This is a repository copy of *Search for gravitational-wave transients associated with magnetar bursts in advanced LIGO and advanced Virgo data from the third observing run*.

White Rose Research Online URL for this paper:
https://eprints.whiterose.ac.uk/212294/

Version: Published Version

Article:
Abbott, R., Abe, H., Acernese, F. et al. (1664 more authors) (2024) Search for gravitational-wave transients associated with magnetar bursts in advanced LIGO and advanced Virgo data from the third observing run. The Astrophysical Journal, 966 (1). p. 137. ISSN 0004-637X

https://doi.org/10.3847/1538-4357/ad27d3

Search for Gravitational-wave Transients Associated with Magnetar Bursts in Advanced LIGO and Advanced Virgo Data from the Third Observing Run

R. Abbott[1], H. Abe[2], F. Acernese[3,4], K. Ackley[5], N. Adhikari[6], R. X. Adhikari[1], V. K. Adkins[7], V. B. Adya[8], C. Affeldt[9,10], D. Agarwal[11], M. Agathos[12,13], K. Agatsuma[14], N. Aggarwal[15], O. D. Aguiar[16], L. Aiello[17], A. Ain[18], P. Ajith[19], T. Akutsu[20,21], S. Albanesi[22,23], R. A. Alfaidi[24], A. Allocca[4,25], P. A. Altin[8], A. Amato[26], C. Anand[5], S. Anand[1], A. Ananyeva[1], S. B. Anderson[1], W. G. Anderson[6], M. Ando[27,28], T. Andrade[29], N. Andres[30], M. Andrés-Carcasona[31], T. Andrić[32], S. V. Angelova[33], S. Ansoldi[34,35], J. M. Antelis[36], S. Antier[37,38], T. Apostolatos[39], E. Z. Appavuravther[40,41], S. Appert[1], S. K. Apple[42], K. Arai[1], A. Araya[43], M. C. Araya[1], J. S. Areeda[44], M. Arène[45], N. Aritomi[20], N. Arnaud[46,47], M. Arogeti[48], S. M. Aronson[7], H. Asada[49], Y. Asali[50], G. Ashton[51], Y. Aso[52,53], M. Assiduo[54,55], S. Assis de Souza Melo[47], S. M. Aston[56], P. Astone[57], F. Aubin[55], K. AultONeal[36], C. Austin[7], S. Babak[45], F. Badaracco[58], M. K. M. Bader[59], C. Badger[60], S. Bae[61], Y. Bae[62], A. M. Baer[63], S. Bagnasco[23], Y. Bai[1], J. Baird[45], R. Bajpai[64], T. Baka[65], M. Ball[66], G. Ballardin[47], S. W. Ballmer[67], A. Balsamo[63], G. Baltus[68], S. Banagiri[15], B. Banerjee[32], D. Bankar[11], J. C. Barayoga[1], C. Barbieri[69,70,71], B. C. Barish[1], D. Barker[72], P. Barneo[29], F. Barone[4,73], B. Barr[24], L. Barsotti[74], M. Barsuglia[45], D. Barta[75], J. Bartlett[72], M. A. Barton[24], I. Bartos[76], S. Basak[19], R. Bassiri[77], A. Basti[18,78], M. Bawaj[40,79], J. C. Bayley[24], M. Bazzan[80,81], B. R. Becher[82], B. Bécsy[83], V. M. Bedakihale[84], F. Beirnaert[85], M. Bejger[86], I. Belahcene[46], V. Benedetto[87], D. Beniwal[88], M. G. Benjamin[89], T. F. Bennett[90], J. D. Bentley[14], M. BenYaala[33], S. Bera[11], M. Berbel[91], F. Bergamin[9,10], B. K. Berger[77], S. Bernuzzi[13], D. Bersanetti[92], A. Bertolini[59], J. Betzwieser[56], D. Beveridge[93], R. Bhandare[94], A. V. Bhandari[11], U. Bhardwaj[38,59], R. Bhatt[1], D. Bhattacharjee[95], S. Bhaumik[76], A. Bianchi[59,96], I. A. Bilenko[97], G. Billingsley[1], S. Bini[98,99], R. Birney[100], O. Birnholtz[101], S. Biscans[1,74], M. Bischi[54,55], S. Biscoveanu[74], A. Bisht[9,10], B. Biswas[11], M. Bitossi[18,47], M.-A. Bizouard[37], J. K. Blackburn[1], C. D. Blair[93], D. G. Blair[93], R. M. Blair[72], F. Bobba[102,103], N. Bode[9,10], M. Boër[37], G. Bogaert[37], M. Boldrini[57,104], G. N. Bolingbroke[88], L. D. Bonavena[80], F. Bondu[105], E. Bonilla[77], R. Bonnand[30], P. Booker[9,10], B. A. Boom[59], R. Bork[1], V. Boschi[18], N. Bose[106], S. Bose[11], V. Bossilkov[93], V. Boudart[68], Y. Bouffanais[80,81], A. Bozzi[47], C. Bradaschia[18], P. R. Brady[6], A. Bramley[56], A. Branch[56], M. Branchesi[32,107], J. E. Brau[66], M. Breschi[13], T. Briant[108], J. H. Briggs[24], A. Brillet[37], M. Brinkmann[9,10], P. Brockill[6], A. F. Brooks[1], J. Brooks[47], D. D. Brown[88], S. Brunett[1], G. Bruno[58], R. Bruntz[63], J. Bryant[14], F. Bucci[55], T. Bulik[109], H. J. Bulten[59], A. Buonanno[110,111], K. Burtnyk[72], R. Buscicchio[14], D. Buskulic[30], C. Buy[112], R. L. Byer[77], G. S. Cabourn Davies[51], G. Cabras[34,35], R. Cabrita[58], L. Cadonati[48], M. Caesar[113], G. Cagnoli[26], C. Cahillane[72], J. Calderón Bustillo[114], J. D. Callaghan[24], T. A. Callister[115,116], E. Calloni[4,25], J. Cameron[93], J. B. Camp[117], M. Canepa[92,118], S. Canevarolo[65], M. Cannavacciuolo[102], K. C. Cannon[28], H. Cao[88], Z. Cao[119], E. Capocasa[20,45], E. Capote[67], G. Carapella[102,103], F. Carbognani[47], M. Carlassara[9,10], J. B. Carlin[120], M. F. Carney[15], M. Carpinelli[47,121,122], G. Carrillo[66], G. Carullo[18,78], T. L. Carver[17], J. Casanueva Diaz[47], C. Casentini[123,124], G. Castaldi[125,126], S. Caudill[59,65], M. Cavaglià[95], F. Cavalier[46], R. Cavalieri[47], G. Cella[18], P. Cerdá-Durán[127], E. Cesarini[124], W. Chaibi[37], S. Chalathadka Subrahmanya[128], E. Champion[129], C.-H. Chan[130], C. Chan[28], C. L. Chan[131], K. Chan[131], M. Chan[132], K. Chandra[106], I. P. Chang[130], P. Chanial[47], S. Chao[130], C. Chapman-Bird[24], P. Charlton[133], E. A. Chase[15], E. Chassande-Mottin[45], C. Chatterjee[93], Debarati Chatterjee[11], Deep Chatterjee[6], M. Chaturvedi[94], S. Chaty[45], C. Chen[134,135], D. Chen[52], H. Y. Chen[74], J. Chen[130], K. Chen[136], X. Chen[93], Y.-B. Chen[137], Y.-R. Chen[138], Z. Chen[17], H. Cheng[76], C. K. Cheong[131], H. Y. Cheung[131], H. Y. Chia[76], F. Chiadini[103,139], C-Y. Chiang[140], G. Chiarini[81], R. Chierici[141], A. Chincarini[92], M. L. Chiofalo[18,78], A. Chiummo[47], R. K. Choudhary[93], S. Choudhary[11], N. Christensen[37], Q. Chu[93], Y-K. Chu[140], S. S. Y. Chua[8], K. W. Chung[60], G. Ciani[80,81], P. Ciecielag[86], M. Cieślar[86], M. Cifaldi[123,124], A. A. Ciobanu[88], R. Ciolfi[81,142], F. Cipriano[37], F. Clara[72], J. A. Clark[1,48], P. Clearwater[143], S. Clesse[144], F. Cleva[37], E. Coccia[32,107], E. Codazzo[32], P.-F. Cohadon[108], D. E. Cohen[46], M. Colleoni[145], C. G. Collette[146], A. Colombo[69,70], M. Colpi[69,70], C. M. Compton[72], M. Constancio, Jr.[16], L. Conti[81], S. J. Cooper[14], P. Corban[56], T. R. Corbitt[7], I. Cordero-Carrión[147], S. Corezzi[40,79], K. R. Corley[50], N. J. Cornish[83], D. Corre[46], A. Corsi[148], S. Cortese[47], C. A. Costa[16], R. Cotesta[111], R. Cottingham[56], M. W. Coughlin[149], J.-P. Coulon[37], S. T. Countryman[50], B. Cousins[150], P. Couvares[1], D. M. Coward[93], M. J. Cowart[56], D. C. Coyne[1], R. Coyne[151], J. D. E. Creighton[6], T. D. Creighton[89], A. W. Criswell[149], M. Croquette[108], S. G. Crowder[152], J. R. Cudell[68], T. J. Cullen[7], A. Cumming[24], R. Cummings[24], L. Cunningham[24], E. Cuoco[18,47,153], M. Curyło[109], P. Dabadie[26], T. Dal Canton[46], S. Dall'Osso[32], G. Dálya[85,154], A. Dana[77], B. D'Angelo[92,118], S. Danilishin[59,155], S. D'Antonio[124], K. Danzmann[9,10], C. Darsow-Fromm[128], A. Dasgupta[84], L. E. H. Datrier[24], Sayak Datta[11], Sayantani Datta[156], V. Dattilo[47], I. Dave[94], M. Davier[46], D. Davis[1], M. C. Davis[113], E. J. Daw[157], R. Dean[113], D. DeBra[77], M. Deenadayalan[11], J. Degallaix[158], M. De Laurentis[4,25], S. Déléglise[108], V. Del Favero[129], F. De Lillo[58], N. De Lillo[24], D. Dell'Aquila[121], W. Del Pozzo[18,78], L. M. DeMarchi[15], F. De Matteis[123,124], V. D'Emilio[17], N. Demos[74], T. Dent[114], A. Depasse[58], R. De Pietri[159,160], R. De Rosa[4,25], C. De Rossi[47], R. DeSalvo[125,126,161], R. De Simone[139], S. Dhurandhar[11], M. C. Díaz[89], N. A. Didio[67], T. Dietrich[111], L. Di Fiore[4], C. Di Fronzo[14], C. Di Giorgio[102,103], F. Di Giovanni[127], M. Di Giovanni[32],

T. Di Girolamo[4,25], A. Di Lieto[18,78], A. Di Michele[79], B. Ding[146], S. Di Pace[57,104], I. Di Palma[57,104],
F. Di Renzo[18,78], A. K. Divakarla[76], A. Dmitriev[14], Z. Doctor[15], L. Donahue[162], L. D'Onofrio[4,25], F. Donovan[74],
K. L. Dooley[17], S. Doravari[11], M. Drago[57,104], J. C. Driggers[72], Y. Drori[1], J.-G. Ducoin[46], P. Dupej[24], U. Dupletsa[32],
O. Durante[102,103], D. D'Urso[121,122], P.-A. Duverne[46], S. E. Dwyer[72], C. Eassa[72], P. J. Easter[5], M. Ebersold[163], T. Eckhardt[128],
G. Eddolls[24], B. Edelman[66], T. B. Edo[1], O. Edy[51], A. Effler[56], S. Eguchi[132], J. Eichholz[8], S. S. Eikenberry[76],
M. Eisenmann[20,30], R. A. Eisenstein[74], A. Ejlli[17], E. Engelby[44], Y. Enomoto[27], L. Errico[4,25], R. C. Essick[164], H. Estellés[145],
D. Estevez[165], Z. Etienne[166], T. Etzel[1], M. Evans[74], T. M. Evans[56], T. Evstafyeva[12], B. E. Ewing[150], F. Fabrizi[54,55],
F. Faedi[55], V. Fafone[32,123,124], H. Fair[67], S. Fairhurst[17], P. C. Fan[162], A. M. Farah[167], S. Farinon[92], B. Farr[66],
W. M. Farr[115,116], E. J. Fauchon-Jones[17], G. Favaro[80], M. Favata[168], M. Fays[68], M. Fazio[169], J. Feicht[1], M. M. Fejer[77],
E. Fenyvesi[75,170], D. L. Ferguson[171], A. Fernandez-Galiana[74], I. Ferrante[18,78], T. A. Ferreira[16], F. Fidecaro[18,78],
P. Figura[109], A. Fiori[18,78], I. Fiori[47], M. Fishbach[15], R. P. Fisher[63], R. Fittipaldi[103,172], V. Fiumara[103,173],
R. Flaminio[20,30], E. Floden[149], H. K. Fong[28], J. A. Font[127,174], B. Fornal[161], P. W. F. Forsyth[8], A. Franke[128], S. Frasca[57,104],
F. Frasconi[18], J. P. Freed[36], Z. Frei[154], A. Freise[59,96], O. Freitas[175], R. Frey[66], P. Fritschel[74], V. V. Frolov[56],
G. G. Fronzé[23], Y. Fujii[176], Y. Fujikawa[177], Y. Fujimoto[178], P. Fulda[76], M. Fyffe[56], H. A. Gabbard[24], B. U. Gadre[111],
J. R. Gair[111], J. Gais[131], S. Galaudage[5], R. Gamba[13], D. Ganapathy[74], A. Ganguly[11], D. Gao[179], S. G. Gaonkar[11],
B. Garaventa[92,118], C. García Núñez[100], C. García-Quirós[145], F. Garufi[4,25], B. Gateley[72], V. Gayathri[76], G.-G. Ge[179],
G. Gemme[92], A. Gennai[18], J. George[94], O. Gerberding[128], L. Gergely[180], P. Gewecke[128], S. Ghonge[48],
Abhirup Ghosh[111], Archisman Ghosh[85], Shaon Ghosh[168], Shrobana Ghosh[17], Tathagata Ghosh[11],
B. Giacomazzo[69,70,71], L. Giacoppo[57,104], J. A. Giaime[7,56], K. D. Giardina[56], D. R. Gibson[100], C. Gier[33], M. Giesler[181],
P. Giri[18,78], F. Gissi[87], S. Gkaitatzis[18,78], J. Glanzer[7], A. E. Gleckl[44], P. Godwin[150], E. Goetz[182], R. Goetz[76],
N. Gohlke[9,10], J. Golomb[1], B. Goncharov[32], G. González[7], M. Gosselin[47], R. Gouaty[30], D. W. Gould[8], S. Goyal[19], B. Grace[8],
A. Grado[4,183], V. Graham[24], M. Granata[158], V. Granata[102], A. Grant[24], S. Gras[74], P. Grassia[1], C. Gray[72], R. Gray[24],
G. Greco[40], A. C. Green[76], R. Green[17], A. M. Gretarsson[36], E. M. Gretarsson[36], D. Griffith[1], W. L. Griffiths[17],
H. L. Griggs[48], G. Grignani[40,79], A. Grimaldi[98,99], E. Grimes[36], S. J. Grimm[32,107], H. Grote[17], S. Grunewald[111],
P. Gruning[46], A. S. Gruson[44], D. Guerra[127], G. M. Guidi[54,55], A. R. Guimaraes[7], G. Guixé[29], H. K. Gulati[84], A. M. Gunny[74],
H.-K. Guo[161], Y. Guo[59], Anchal Gupta[1], Anuradha Gupta[184], I. M. Gupta[150], P. Gupta[59,65], S. K. Gupta[106], R. Gustafson[185],
F. Guzman[186], S. Ha[187], I. P. W. Hadiputrawan[136], L. Haegel[45], S. Haino[140], O. Halim[35], E. D. Hall[74], E. Z. Hamilton[163],
G. Hammond[24], W.-B. Han[188], M. Haney[163], J. Hanks[72], C. Hanna[150], M. D. Hannam[17], O. Hannuksela[59,65], H. Hansen[72],
T. J. Hansen[36], J. Hanson[56], T. Harder[37], K. Haris[59,65], J. Harms[32,107], G. M. Harry[42], I. W. Harry[51], D. Hartwig[128],
K. Hasegawa[189], B. Haskell[86], C.-J. Haster[74], J. S. Hathaway[129], K. Hattori[190], K. Haughian[24], H. Hayakawa[191], K. Hayama[132],
F. J. Hayes[24], J. Healy[129], A. Heidmann[108], A. Heidt[9,10], M. C. Heintze[56], J. Heinze[9,10], J. Heinzel[74], H. Heitmann[37],
F. Hellman[192], P. Hello[46], A. F. Helmling-Cornell[66], G. Hemming[47], M. Hendry[24], I. S. Heng[24], E. Hennes[59],
J. Hennig[193], M. H. Hennig[193], C. Henshaw[48], A. G. Hernandez[90], F. Hernandez Vivanco[5], M. Heurs[9,10], A. L. Hewitt[194],
S. Higginbotham[17], S. Hild[59,155], P. Hill[33], Y. Himemoto[195], A. S. Hines[186], N. Hirata[20], C. Hirose[177], T-C. Ho[136], S. Hochheim[9,10],
D. Hofman[158], J. N. Hohmann[128], D. G. Holcomb[113], N. A. Holland[8], I. J. Hollows[157], Z. J. Holmes[88], K. Holt[56],
D. E. Holz[167], Q. Hong[130], J. Hough[24], S. Hourihane[1], E. J. Howell[93], C. G. Hoy[17], D. Hoyland[14], A. Hreibi[9,10],
B-H. Hsieh[189], H-F. Hsieh[196], C. Hsiung[134], Y. Hsu[130], H-Y. Huang[140], P. Huang[179], Y-C. Huang[138], Y.-J. Huang[140],
Yiting Huang[152], Yiwen Huang[74], M. T. Hübner[5], A. D. Huddart[197], B. Hughey[36], D. C. Y. Hui[198], V. Hui[30], S. Husa[145],
S. H. Huttner[24], R. Huxford[150], T. Huynh-Dinh[56], S. Ide[199], B. Idzkowski[109], A. Iess[123,124], K. Inayoshi[200], Y. Inoue[136],
P. Iosif[201], M. Isi[74], K. Isleif[128], K. Ito[202], Y. Itoh[178,203], B. R. Iyer[19], V. JaberianHamedan[93], T. Jacqmin[108],
P.-E. Jacquet[108], S. J. Jadhav[204], S. P. Jadhav[11], T. Jain[12], A. L. James[17], A. Z. Jan[171], K. Jani[205], J. Janquart[59,65],
K. Janssens[37,206], N. N. Janthalur[204], P. Jaranowski[207], D. Jariwala[76], R. Jaume[145], A. C. Jenkins[60], K. Jenner[88],
C. Jeon[208], W. Jia[74], J. Jiang[76], H.-B. Jin[209,210], G. R. Johns[63], R. Johnston[24], A. W. Jones[93], D. I. Jones[211], P. Jones[14],
R. Jones[24], P. Joshi[150], L. Ju[93], A. Jue[161], P. Jung[62], K. Jung[187], J. Junker[9,10], V. Juste[165], K. Kaihotsu[202], T. Kajita[212],
M. Kakizaki[190], C. V. Kalaghatgi[17,59,65,213], V. Kalogera[15], B. Kamai[1], M. Kamiizumi[191], N. Kanda[178,203],
S. Kandhasamy[11], G. Kang[214], J. B. Kanner[1], Y. Kao[130], S. J. Kapadia[19], D. P. Kapasi[8], C. Karathanasis[31], S. Karki[95],
R. Kashyap[150], M. Kasprzack[1], W. Kastaun[9,10], T. Kato[189], S. Katsanevas[47], E. Katsavounidis[74], W. Katzman[56], T. Kaur[93],
K. Kawabe[72], K. Kawaguchi[189], F. Kéfélian[37], D. Keitel[145], J. S. Key[215], S. Khadka[77], F. Y. Khalili[97], S. Khan[17],
T. Khanam[148], E. A. Khazanov[216], N. Khetan[32,107], M. Khursheed[94], N. Kijbunchoo[8], A. Kim[15], C. Kim[208], J. C. Kim[217],
J. Kim[218], K. Kim[208], W. S. Kim[62], Y.-M. Kim[187], C. Kimball[15], N. Kimura[191], M. Kinley-Hanlon[24], R. Kirchhoff[9,10],
J. S. Kissel[72], S. Klimenko[76], T. Klinger[12], A. M. Knee[182], T. D. Knowles[166], N. Knust[9,10], E. Knyazev[74], Y. Kobayashi[178],
P. Koch[9,10], G. Koekoek[59,155], K. Kohri[219], K. Kokeyama[220], S. Koley[32], P. Kolitsidou[17], M. Kolstein[31], K. Komori[74],
V. Kondrashov[1], A. K. H. Kong[196], A. Kontos[82], N. Koper[9,10], M. Korobko[128], M. Kovalam[93], N. Koyama[177],
D. B. Kozak[1], C. Kozakai[52], V. Kringel[9,10], N. V. Krishnendu[9,10], A. Królak[221,222], G. Kuehn[9,10], F. Kuei[130], P. Kuijer[59],
S. Kulkarni[184], A. Kumar[204], Prayush Kumar[19], Rahul Kumar[72], Rakesh Kumar[84], J. Kume[28], K. Kuns[74], Y. Kuromiya[202],
S. Kuroyanagi[223,224], K. Kwak[187], G. Lacaille[24], P. Lagabbe[30], D. Laghi[112], E. Lalande[225], M. Lalleman[206], T. L. Lam[131],
A. Lamberts[37,226], M. Landry[72], B. B. Lane[74], R. N. Lang[74], J. Lange[171], B. Lantz[77], I. La Rosa[30], A. Lartaux-Vollard[46],

P. D. Lasky[5], M. Laxen[56], A. Lazzarini[1], C. Lazzaro[80,81], P. Leaci[57,104], S. Leavey[9,10], S. LeBohec[161],
Y. K. Lecoeuche[182], E. Lee[189], H. M. Lee[227], H. W. Lee[217], K. Lee[228], R. Lee[138], I. N. Legred[1], J. Lehmann[9,10],
A. Lemaître[229], M. Lenti[55,230], M. Leonardi[20], E. Leonova[38], N. Leroy[46], N. Letendre[30], C. Levesque[225], Y. Levin[5],
J. N. Leviton[185], K. Leyde[45], A. K. Y. Li[1], B. Li[130], J. Li[15], K. L. Li[231], P. Li[232], T. G. F. Li[131], X. Li[137], C-Y. Lin[233],
E. T. Lin[196], F-K. Lin[140], F-L. Lin[234], H. L. Lin[136], L. C.-C. Lin[231], F. Linde[59,213], S. D. Linker[90,125,126], J. N. Linley[24],
T. B. Littenberg[235], G. C. Liu[134], J. Liu[93], K. Liu[130], X. Liu[6], F. Llamas[89], R. K. L. Lo[1], T. Lo[130], L. T. London[38,74],
A. Longo[236], D. Lopez[163], M. Lopez Portilla[65], M. Lorenzini[123,124], V. Loriette[237], M. Lormand[56], G. Losurdo[18],
T. P. Lott[48], J. D. Lough[9,10], C. O. Lousto[129], G. Lovelace[44], J. F. Lucaccioni[238], H. Lück[9,10], D. Lumaca[123,124],
A. P. Lundgren[51], L.-W. Luo[140], J. E. Lynam[63], M. Ma'arif[136], R. Macas[51], J. B. Machtinger[15], M. MacInnis[74],
D. M. Macleod[17], I. A. O. MacMillan[1], A. Macquet[37], I. Magaña Hernandez[6], C. Magazzù[18], R. M. Magee[1],
R. Maggiore[14], M. Magnozzi[92,118], S. Mahesh[166], E. Majorana[57,104], I. Maksimovic[237], S. Maliakal[1], A. Malik[94], N. Man[37],
V. Mandic[149], V. Mangano[57,104], B. R. Mannix[66], G. L. Mansell[72,74], M. Manske[6], M. Mantovani[47], M. Mapelli[80,81],
F. Marchesoni[40,41,239], D. Marín Pina[29], F. Marion[30], Z. Mark[137], S. Márka[50], Z. Márka[50], C. Markakis[12],
A. S. Markosyan[77], A. Markowitz[1], E. Maros[1], A. Marquina[147], S. Marsat[45], F. Martelli[54,55], I. W. Martin[24], R. M. Martin[168],
M. Martinez[31], V. A. Martinez[76], V. Martinez[26], K. Martinovic[60], D. V. Martynov[14], E. J. Marx[74], H. Masalehdan[128],
K. Mason[74], E. Massera[157], A. Masserot[30], M. Masso-Reid[24], S. Mastrogiovanni[45], A. Matas[111], M. Mateu-Lucena[145],
F. Matichard[1,74], M. Matiushechkina[9,10], N. Mavalvala[74], J. J. McCann[93], R. McCarthy[72], D. E. McClelland[8],
P. K. McClincy[150], S. McCormick[56], L. McCuller[74], G. I. McGhee[24], S. C. McGuire[56], C. McIsaac[51], J. McIver[182], T. McRae[8],
S. T. McWilliams[166], D. Meacher[6], M. Mehmet[9,10], A. K. Mehta[111], Q. Meijer[65], A. Melatos[120], D. A. Melchor[44],
G. Mendell[72], A. Menendez-Vazquez[31], C. S. Menoni[169], R. A. Mercer[6], L. Mereni[158], K. Merfeld[66,148], E. L. Merilh[56],
J. D. Merritt[66], M. Merzougui[37], S. Meshkov[1,294], C. Messenger[24], C. Messick[74], P. M. Meyers[120], F. Meylahn[9,10],
A. Mhaske[11], A. Miani[98,99], H. Miao[14], I. Michaloliakos[76], C. Michel[158], Y. Michimura[27], H. Middleton[120],
D. P. Mihaylov[111], L. Milano[25,295], A. L. Miller[58], A. Miller[90], B. Miller[38,59], M. Millhouse[120], J. C. Mills[17], E. Milotti[35,240],
Y. Minenkov[124], N. Mio[241], Ll. M. Mir[31], M. Miravet-Tenés[127], A. Mishkin[76], C. Mishra[242], T. Mishra[76], T. Mistry[157],
S. Mitra[11], V. P. Mitrofanov[97], G. Mitselmakher[76], R. Mittleman[74], O. Miyakawa[191], K. Miyo[191], S. Miyoki[191],
Geoffrey Mo[74], L. M. Modafferi[145], E. Moguel[238], K. Mogushi[95], S. R. P. Mohapatra[74], S. R. Mohite[6], I. Molina[44],
M. Molina-Ruiz[192], M. Mondin[90], M. Montani[54,55], C. J. Moore[14], J. Moragues[145], D. Moraru[72], F. Morawski[86], A. More[11],
C. Moreno[36], G. Moreno[72], Y. Mori[202], S. Morisaki[6], N. Morisue[178], Y. Moriwaki[190], B. Mours[165],
C. M. Mow-Lowry[59,96], S. Mozzon[51], F. Muciaccia[57,104], Arunava Mukherjee[243], D. Mukherjee[150], Soma Mukherjee[89],
Subroto Mukherjee[84], Suvodip Mukherjee[38,164], N. Mukund[9,10], A. Mullavey[56], J. Munch[88], E. A. Muñiz[67],
P. G. Murray[24], R. Musenich[92,118], S. Muusse[88], S. L. Nadji[9,10], K. Nagano[244], A. Nagar[23,245], K. Nakamura[20],
H. Nakano[246], M. Nakano[189], Y. Nakayama[202], V. Napolano[47], I. Nardecchia[123,124], T. Narikawa[189], H. Narola[65],
L. Naticchioni[57], B. Nayak[90], R. K. Nayak[247], B. F. Neil[93], J. Neilson[87,103], A. Nelson[186], T. J. N. Nelson[56], M. Nery[9,10],
P. Neubauer[238], A. Neunzert[215], K. Y. Ng[74], S. W. S. Ng[88], C. Nguyen[45], P. Nguyen[66], T. Nguyen[74], L. Nguyen Quynh[248],
J. Ni[149], W.-T. Ni[138,179,209], S. A. Nichols[7], T. Nishimoto[189], A. Nishizawa[28], S. Nissanke[38,59], E. Nitoglia[141], F. Nocera[47],
M. Norman[17], C. North[17], S. Nozaki[190], G. Nurbek[89], L. K. Nuttall[51], Y. Obayashi[189], J. Oberling[72], B. D. O'Brien[76],
J. O'Dell[197], E. Oelker[24], W. Ogaki[189], G. Oganesyan[32,107], J. J. Oh[62], K. Oh[198], S. H. Oh[62], M. Ohashi[191],
T. Ohashi[178], M. Ohkawa[177], F. Ohme[9,10], H. Ohta[28], M. A. Okada[16], Y. Okutani[199], C. Olivetto[47], K. Oohara[189,249],
R. Oram[56], B. O'Reilly[56], R. G. Ormiston[149], N. D. Ormsby[63], R. O'Shaughnessy[129], E. O'Shea[181], S. Oshino[191],
S. Ossokine[111], C. Osthelder[1], S. Otabe[2], D. J. Ottaway[88], H. Overmier[56], A. E. Pace[150], G. Pagano[18,78], R. Pagano[7],
M. A. Page[93], G. Pagliaroli[32,107], A. Pai[106], S. A. Pai[94], S. Pal[247], J. R. Palamos[66], O. Palashov[216], C. Palomba[57], H. Pan[130],
K.-C. Pan[138,196], P. K. Panda[204], P. T. H. Pang[59,65], C. Pankow[15], F. Pannarale[57,104], B. C. Pant[94], F. H. Panther[93],
F. Paoletti[18], A. Paoli[47], A. Paolone[57,250], G. Pappas[201], A. Parisi[134], H. Park[6], J. Park[251], W. Parker[56],
D. Pascucci[59,85], A. Pasqualetti[47], R. Passaquieti[18,78], D. Passuello[18], M. Patel[63], M. Pathak[88], B. Patricelli[18,47],
A. S. Patron[7], S. Paul[66], E. Payne[5], M. Pedraza[1], R. Pedurand[103], M. Pegoraro[81], A. Pele[56], F. E. Peña Arellano[191],
S. Penano[77], S. Penn[252], A. Perego[98,99], A. Pereira[26], T. Pereira[253], C. J. Perez[72], C. Périgois[30], C. C. Perkins[76],
A. Perreca[98,99], S. Perriès[141], D. Pesios[201], J. Petermann[128], D. Petterson[1], H. P. Pfeiffer[111], H. Pham[56], K. A. Pham[149],
K. S. Phukon[59,213], H. Phurailatpam[131], O. J. Piccinni[57], M. Pichot[37], M. Piendibene[18,78], F. Piergiovanni[54,55],
L. Pierini[57,104], V. Pierro[87,103], G. Pillant[47], M. Pillas[46], F. Pilo[18], L. Pinard[158], C. Pineda-Bosque[90], I. M. Pinto[87,103,254],
M. Pinto[47], B. J. Piotrzkowski[6], K. Piotrzkowski[58], M. Pirello[72], M. D. Pitkin[194], A. Placidi[40,79], E. Placidi[57,104],
M. L. Planas[145], W. Plastino[236,255], C. Pluchar[256], R. Poggiani[18,78], E. Polini[30], D. Y. T. Pong[131], S. Ponrathnam[11],
E. K. Porter[45], R. Poulton[47], A. Poverman[82], J. Powell[143], M. Pracchia[30], T. Pradier[165], A. K. Prajapati[84], K. Prasai[77],
R. Prasanna[204], G. Pratten[14], M. Principe[87,103,254], G. A. Prodi[99,257], L. Prokhorov[14], P. Prosposito[123,124], L. Prudenzi[111],
A. Puecher[59,65], M. Punturo[40], F. Puosi[18,78], P. Puppo[57], M. Pürrer[111], H. Qi[17], N. Quartey[63], V. Quetschke[89],
P. J. Quinonez[36], R. Quitzow-James[95], F. J. Raab[72], G. Raaijmakers[38,59], H. Radkins[72], N. Radulesco[37], P. Raffai[154],
S. X. Rail[225], S. Raja[94], C. Rajan[94], K. E. Ramirez[56], T. D. Ramirez[44], A. Ramos-Buades[111], J. Rana[150], P. Rapagnani[57,104],

A. Ray[6], V. Raymond[17], N. Raza[182], M. Razzano[18,78], J. Read[44], L. A. Rees[42], T. Regimbau[30], L. Rei[92], S. Reid[33], S. W. Reid[63], D. H. Reitze[1,76], P. Relton[17], A. Renzini[1], P. Rettegno[22,23], B. Revenu[45], A. Reza[59], M. Rezac[44], F. Ricci[57,104], D. Richards[197], J. W. Richardson[258], L. Richardson[186], G. Riemenschneider[22,23], K. Riles[185], S. Rinaldi[18,78], K. Rink[182], N. A. Robertson[1], R. Robie[1], F. Robinet[46], A. Rocchi[124], S. Rodriguez[44], L. Rolland[30], J. G. Rollins[1], M. Romanelli[105], R. Romano[3,4], C. L. Romel[72], A. Romero[31], I. M. Romero-Shaw[5], J. H. Romie[56], S. Ronchini[32,107], L. Rosa[4,25], C. A. Rose[6], D. Rosińska[109], M. P. Ross[259], S. Rowan[24], S. J. Rowlinson[14], S. Roy[65], Santosh Roy[11], Soumen Roy[260], D. Rozza[121,122], P. Ruggi[47], K. Ruiz-Rocha[205], K. Ryan[72], S. Sachdev[150], T. Sadecki[72], J. Sadiq[114], S. Saha[196], Y. Saito[191], K. Sakai[261], M. Sakellariadou[60], S. Sakon[150], O. S. Salafia[69,70,71], F. Salces-Carcoba[1], L. Salconi[47], M. Saleem[149], F. Salemi[98,99], A. Samajdar[70], E. J. Sanchez[1], J. H. Sanchez[44], L. E. Sanchez[1], N. Sanchis-Gual[262], J. R. Sanders[263], A. Sanuy[29], T. R. Saravanan[11], N. Sarin[5], B. Sassolas[158], H. Satari[93], B. S. Sathyaprakash[17,150], O. Sauter[76], R. L. Savage[72], V. Savant[11], T. Sawada[178], H. L. Sawant[11], S. Sayah[158], D. Schaetzl[1], M. Scheel[137], J. Scheuer[15], M. G. Schiworski[88], P. Schmidt[14], S. Schmidt[65], R. Schnabel[128], M. Schneewind[9,10], R. M. S. Schofield[66], A. Schönbeck[128], B. W. Schulte[9,10], B. F. Schutz[9,10,17], E. Schwartz[17], J. Scott[24], S. M. Scott[8], M. Seglar-Arroyo[30], Y. Sekiguchi[264], D. Sellers[56], A. S. Sengupta[260], D. Sentenac[47], E. G. Seo[131], V. Sequino[4,25], A. Sergeev[216], Y. Setyawati[9,10,65], T. Shaffer[72], M. S. Shahriar[15], M. A. Shaikh[19], B. Shams[161], L. Shao[200], A. Sharma[32,107], P. Sharma[94], P. Shawhan[110], N. S. Shcheblanov[229], A. Sheela[242], Y. Shikano[265,266], M. Shikauchi[28], H. Shimizu[267], K. Shimode[191], H. Shinkai[268], T. Shishido[53], A. Shoda[20], D. H. Shoemaker[74], D. M. Shoemaker[171], S. ShyamSundar[94], M. Sieniawska[58], D. Sigg[72], L. Silenzi[40,41], L. P. Singer[117], D. Singh[150], M. K. Singh[19], N. Singh[109], A. Singha[59,155], A. M. Sintes[145], V. Sipala[121,122], V. Skliris[17], B. J. J. Slagmolen[8], T. J. Slaven-Blair[93], J. Smetana[14], J. R. Smith[44], L. Smith[24], R. J. E. Smith[5], J. Soldateschi[55,230,269], S. N. Somala[270], K. Somiya[2], I. Song[196], K. Soni[11], V. Sordini[141], F. Sorrentino[92], N. Sorrentino[18,78], R. Soulard[37], T. Souradeep[11,271], E. Sowell[148], V. Spagnuolo[59,155], A. P. Spencer[24], M. Spera[80,81], P. Spinicelli[47], A. K. Srivastava[84], V. Srivastava[67], K. Staats[15], C. Stachie[37], F. Stachurski[24], D. A. Steer[45], J. Steinlechner[59,155], S. Steinlechner[59,155], N. Stergioulas[201], D. J. Stops[14], M. Stover[238], K. A. Strain[24], L. C. Strang[120], G. Stratta[57,272], M. D. Strong[7], A. Strunk[72], R. Sturani[253], A. L. Stuver[113], M. Suchenek[86], S. Sudhagar[11], V. Sudhir[74], R. Sugimoto[244,273], H. G. Suh[6], A. G. Sullivan[50], T. Z. Summerscales[274], L. Sun[8], S. Sunil[84], A. Sur[86], J. Suresh[28], P. J. Sutton[17], Takamasa Suzuki[177], Takanori Suzuki[2], Toshikazu Suzuki[189], B. L. Swinkels[59], M. J. Szczepańczyk[76], P. Szewczyk[109], M. Tacca[59], H. Tagoshi[189], S. C. Tait[24], H. Takahashi[275], R. Takahashi[20], S. Takano[27], H. Takeda[27], M. Takeda[178], C. J. Talbot[33], C. Talbot[1], K. Tanaka[276], Taiki Tanaka[189], Takahiro Tanaka[277], A. J. Tanasijczuk[58], S. Tanioka[191], D. B. Tanner[76], D. Tao[1], L. Tao[76], R. D. Tapia[150], E. N. Tapia San Martín[59], C. Taranto[123], A. Taruya[278], J. D. Tasson[162], R. Tenorio[145], J. E. S. Terhune[113], L. Terkowski[128], M. P. Thirugnanasambandam[11], M. Thomas[56], P. Thomas[72], E. E. Thompson[48], J. E. Thompson[17], S. R. Thondapu[94], K. A. Thorne[56], E. Thrane[5], Shubhanshu Tiwari[163], Srishti Tiwari[11], V. Tiwari[17], A. M. Toivonen[149], A. E. Tolley[51], T. Tomaru[20], T. Tomura[191], M. Tonelli[18,78], Z. Tornasi[24], A. Torres-Forné[127], C. I. Torrie[1], I. Tosta e Melo[122], D. Töyrä[8], A. Trapananti[40,41], F. Travasso[40,41], G. Traylor[56], M. Trevor[110], M. C. Tringali[47], A. Tripathee[185], L. Troiano[103,279], A. Trovato[45], L. Trozzo[4,191], R. J. Trudeau[1], D. Tsai[130], K. W. Tsang[59,65,280], T. Tsang[281], J-S. Tsao[234], M. Tse[74], R. Tso[137], S. Tsuchida[178], L. Tsukada[150], D. Tsuna[28], T. Tsutsui[28], K. Turbang[206,282], M. Turconi[37], D. Tuyenbayev[178], A. S. Ubhi[14], N. Uchikata[189], T. Uchiyama[191], R. P. Udall[1], A. Ueda[283], T. Uehara[284,285], K. Ueno[28], G. Ueshima[286], C. S. Unnikrishnan[287], A. L. Urban[7], T. Ushiba[191], A. Utina[59,155], G. Vajente[1], A. Vajpeyi[5], G. Valdes[186], M. Valentini[98,99,184], V. Valsan[6], N. van Bakel[59], M. van Beuzekom[59], M. van Dael[59,288], J. F. J. van den Brand[59,96,155], C. Van Den Broeck[59,65], D. C. Vander-Hyde[67], H. van Haevermaet[206], J. V. van Heijningen[58], M. H. P. M. van Putten[289], N. van Remortel[206], M. Vardaro[59,213], A. F. Vargas[120], V. Varma[111], M. Vasúth[75], A. Vecchio[14], G. Vedovato[81], J. Veitch[24], P. J. Veitch[88], J. Venneberg[9,10], G. Venugopalan[1], D. Verkindt[30], P. Verma[222], Y. Verma[94], S. M. Vermeulen[17], D. Veske[50], F. Vetrano[54], A. Viceré[54,55], S. Vidyant[67], A. D. Viets[290], A. Vijaykumar[19], V. Villa-Ortega[114], J.-Y. Vinet[37], A. Virtuoso[35,240], S. Vitale[74], H. Vocca[40,79], E. R. G. von Reis[72], J. S. A. von Wrangel[9,10], C. Vorvick[72], S. P. Vyatchanin[97], L. E. Wade[238], M. Wade[238], K. J. Wagner[129], R. C. Walet[59], M. Walker[63], G. S. Wallace[33], L. Wallace[1], J. Wang[179], J. Z. Wang[185], W. H. Wang[89], R. L. Ward[8], J. Warner[72], M. Was[30], T. Washimi[20], N. Y. Washington[1], J. Watchi[146], B. Weaver[72], C. R. Weaving[51], S. A. Webster[24], M. Weinert[9,10], A. J. Weinstein[1], R. Weiss[74], C. M. Weller[259], R. A. Weller[205], F. Wellmann[9,10], L. Wen[93], P. Weßels[9,10], K. Wette[8], J. T. Whelan[129], D. D. White[44], B. F. Whiting[76], C. Whittle[74], D. Wilken[9,10], D. Williams[24], M. J. Williams[24], A. R. Williamson[51], J. L. Willis[1], B. Willke[9,10], D. J. Wilson[256], C. C. Wipf[1], T. Wlodarczyk[111], G. Woan[24], J. Woehler[9,10], J. K. Wofford[129], D. Wong[182], I. C. F. Wong[131], M. Wright[24], C. Wu[138], D. S. Wu[9,10], H. Wu[138], D. M. Wysocki[6], L. Xiao[1], T. Yamada[267], H. Yamamoto[1], K. Yamamoto[1], T. Yamamoto[191], K. Yamashita[202], R. Yamazaki[199], F. W. Yang[161], K. Z. Yang[149], L. Yang[169], Y.-C. Yang[130], Y. Yang[291], Yang Yang[76], M. J. Yap[8], D. W. Yeeles[17], S.-W. Yeh[138], A. B. Yelikar[129], M. Ying[130], J. Yokoyama[27,28], T. Yokozawa[191], J. Yoo[181], T. Yoshioka[202], Hang Yu[137], Haocun Yu[74], H. Yuzurihara[189], A. Zadrożny[222], M. Zanolin[36], S. Zeidler[292], T. Zelenova[47], J.-P. Zendri[81], M. Zevin[167], M. Zhan[179], H. Zhang[234],

J. Zhang[93] , L. Zhang[1], R. Zhang[76] , T. Zhang[14], Y. Zhang[186], C. Zhao[93] , G. Zhao[146], Y. Zhao[20,189] , Yue Zhao[161],
R. Zhou[192], Z. Zhou[15], X. J. Zhu[5] , Z.-H. Zhu[119,232] , M. E. Zucker[1,74], J. Zweizig[293] , and
The LIGO Scientific Collaboration, the Virgo Collaboration, and the KAGRA Collaboration

[1] LIGO Laboratory, California Institute of Technology, Pasadena, CA 91125, USA
[2] Graduate School of Science, Tokyo Institute of Technology, Meguro-ku, Tokyo 152-8551, Japan
[3] Dipartimento di Farmacia, Università di Salerno, I-84084 Fisciano, Salerno, Italy
[4] INFN, Sezione di Napoli, Complesso Universitario di Monte S. Angelo, I-80126 Napoli, Italy
[5] OzGrav, School of Physics & Astronomy, Monash University, Clayton 3800, Victoria, Australia
[6] University of Wisconsin-Milwaukee, Milwaukee, WI 53201, USA
[7] Louisiana State University, Baton Rouge, LA 70803, USA
[8] OzGrav, Australian National University, Canberra, Australian Capital Territory 0200, Australia
[9] Max Planck Institute for Gravitational Physics (Albert Einstein Institute), D-30167 Hannover, Germany
[10] Leibniz Universität Hannover, D-30167 Hannover, Germany
[11] Inter-University Centre for Astronomy and Astrophysics, Pune 411007, India
[12] University of Cambridge, Cambridge CB2 1TN, UK
[13] Theoretisch-Physikalisches Institut, Friedrich-Schiller-Universität Jena, D-07743 Jena, Germany
[14] University of Birmingham, Birmingham B15 2TT, UK
[15] Northwestern University, Evanston, IL 60208, USA
[16] Instituto Nacional de Pesquisas Espaciais, 12227-010 São José dos Campos, São Paulo, Brazil
[17] Cardiff University, Cardiff CF24 3AA, UK
[18] INFN, Sezione di Pisa, I-56127 Pisa, Italy
[19] International Centre for Theoretical Sciences, Tata Institute of Fundamental Research, Bengaluru 560089, India
[20] Gravitational Wave Science Project, National Astronomical Observatory of Japan (NAOJ), Mitaka City, Tokyo 181-8588, Japan
[21] Advanced Technology Center, National Astronomical Observatory of Japan (NAOJ), Mitaka City, Tokyo 181-8588, Japan
[22] Dipartimento di Fisica, Università degli Studi di Torino, I-10125 Torino, Italy
[23] INFN, Sezione di Torino, I-10125 Torino, Italy
[24] SUPA, University of Glasgow, Glasgow G12 8QQ, UK
[25] Università di Napoli "Federico II," Complesso Universitario di Monte S. Angelo, I-80126 Napoli, Italy
[26] Université de Lyon, Université Claude Bernard Lyon 1, CNRS, Institut Lumière Matière, F-69622 Villeurbanne, France
[27] Department of Physics, The University of Tokyo, Bunkyo-ku, Tokyo 113-0033, Japan
[28] Research Center for the Early Universe (RESCEU), The University of Tokyo, Bunkyo-ku, Tokyo 113-0033, Japan
[29] Institut de Ciències del Cosmos (ICCUB), Universitat de Barcelona, C/ Martí i Franquès 1, Barcelona 08028, Spain
[30] Univ. Savoie Mont Blanc, CNRS, Laboratoire d'Annecy de Physique des Particules—IN2P3, F-74000 Annecy, France
[31] Institut de Física d'Altes Energies (IFAE), Barcelona Institute of Science and Technology, and ICREA, E-08193 Barcelona, Spain
[32] Gran Sasso Science Institute (GSSI), I-67100 L'Aquila, Italy
[33] SUPA, University of Strathclyde, Glasgow G1 1XQ, UK
[34] Dipartimento di Scienze Matematiche, Informatiche e Fisiche, Università di Udine, I-33100 Udine, Italy
[35] INFN, Sezione di Trieste, I-34127 Trieste, Italy
[36] Embry-Riddle Aeronautical University, Prescott, AZ 86301, USA
[37] Artemis, Université Côte d'Azur, Observatoire de la Côte d'Azur, CNRS, F-06304 Nice, France
[38] GRAPPA, Anton Pannekoek Institute for Astronomy and Institute for High-Energy Physics, University of Amsterdam, Science Park 904, 1098 XH Amsterdam,
Netherlands
[39] National and Kapodistrian University of Athens, School of Science Building, 2nd floor, Panepistimiopolis, 15771 Ilissia, Greece
[40] INFN, Sezione di Perugia, I-06123 Perugia, Italy
[41] Università di Camerino, Dipartimento di Fisica, I-62032 Camerino, Italy
[42] American University, Washington, DC 20016, USA
[43] Earthquake Research Institute, The University of Tokyo, Bunkyo-ku, Tokyo 113-0032, Japan
[44] California State University Fullerton, Fullerton, CA 92831, USA
[45] Université de Paris, CNRS, Astroparticule et Cosmologie, F-75006 Paris, France
[46] Université Paris-Saclay, CNRS/IN2P3, IJCLab, 91405 Orsay, France
[47] European Gravitational Observatory (EGO), I-56021 Cascina, Pisa, Italy
[48] Georgia Institute of Technology, Atlanta, GA 30332, USA
[49] Department of Mathematics and Physics, Graduate School of Science and Technology, Hirosaki University, Hirosaki, Aomori 036-8561, Japan
[50] Columbia University, New York, NY 10027, USA
[51] University of Portsmouth, Portsmouth PO1 3FX, UK
[52] Kamioka Branch, National Astronomical Observatory of Japan (NAOJ), Kamioka-cho, Hida City, Gifu 506-1205, Japan
[53] The Graduate University for Advanced Studies (SOKENDAI), Mitaka City, Tokyo 181-8588, Japan
[54] Università degli Studi di Urbino "Carlo Bo," I-61029 Urbino, Italy
[55] INFN, Sezione di Firenze, I-50019 Sesto Fiorentino, Firenze, Italy
[56] LIGO Livingston Observatory, Livingston, LA 70754, USA
[57] INFN, Sezione di Roma, I-00185 Roma, Italy
[58] Université catholique de Louvain, B-1348 Louvain-la-Neuve, Belgium
[59] Nikhef, Science Park 105, 1098 XG Amsterdam, Netherlands
[60] King's College London, University of London, London WC2R 2LS, UK
[61] Korea Institute of Science and Technology Information, Daejeon 34141, Republic of Korea
[62] National Institute for Mathematical Sciences, Daejeon 34047, Republic of Korea
[63] Christopher Newport University, Newport News, VA 23606, USA
[64] School of High Energy Accelerator Science, The Graduate University for Advanced Studies (SOKENDAI), Tsukuba City, Ibaraki 305-0801, Japan
[65] Institute for Gravitational and Subatomic Physics (GRASP), Utrecht University, Princetonplein 1, 3584 CC Utrecht, Netherlands
[66] University of Oregon, Eugene, OR 97403, USA
[67] Syracuse University, Syracuse, NY 13244, USA
[68] Université de Liège, B-4000 Liège, Belgium
[69] Università degli Studi di Milano-Bicocca, I-20126 Milano, Italy
[70] INFN, Sezione di Milano-Bicocca, I-20126 Milano, Italy

[71] INAF, Osservatorio Astronomico di Brera sede di Merate, I-23807 Merate, Lecco, Italy
[72] LIGO Hanford Observatory, Richland, WA 99352, USA
[73] Dipartimento di Medicina, Chirurgia e Odontoiatria "Scuola Medica Salernitana,"Università di Salerno, I-84081 Baronissi, Salerno, Italy
[74] LIGO Laboratory, Massachusetts Institute of Technology, Cambridge, MA 02139, USA
[75] Wigner RCP, RMKI, H-1121 Budapest, Konkoly Thege Miklós út 29-33, Hungary
[76] University of Florida, Gainesville, FL 32611, USA
[77] Stanford University, Stanford, CA 94305, USA
[78] Università di Pisa, I-56127 Pisa, Italy
[79] Università di Perugia, I-06123 Perugia, Italy
[80] Università di Padova, Dipartimento di Fisica e Astronomia, I-35131 Padova, Italy
[81] INFN, Sezione di Padova, I-35131 Padova, Italy
[82] Bard College, Annandale-On-Hudson, NY 12504, USA
[83] Montana State University, Bozeman, MT 59717, USA
[84] Institute for Plasma Research, Bhat, Gandhinagar 382428, India
[85] Universiteit Gent, B-9000 Gent, Belgium
[86] Nicolaus Copernicus Astronomical Center, Polish Academy of Sciences, 00-716, Warsaw, Poland
[87] Dipartimento di Ingegneria, Università del Sannio, I-82100 Benevento, Italy
[88] OzGrav, University of Adelaide, Adelaide, South Australia 5005, Australia
[89] The University of Texas Rio Grande Valley, Brownsville, TX 78520, USA
[90] California State University, Los Angeles, Los Angeles, CA 90032, USA
[91] Departamento de Matemáticas, Universitat Autònoma de Barcelona, Edificio C Facultad de Ciencias 08193 Bellaterra (Barcelona), Spain
[92] INFN, Sezione di Genova, I-16146 Genova, Italy
[93] OzGrav, University of Western Australia, Crawley, Western Australia 6009, Australia
[94] RRCAT, Indore, Madhya Pradesh 452013, India
[95] Missouri University of Science and Technology, Rolla, MO 65409, USA
[96] Vrije Universiteit Amsterdam, 1081 HV Amsterdam, Netherlands
[97] Lomonosov Moscow State University, Moscow 119991, Russia
[98] Università di Trento, Dipartimento di Fisica, I-38123 Povo, Trento, Italy
[99] INFN, Trento Institute for Fundamental Physics and Applications, I-38123 Povo, Trento, Italy
[100] SUPA, University of the West of Scotland, Paisley PA1 2BE, UK
[101] Bar-Ilan University, Ramat Gan, 5290002, Israel
[102] Dipartimento di Fisica "E.R. Caianiello,"Università di Salerno, I-84084 Fisciano, Salerno, Italy
[103] INFN, Sezione di Napoli, Gruppo Collegato di Salerno, Complesso Universitario di Monte S. Angelo, I-80126 Napoli, Italy
[104] Università di Roma "La Sapienza," I-00185 Roma, Italy
[105] Univ Rennes, CNRS, Institut FOTON—UMR6082, F-3500 Rennes, France
[106] Indian Institute of Technology Bombay, Powai, Mumbai 400 076, India
[107] INFN, Laboratori Nazionali del Gran Sasso, I-67100 Assergi, Italy
[108] Laboratoire Kastler Brossel, Sorbonne Université, CNRS, ENS-Université PSL, Collège de France, F-75005 Paris, France
[109] Astronomical Observatory Warsaw University, 00-478 Warsaw, Poland
[110] University of Maryland, College Park, MD 20742, USA
[111] Max Planck Institute for Gravitational Physics (Albert Einstein Institute), D-14476 Potsdam, Germany
[112] L2IT, Laboratoire des 2 Infinis—Toulouse, Université de Toulouse, CNRS/IN2P3, UPS, F-31062 Toulouse Cedex 9, France
[113] Villanova University, Villanova, PA 19085, USA
[114] IGFAE, Universidade de Santiago de Compostela, Galicia 15782 Spain
[115] Stony Brook University, Stony Brook, NY 11794, USA
[116] Center for Computational Astrophysics, Flatiron Institute, New York, NY 10010, USA
[117] NASA Goddard Space Flight Center, Greenbelt, MD 20771, USA
[118] Dipartimento di Fisica, Università degli Studi di Genova, I-16146 Genova, Italy
[119] Department of Astronomy, Beijing Normal University, Beijing 100875, People's Republic of China
[120] OzGrav, University of Melbourne, Parkville, Victoria 3010, Australia
[121] Università degli Studi di Sassari, I-07100 Sassari, Italy
[122] INFN, Laboratori Nazionali del Sud, I-95125 Catania, Italy
[123] Università di Roma Tor Vergata, I-00133 Roma, Italy
[124] INFN, Sezione di Roma Tor Vergata, I-00133 Roma, Italy
[125] University of Sannio at Benevento, I-82100 Benevento, Italy
[126] INFN, Sezione di Napoli, I-80100 Napoli, Italy
[127] Departamento de Astronomía y Astrofísica, Universitat de València, E-46100 Burjassot, València, Spain
[128] Universität Hamburg, D-22761 Hamburg, Germany
[129] Rochester Institute of Technology, Rochester, NY 14623, USA
[130] National Tsing Hua University, Hsinchu City, 30013 Taiwan, People's Republic of China
[131] The Chinese University of Hong Kong, Shatin, NT, Hong Kong
[132] Department of Applied Physics, Fukuoka University, Jonan, Fukuoka City, Fukuoka 814-0180, Japan
[133] OzGrav, Charles Sturt University, Wagga Wagga, New South Wales 2678, Australia
[134] Department of Physics, Tamkang University, Danshui Dist., New Taipei City 25137, Taiwan
[135] Department of Physics and Institute of Astronomy, National Tsing Hua University, Hsinchu 30013, Taiwan
[136] Department of Physics, Center for High Energy and High Field Physics, National Central University, Zhongli District, Taoyuan City 32001, Taiwan
[137] CaRT, California Institute of Technology, Pasadena, CA 91125, USA
[138] Department of Physics, National Tsing Hua University, Hsinchu 30013, Taiwan
[139] Dipartimento di Ingegneria Industriale (DIIN), Università di Salerno, I-84084 Fisciano, Salerno, Italy
[140] Institute of Physics, Academia Sinica, Nankang, Taipei 11529, Taiwan
[141] Université Lyon, Université Claude Bernard Lyon 1, CNRS, IP2I Lyon/IN2P3, UMR 5822, F-69622 Villeurbanne, France
[142] INAF, Osservatorio Astronomico di Padova, I-35122 Padova, Italy
[143] OzGrav, Swinburne University of Technology, Hawthorn VIC 3122, Australia
[144] Université libre de Bruxelles, Avenue Franklin Roosevelt 50-1050 Bruxelles, Belgium

[145] IAC3–IEEC, Universitat de les Illes Balears, E-07122 Palma de Mallorca, Spain
[146] Université Libre de Bruxelles, Brussels 1050, Belgium
[147] Departamento de Matemáticas, Universitat de València, E-46100 Burjassot, València, Spain
[148] Texas Tech University, Lubbock, TX 79409, USA
[149] University of Minnesota, Minneapolis, MN 55455, USA
[150] The Pennsylvania State University, University Park, PA 16802, USA
[151] University of Rhode Island, Kingston, RI 02881, USA
[152] Bellevue College, Bellevue, WA 98007, USA
[153] Scuola Normale Superiore, Piazza dei Cavalieri, 7-56126 Pisa, Italy
[154] Eötvös University, Budapest 1117, Hungary
[155] Maastricht University, P.O. Box 616, 6200 MD Maastricht, Netherlands
[156] Chennai Mathematical Institute, Chennai 603103, India
[157] The University of Sheffield, Sheffield S10 2TN, UK
[158] Université Lyon, Université Claude Bernard Lyon 1, CNRS, Laboratoire des Matériaux Avancés (LMA), IP2I Lyon/IN2P3, UMR 5822, F-69622 Villeurbanne, France
[159] Dipartimento di Scienze Matematiche, Fisiche e Informatiche, Università di Parma, I-43124 Parma, Italy
[160] INFN, Sezione di Milano Bicocca, Gruppo Collegato di Parma, I-43124 Parma, Italy
[161] The University of Utah, Salt Lake City, UT 84112, USA
[162] Carleton College, Northfield, MN 55057, USA
[163] University of Zurich, Winterthurerstrasse 190, 8057 Zurich, Switzerland
[164] Perimeter Institute, Waterloo, ON N2L 2Y5, Canada
[165] Université de Strasbourg, CNRS, IPHC UMR 7178, F-67000 Strasbourg, France
[166] West Virginia University, Morgantown, WV 26506, USA
[167] University of Chicago, Chicago, IL 60637, USA
[168] Montclair State University, Montclair, NJ 07043, USA
[169] Colorado State University, Fort Collins, CO 80523, USA
[170] Institute for Nuclear Research, Bem t'er 18/c, H-4026 Debrecen, Hungary
[171] University of Texas, Austin, TX 78712, USA
[172] CNR-SPIN, c/o Università di Salerno, I-84084 Fisciano, Salerno, Italy
[173] Scuola di Ingegneria, Università della Basilicata, I-85100 Potenza, Italy
[174] Observatori Astronòmic, Universitat de València, E-46980 Paterna, València, Spain
[175] Centro de Física das Universidades do Minho e do Porto, Universidade do Minho, Campus de Gualtar, PT-4710-057 Braga, Portugal
[176] Department of Astronomy, The University of Tokyo, Mitaka City, Tokyo 181-8588, Japan
[177] Faculty of Engineering, Niigata University, Nishi-ku, Niigata City, Niigata 950-2181, Japan
[178] Department of Physics, Graduate School of Science, Osaka City University, Sumiyoshi-ku, Osaka City, Osaka 558-8585, Japan
[179] State Key Laboratory of Magnetic Resonance and Atomic and Molecular Physics, Innovation Academy for Precision Measurement Science and Technology (APM), Chinese Academy of Sciences, Xiao Hong Shan, Wuhan 430071, People's Republic of China
[180] University of Szeged, Dóm tér 9, Szeged 6720, Hungary
[181] Cornell University, Ithaca, NY 14850, USA
[182] University of British Columbia, Vancouver, BC V6T 1Z4, Canada
[183] INAF, Osservatorio Astronomico di Capodimonte, I-80131 Napoli, Italy
[184] The University of Mississippi, University, MS 38677, USA
[185] University of Michigan, Ann Arbor, MI 48109, USA
[186] Texas A&M University, College Station, TX 77843, USA
[187] Ulsan National Institute of Science and Technology, Ulsan 44919, Republic of Korea
[188] Shanghai Astronomical Observatory, Chinese Academy of Sciences, Shanghai 200030, People's Republic of China
[189] Institute for Cosmic Ray Research (ICRR), KAGRA Observatory, The University of Tokyo, Kashiwa City, Chiba 277-8582, Japan
[190] Faculty of Science, University of Toyama, Toyama City, Toyama 930-8555, Japan
[191] Institute for Cosmic Ray Research (ICRR), KAGRA Observatory, The University of Tokyo, Kamioka-cho, Hida City, Gifu 506-1205, Japan
[192] University of California, Berkeley, CA 94720, USA
[193] Maastricht University, 6200 MD, Maastricht, Netherlands
[194] Lancaster University, Lancaster LA1 4YW, UK
[195] College of Industrial Technology, Nihon University, Narashino City, Chiba 275-8575, Japan
[196] Institute of Astronomy, National Tsing Hua University, Hsinchu 30013, Taiwan
[197] Rutherford Appleton Laboratory, Didcot OX11 0DE, UK
[198] Department of Astronomy & Space Science, Chungnam National University, Yuseong-gu, Daejeon 34134, Republic of Korea
[199] Department of Physical Sciences, Aoyama Gakuin University, Sagamihara City, Kanagawa 252-5258, Japan
[200] Kavli Institute for Astronomy and Astrophysics, Peking University, Haidian District, Beijing 100871, People's Republic of China
[201] Aristotle University of Thessaloniki, University Campus, 54124 Thessaloniki, Greece
[202] Graduate School of Science and Engineering, University of Toyama, Toyama City, Toyama 930-8555, Japan
[203] Nambu Yoichiro Institute of Theoretical and Experimental Physics (NITEP), Osaka City University, Sumiyoshi-ku, Osaka City, Osaka 558-8585, Japan
[204] Directorate of Construction, Services & Estate Management, Mumbai 400094, India
[205] Vanderbilt University, Nashville, TN 37235, USA
[206] Universiteit Antwerpen, Prinsstraat 13, 2000 Antwerpen, Belgium
[207] University of Białystok, 15-424 Białystok, Poland
[208] Ewha Womans University, Seoul 03760, Republic of Korea
[209] National Astronomical Observatories, Chinese Academic of Sciences, Chaoyang District, Beijing, People's Republic of China
[210] School of Astronomy and Space Science, University of Chinese Academy of Sciences, Chaoyang District, Beijing, People's Republic of China
[211] University of Southampton, Southampton SO17 1BJ, UK
[212] Institute for Cosmic Ray Research (ICRR), The University of Tokyo, Kashiwa City, Chiba 277-8582, Japan
[213] Institute for High-Energy Physics, University of Amsterdam, Science Park 904, 1098 XH Amsterdam, Netherlands
[214] Chung-Ang University, Seoul 06974, Republic of Korea
[215] University of Washington Bothell, Bothell, WA 98011, USA
[216] Institute of Applied Physics, Nizhny Novgorod, 603950, Russia

[217] Inje University Gimhae, South Gyeongsang 50834, Republic of Korea
[218] Department of Physics, Myongji University, Yongin 17058, Republic of Korea
[219] Institute of Particle and Nuclear Studies (IPNS), High Energy Accelerator Research Organization (KEK), Tsukuba City, Ibaraki 305-0801, Japan
[220] School of Physics and Astronomy, Cardiff University, Cardiff CF24 3AA, UK
[221] Institute of Mathematics, Polish Academy of Sciences, 00656 Warsaw, Poland
[222] National Center for Nuclear Research, 05-400 Świerk-Otwock, Poland
[223] Instituto de Fisica Teorica, 28049 Madrid, Spain
[224] Department of Physics, Nagoya University, Chikusa-ku, Nagoya, Aichi 464-8602, Japan
[225] Université de Montréal/Polytechnique, Montreal, Quebec H3T 1J4, Canada
[226] Laboratoire Lagrange, Université Côte d'Azur, Observatoire Côte d'Azur, CNRS, F-06304 Nice, France
[227] Seoul National University, Seoul 08826, Republic of Korea
[228] Sungkyunkwan University, Seoul 03063, Republic of Korea
[229] NAVIER, École des Ponts, Univ Gustave Eiffel, CNRS, Marne-la-Vallée, France
[230] Università di Firenze, Sesto Fiorentino I-50019, Italy
[231] Department of Physics, National Cheng Kung University, Tainan City 701, Taiwan
[232] School of Physics and Technology, Wuhan University, Wuhan, Hubei, 430072, People's Republic of China
[233] National Center for High-performance computing, National Applied Research Laboratories, Hsinchu Science Park, Hsinchu City 30076, Taiwan
[234] Department of Physics, National Taiwan Normal University, Sec. 4, Taipei 116, Taiwan
[235] NASA Marshall Space Flight Center, Huntsville, AL 35811, USA
[236] INFN, Sezione di Roma Tre, I-00146 Roma, Italy
[237] ESPCI, CNRS, F-75005 Paris, France
[238] Kenyon College, Gambier, OH 43022, USA
[239] School of Physics Science and Engineering, Tongji University, Shanghai 200092, People's Republic of China
[240] Dipartimento di Fisica, Università di Trieste, I-34127 Trieste, Italy
[241] Institute for Photon Science and Technology, The University of Tokyo, Bunkyo-ku, Tokyo 113-8656, Japan
[242] Indian Institute of Technology Madras, Chennai 600036, India
[243] Saha Institute of Nuclear Physics, Bidhannagar, West Bengal 700064, India
[244] Institute of Space and Astronautical Science (JAXA), Chuo-ku, Sagamihara City, Kanagawa 252-0222, Japan
[245] Institut des Hautes Etudes Scientifiques, F-91440 Bures-sur-Yvette, France
[246] Faculty of Law, Ryukoku University, Fushimi-ku, Kyoto City, Kyoto 612-8577, Japan
[247] Indian Institute of Science Education and Research, Kolkata, Mohanpur, West Bengal 741252, India
[248] Department of Physics, University of Notre Dame, Notre Dame, IN 46556, USA
[249] Graduate School of Science and Technology, Niigata University, Nishi-ku, Niigata City, Niigata 950-2181, Japan
[250] Consiglio Nazionale delle Ricerche—Istituto dei Sistemi Complessi, Piazzale Aldo Moro 5, I-00185 Roma, Italy
[251] Korea Astronomy and Space Science Institute (KASI), Yuseong-gu, Daejeon 34055, Republic of Korea
[252] Hobart and William Smith Colleges, Geneva, NY 14456, USA
[253] International Institute of Physics, Universidade Federal do Rio Grande do Norte, Natal RN 59078-970, Brazil
[254] Museo Storico della Fisica e Centro Studi e Ricerche "Enrico Fermi," I-00184 Roma, Italy
[255] Dipartimento di Matematica e Fisica, Università degli Studi Roma Tre, I-00146 Roma, Italy
[256] University of Arizona, Tucson, AZ 85721, USA
[257] Università di Trento, Dipartimento di Matematica, I-38123 Povo, Trento, Italy
[258] University of California, Riverside, Riverside, CA 92521, USA
[259] University of Washington, Seattle, WA 98195, USA
[260] Indian Institute of Technology, Palaj, Gandhinagar, Gujarat 382355, India
[261] Department of Electronic Control Engineering, National Institute of Technology, Nagaoka College, Nagaoka City, Niigata 940-8532, Japan
[262] Departamento de Matemática da Universidade de Aveiro and Centre for Research and Development in Mathematics and Applications, Campus de Santiago, 3810-183 Aveiro, Portugal
[263] Marquette University, Milwaukee, WI 53233, USA
[264] Faculty of Science, Toho University, Funabashi City, Chiba 274-8510, Japan
[265] Graduate School of Science and Technology, Gunma University, Maebashi, Gunma 371-8510, Japan
[266] Institute for Quantum Studies, Chapman University, Orange, CA 92866, USA
[267] Accelerator Laboratory, High Energy Accelerator Research Organization (KEK), Tsukuba City, Ibaraki 305-0801, Japan
[268] Faculty of Information Science and Technology, Osaka Institute of Technology, Hirakata City, Osaka 573-0196, Japan
[269] INAF, Osservatorio Astrofisico di Arcetri, Largo E. Fermi 5, I-50125 Firenze, Italy
[270] Indian Institute of Technology Hyderabad, Sangareddy, Khandi, Telangana 502285, India
[271] Indian Institute of Science Education and Research, Pune, Maharashtra 411008, India
[272] Istituto di Astrofisica e Planetologia Spaziali di Roma, Via del Fosso del Cavaliere, 100, 00133 Roma RM, Italy
[273] Department of Space and Astronautical Science, The Graduate University for Advanced Studies (SOKENDAI), Sagamihara City, Kanagawa 252-5210, Japan
[274] Andrews University, Berrien Springs, MI 49104, USA
[275] Research Center for Space Science, Advanced Research Laboratories, Tokyo City University, Setagaya, Tokyo 158-0082, Japan
[276] Institute for Cosmic Ray Research (ICRR), Research Center for Cosmic Neutrinos (RCCN), The University of Tokyo, Kashiwa City, Chiba 277-8582, Japan
[277] Department of Physics, Kyoto University, Sakyou-ku, Kyoto City, Kyoto 606-8502, Japan
[278] Yukawa Institute for Theoretical Physics (YITP), Kyoto University, Sakyou-ku, Kyoto City, Kyoto 606-8502, Japan
[279] Dipartimento di Scienze Aziendali—Management and Innovation Systems (DISA-MIS), Università di Salerno, I-84084 Fisciano, Salerno, Italy
[280] Van Swinderen Institute for Particle Physics and Gravity, University of Groningen, Nijenborgh 4, 9747 AG Groningen, Netherlands
[281] Faculty of Science, Department of Physics, The Chinese University of Hong Kong, Shatin, N.T., Hong Kong
[282] Vrije Universiteit Brussel, Pleinlaan 2, 1050 Brussel, Belgium
[283] Applied Research Laboratory, High Energy Accelerator Research Organization (KEK), Tsukuba City, Ibaraki 305-0801, Japan
[284] Department of Communications Engineering, National Defense Academy of Japan, Yokosuka City, Kanagawa 239-8686, Japan
[285] Department of Physics, University of Florida, Gainesville, FL 32611, USA
[286] Department of Information and Management Systems Engineering, Nagaoka University of Technology, Nagaoka City, Niigata 940-2188, Japan
[287] Tata Institute of Fundamental Research, Mumbai 400005, India
[288] Eindhoven University of Technology, Postbus 513, 5600 MB Eindhoven, Netherlands
[289] Department of Physics and Astronomy, Sejong University, Gwangjin-gu, Seoul 143-747, Republic of Korea
[290] Concordia University Wisconsin, Mequon, WI 53097, USA
[291] Department of Electrophysics, National Yang Ming Chiao Tung University, Hsinchu, Taiwan

[292] Department of Physics, Rikkyo University, Toshima-ku, Tokyo 171-8501, Japan
[293] LIGO Laboratory, California Institute of Technology, Pasadena, CA 91125, USA

Abstract

Gravitational waves are expected to be produced from neutron star oscillations associated with magnetar giant flares and short bursts. We present the results of a search for short-duration (milliseconds to seconds) and long-duration ($\sim$100 s) transient gravitational waves from 13 magnetar short bursts observed during Advanced LIGO, Advanced Virgo, and KAGRA's third observation run. These 13 bursts come from two magnetars, SGR 1935 +2154 and Swift J1818.0−1607. We also include three other electromagnetic burst events detected by Fermi-GBM which were identified as likely coming from one or more magnetars, but they have no association with a known magnetar. No magnetar giant flares were detected during the analysis period. We find no evidence of gravitational waves associated with any of these 16 bursts. We place upper limits on the rms of the integrated incident gravitational-wave strain that reach $3.6 \times 10^{-23}/\sqrt{\mathrm{Hz}}$ at 100 Hz for the short-duration search and $1.1 \times 10^{-22}/\sqrt{\mathrm{Hz}}$ at 450 Hz for the long-duration search. For a ringdown signal at 1590 Hz targeted by the short-duration search the limit is set to $2.3 \times 10^{-22}/\sqrt{\mathrm{Hz}}$. Using the estimated distance to each magnetar, we derive upper limits on the emitted gravitational-wave energy of 1.5×10^{44} erg (1.0×10^{44} erg) for SGR 1935+2154 and 9.4×10^{43} erg (1.3×10^{44} erg) for Swift J1818.0−1607, for the short-duration (long-duration) search. Assuming isotropic emission of electromagnetic radiation of the burst fluences, we constrain the ratio of gravitational-wave energy to electromagnetic energy for bursts from SGR 1935+2154 with the available fluence information. The lowest of these ratios is 4.5×10^3.

Unified Astronomy Thesaurus concepts: Magnetars (992); Gravitational waves (678); X-ray bursts (1814); Stellar oscillations (1617)

Supporting material: machine-readable tables

1. Introduction

Magnetars—highly magnetized neutron stars—exhibit intermittent bursts of hard X-rays and soft gamma-rays with typical peak luminosities $\lesssim 10^{43}$ erg s^{-1} (see Kaspi & Beloborodov 2017, for a review). Galactic (Evans et al. 1980; Hurley et al. 1999, 2005; Mereghetti et al. 2005; Boggs et al. 2007) and extragalactic (Mazets et al. 2008; Abadie et al. 2012; Burns et al. 2021; Svinkin et al. 2021) giant flares have peak luminosities up to five orders of magnitude larger. Although the mechanisms that cause these bursts and giant flares are not well understood, many models predict accompanying gravitational-wave emission from excited core and/or crust oscillations (Ioka 2001; Ciolfi et al. 2011; Corsi & Owen 2011; Kashiyama & Ioka 2011; Zink et al. 2012). This hypothesis is enhanced by the identification of quasiperiodic oscillations (QPOs) in the tails of giant flares (Barat et al. 1983; Israel et al. 2005; Strohmayer & Watts 2005, 2006; Watts & Strohmayer 2006), and possibly fainter bursts (Huppenkothen et al. 2014a, 2014b), which have been attributed to various oscillations of the stellar crust and core (e.g., Duncan 1998; Messios et al. 2001; Piro 2005; Glampedakis et al. 2006; Strohmayer & Watts 2006; Levin 2007; Colaiuda & Kokkotas 2011; Glampedakis & Jones 2014).

Initial estimates for the potential gravitational-wave emission from giant flares were optimistic that the fundamental oscillation mode (*f*-mode) of magnetars could be excited by the catastrophic rearrangement of the star's interior magnetic field. These *f*-modes are excited at frequencies between $\sim$1 and 3 kHz, and could potentially emit up to $\sim$10^{49} erg (Ioka 2001; Corsi & Owen 2011) for $\sim$100 ms (Lindblom & Detweiler 1983; McDermott et al. 1988; Wen et al. 2019), making them detectable with the Advanced LIGO (Aasi et al. 2015), Advanced Virgo (Acernese et al. 2015), and KAGRA (Akutsu et al. 2019, 2021) gravitational-wave observatories (Abbott et al. 2018). Detailed calculations of the rearrangement of the neutron star's magnetic field using analytic calculations (Levin & van Hoven 2011) and numerical relativity simulations (Ciolfi et al. 2011; Ciolfi & Rezzolla 2012; Zink et al. 2012; Tsokaros et al. 2021) yield more realistic estimates for the gravitational-wave energy emitted in the *f*-mode during these events. These models suggest that gravitational waves associated with Galactic magnetar flares are not observable with the current generation of observatories, but instead require the sensitivity of at least third-generation observatories such as the Einstein Telescope (Punturo et al. 2010) or Cosmic Explorer (Reitze et al. 2019; Evans et al. 2021), or dedicated kilohertz facilities such as the proposed NEMO observatory (Ackley et al. 2020).

Other oscillation modes in the star, which are generally longer lived and at lower frequencies than the *f*-mode, may be excited. These include buoyancy modes (*g*-modes) and Alfvén modes where the magnetic field provides the oscillation restoring force. The latter of these modes has been suggested as potential long-lived gravitational-wave sources from magnetar giant flares (Kashiyama & Ioka 2011; Zink et al. 2012), with the resonant frequency correlated to the initial rise time of the magnetar giant flare (Hurley et al. 1999, 2005; Mazets et al. 2008). The damping time and mode excitation amplitude of these modes are largely unknown, making them interesting candidates for longer-lived gravitational-wave signals.

Only one Galactic giant flare has been observed coincident with a LIGO–Virgo observing run: the 2004 giant flare from SGR 1806−20. Upper limits on the gravitational-wave energy associated with the burst were determined to be between $\sim$10^{46} and 10^{52} erg, depending on the assumed waveform model

---

[294] Deceased, 2020 August.
[295] Deceased, 2021 April.

Table 1
List of Magnetar Short Bursts Considered for this Search from the Interplanetary Network Master Burst List (Hurley 2021), and the Available Gravitational-wave Detectors: LHO (H), LLO (L), and Virgo (V)

Burst	Source	Date	Time (UTC)	Detectors	$E_{\mathrm{EM}}^{\mathrm{iso}}$(erg)	GCN Circulars
2651	SGR 1935+2154	2019 Nov 4	01:54:37	H V[a]	⋯	26169
2652	SGR 1935+2154	2019 Nov 4	02:53:31	H V	1.4×10^{39}	26163, 26151
2653	SGR 1935+2154	2019 Nov 4	04:26:55	H L V	1.1×10^{39}	26163
2654	SGR 1935+2154	2019 Nov 4	06:34:00	H L V	⋯	26153
2655	SGR 1935+2154	2019 Nov 4	09:17:53	H L	5.7×10^{39}	26163, 26154
2656	SGR 1935+2154	2019 Nov 4	10:44:26	H L	2.2×10^{40}	26242, 26163, 26158, 26157
2657	SGR 1935+2154	2019 Nov 4	12:38:38	H L V	2.7×10^{39}	26163
2660	SGR 1935+2154	2019 Nov 4	15:36:47	H V	1.2×10^{39}	⋯
2661	SGR 1935+2154	2019 Nov 4	20:29:39	H V	1.3×10^{39}	26165, 26166
2665	SGR 1935+2154	2019 Nov 5	06:11:08	H V	7.8×10^{40}	26242
2668	SGR 1935+2154	2019 Nov 15	20:48:41	L V	7.7×10^{38}	⋯
2669	⋯	2020 Feb 3	03:17:11	H L V	⋯	26980
2670	⋯	2020 Feb 3	03:44:03	H L V	⋯	26969, 26980
2671	⋯	2020 Feb 3	20:39:37	H L V	⋯	26980
2673	Swift J1818.0−1607	2020 Feb 28	22:19:32	L V	⋯	⋯
2674	Swift J1818.0−1607	2020 Mar 12	21:16:47	H L V	⋯	27373

Notes. Three electromagnetic bursts (2669, 2670, and 2671) were not identified with a source and are thought to likely come from one or more magnetar(s), as reported in GCN Circular 26980 (Lesage 2020) and in the Fermi-GBM (Meegan et al. 2009) onboard Trigger Catalog, available online (https://heasarc.gsfc.nasa.gov/W3Browse/fermi/fermigtrig.html). The isotropic electromagnetic energy ($E_{\mathrm{EM}}^{\mathrm{iso}}$) is estimated from the fluence given in Lin et al. (2020) assuming a distance of 9.0 kpc for SGR 1935+2154. Distances to these sources with uncertainties (Olausen & Kaspi 2014; the McGill Online Magnetar Catalog is available at https://www.physics.mcgill.ca/p̄ulsar/magnetar/main.html) are 9.0 ± 2.5 kpc for SGR 1935+2154 (Zhong et al. 2020), 4.8 to 8.1 kpc for Swift J1818.0−1607 (Karuppusamy et al. 2020), and 3.8 ± 0.5 kpc for 1 RXS J170849 (Durant & van Kerkwijk 2006).
[a] Burst 2651 occurred 87 s before Virgo was in observation mode.

(Kalmus et al. 2007; Abbott et al. 2008a; Kalmus 2009). A stacked search was performed on a series of bursts from the same magnetar occurring in the same minute, reducing the above upper limits to $\sim 10^{45}$ and 10^{50} erg assuming the same f-mode frequency and damping time for each burst (Abbott et al. 2009; Kalmus 2009; Kalmus et al. 2009). Further searches for f-modes in 1279 bursts from six different magnetars yielded upper limits between $\sim 10^{44}$ and 10^{47} erg (Abadie et al. 2011), while the first search for f-modes in the advanced era of gravitational-wave interferometers yielded comparable upper limits for four bursts from two magnetars (Abbott et al. 2019; Schale 2019). These energy upper limits are in the range of possible gravitational-wave energies given the most optimistic predictions (Ioka 2001; Corsi & Owen 2011).

Longer-duration searches initially targeted the QPO frequencies in the tail of the giant flare of SGR 1806−20, with upper limits of various modes at $\lesssim 10^{46}$ erg (Abbott et al. 2007; Matone & Márka 2007), comparable to the electromagnetic energy emitted from the giant flare. A study was performed on a method to detect gravitational waves targeting repeated QPOs (Murphy et al. 2013). A search for long-duration gravitational waves from four magnetar bursts was performed using LIGO's sixth science run (S6) data (Quitzow-James 2016; Quitzow-James et al. 2017). The best upper limits from magnetar bursts come from recent observations in the Advanced LIGO–Virgo

second observing run (O2), with gravitational-wave energies constrained to less than $\sim 10^{44}$–10^{48} erg, again depending on the signal model, frequency, and damping time (Abbott et al. 2019; Schale 2019). We previously placed limits on gravitational-wave emission from purported extragalactic magnetar giant flares (Abbott et al. 2008b; Abadie et al. 2012),[296] with long-duration searches constraining the gravitational-wave energy emitted to between $\sim 10^{49}$ and 10^{52} erg for four different giant flares (Macquet et al. 2021).

In this paper, we report on a search for gravitational waves coincident with 13 magnetar short bursts from SGR 1935 +2154, Swift J1818.0−1607, and three electromagnetic bursts from an unidentified source (or sources) during the LIGO–Virgo–KAGRA third observing run (O3). Targeted gravitational-wave searches associated with magnetar bursts can broadly be split in two categories following theoretical predictions of short-duration and long-duration signals. For each magnetar burst we carry out a short-duration and long-duration search. We find no evidence of gravitational-wave signals and hence place upper limits on the gravitational-wave strain and energy for each burst considered.

---

[296] GRB 070222, included in a search targeting gamma-ray bursts (Aasi et al. 2014), was later determined to likely be an extragalactic magnetar giant flare (Burns et al. 2021; Macquet et al. 2021).

Table 2
On-source Window, Off-source Window, and Frequency Range of Searches Performed

Search	Pipeline	On-source Window (s)	On-source Interval (s)	Off-source Window (s)	Frequency Range (Hz)
Centered on source	X-pipeline	8	$[-4, +4]$	10,800	50–4000
Delayed on source	X-pipeline	500	$[+4, +504]$	10,800	50–4000
Long duration	STAMP	1604	$[-4, +1600]$	59,040	24–2500

Note. The on-source interval is centered around the magnetar burst time.

2. Methodology

The O3 observing run extended from 2019 April 1 to 2020 March 27, with three gravitational-wave detectors taking data: LIGO Hanford Observatory (LHO), LIGO Livingston Observatory (LLO), and Virgo, all of which had been upgraded so that the binary neutron star inspiral ranges increased by a factor of 1.53 for LLO, 1.64 for LHO, and 1.73 for Virgo (Davis et al. 2021) compared to their performance during O2. For each detector, several data quality checks are performed to mitigate terrestrial noise (Davis et al. 2021). In addition, multidetector analyses are used to mitigate nonastrophysical features present in the data. In 2020 January, a new technique was implemented to mitigate the impact in LIGO detectors of scattered light, a transient noise coupled with ground motion. Data available for bursts that occurred in February and March show a lower transient noise rate.

The list of magnetar short bursts and giant flares from Hurley (2021) provides the source object and observation time for each burst. In both the long-duration and short-duration searches, we describe the data in which we look for a signal as the "on-source" window, while the time around this composing the background as the "off-source" window. Analysis requirements include at least two gravitational-wave detectors in observation mode, sufficiently good data quality, and sufficient data available in the burst's on-source window. Several bursts did not meet the two-detector criterion (one detector available for bursts 2651, 2658, 2659, and 2667 in Hurley 2021; and none for 2662, 2663, and 2664), had poor data quality (2650 and 2672), or had very little data available in the on-source window (2650). Considering these requirements, 12 magnetar short bursts from known sources and three electromagnetic bursts thought to likely be magnetar short bursts from an unknown source or sources occurred when at least two detectors were in observation mode with sufficiently good data quality and are included in this search. In addition, although burst 2651 occurred when LHO was in observation mode and 87 s before Virgo was in observation mode (LLO was not taking data), data were available for most of the long-duration search on-source window, thus the burst was analyzed by the long-duration search only. 11 of the short bursts were from SGR 1935+2154 (Cummings et al. 2014), a magnetar that emitted a fast radio burst in 2020 April (Kirsten et al. 2020), and two of the short bursts were from Swift J1818.0−1607, a magnetar discovered in 2020 (Evans et al. 2020).

The source or sources of the remaining three electromagnetic bursts, detected by Fermi-GBM (Meegan et al. 2009), are unknown as they have very poor sky localization. These three electromagnetic bursts were accompanied by a fourth burst which did not meet the two-detector condition necessary for our analysis, but all four of these bursts occurred in a 33 hr window of time between 2020 February 3 and February 4. Because of their temporal proximity, we search for a signal

Table 3
False Alarm Statistic for the Most Significant Cluster Found for Each Burst by All Searches

Burst	Long-duration FBS	Centered (8 s) p-value	Delayed (500 s) p-value
2651	9.1×10^{-1}	…	…
2652	2.1×10^{-1}	1.0	4.1×10^{-1}
2653	7.7×10^{-1}	1.8×10^{-2}	3.5×10^{-3}
2654	8.5×10^{-1}	9.9×10^{-2}	6.6×10^{-1}
2655	7.8×10^{-1}	1.0	7.3×10^{-1}
2656	9.7×10^{-1}	8.6×10^{-3}	5.2×10^{-1}
2657	1.6×10^{-1}	6.7×10^{-2}	4.8×10^{-1}
2660	2.2×10^{-2}	4.8×10^{-1}	4.9×10^{-1}
2661	9.0×10^{-1}	1.9×10^{-1}	7.4×10^{-1}
2665	8.2×10^{-1}	…	…
2668	9.9×10^{-1}	1.0	4.3×10^{-1}
2669	…	1.0	6.3×10^{-1}
2670	…	2.9×10^{-1}	7.8×10^{-1}
2671	…	3.4×10^{-1}	…
2673	6.8×10^{-1}	1.0	4.8×10^{-1}
2674	5.9×10^{-1}	1.0	5.0×10^{-2}

Note. FBS is reported for the long-duration search, and the p-value for the short-duration searches. A p-value of 1 indicates that there were no clusters in the on-source window that survive the cluster selection process. Table entries of "…" indicate that no value is recorded, because no search was run. Bursts 2669–2671 are from the magnetar with no identified source, and the long-duration search was not conducted on these. Bursts 2651 and 2665 are missing segments of data from the on-source window such that the short-duration searches could not run, and burst 2671 has data missing in the delayed on-source window such that the delayed on-source search could not be run.

(This table is available in machine-readable form.)

assuming that they were emitted by the same magnetar. Only two known Galactic magnetars are in the 3σ sky position error region of all four electromagnetic bursts. In order to run a directional search and obtain the upper limits, we consider the source of these bursts to be 1 RXS J170849 at 3.8 kpc (Durant & van Kerkwijk 2006), and note that the directional sensitivity of the detector network changes very little between neighboring sky positions. The sources, times, active detectors, and the isotropic electromagnetic energy ($E_{\rm EM}^{\rm iso}$) of each burst included in this search are listed in Table 1; fluence information for some of the bursts from SGR 1935+2154 were obtained from Lin et al. (2020) and used to estimate $E_{\rm EM}^{\rm iso}$.
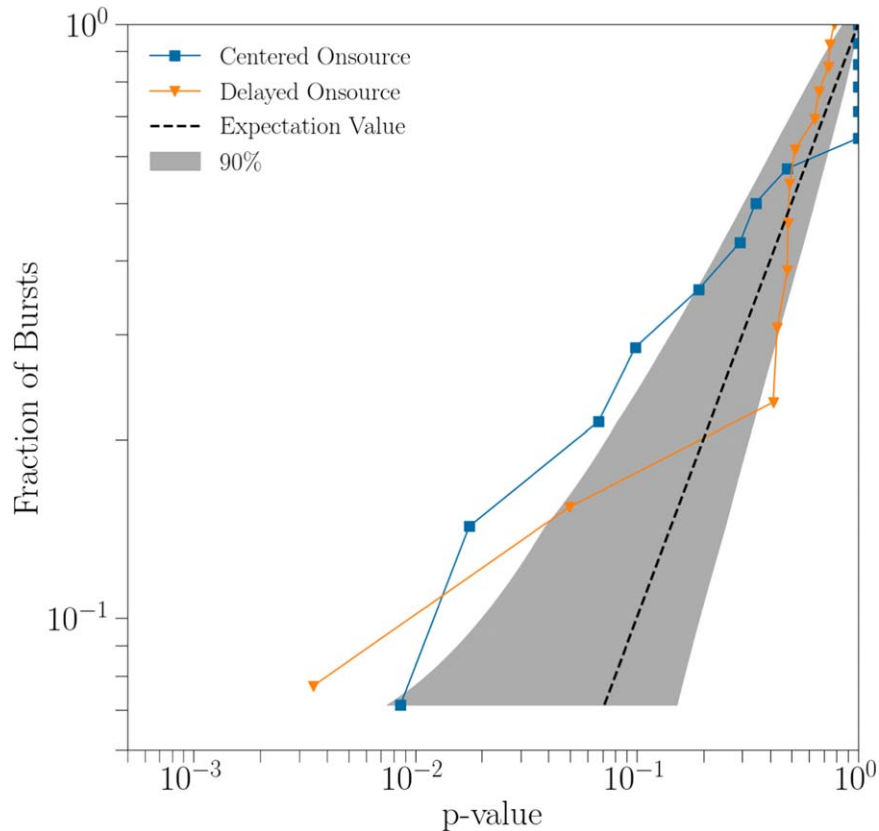
Figure 1. Cumulative distribution of the *p*-values of the most significant clusters found by the short-duration searches. The expectation value and 90% confidence interval are calculated numerically as in Abbott et al. (2023); the expectation value is calculated assuming a uniform distribution of *p*-values (given by the null hypothesis), with each point having a 90% probability of landing in the shaded region. The lowest *p*-value in the delayed on-source search is 3.5×10^{-3} from burst 2653, and is determined to be most likely an instrumental artifact through arguments invoking both astrophysics and the characteristics of the detector. Several centered on-source search clusters fall outside of the 90% confidence interval, which is not unlikely given how few data points there are, and many of them have properties inconsistent with what one would expect from an astrophysical source. Although the most significant of these, which appears in burst 2656, has a *p*-value (8.6×10^{-3}) and a peak frequency (1577 Hz) which are consistent with expectations for an *f*-mode, we provide arguments for why this is not the case in Section 3.1.
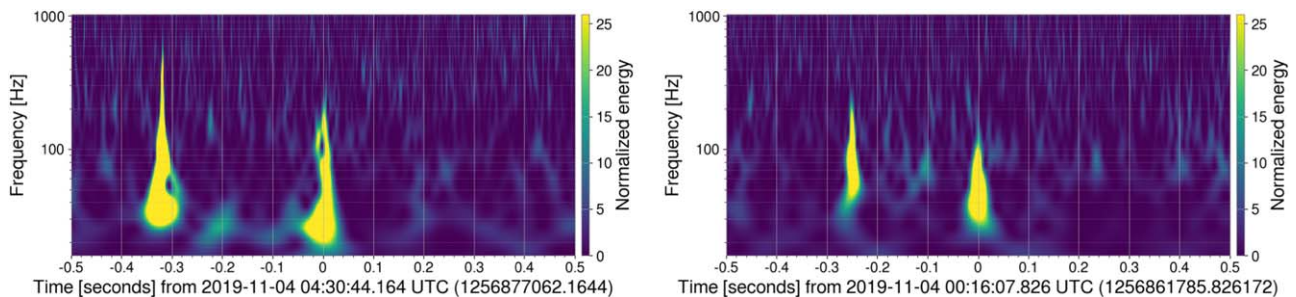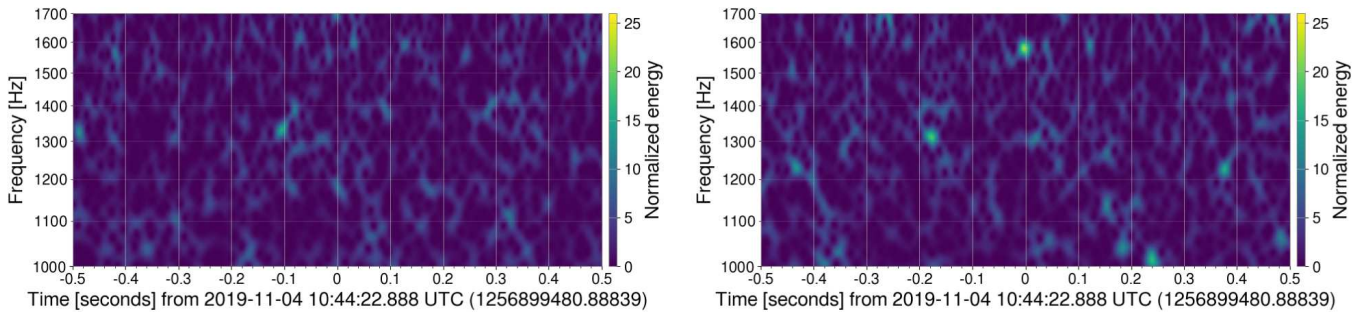

Figure 2. Spectrograms of the LHO data (left) at the time of the most significant cluster found in the on-source window of burst 2653, and an instrumental artifact appearing also in the LHO data (right). The time separation between these two events is $\sim$15,277 s, which is larger than the size of the background window in our analysis, and therefore the instrumental artifact was not included in the background. These two spectrograms display very similar structure, with similar double short-duration transients separated in both cases by $\sim$0.3 s. Several instrumental artifacts of this nature are found by Omicron (Robinet et al. 2020) within the day of burst 2653. The second most significant cluster in the same delayed on-source analysis of burst 2653 also has this same double-peaked structure.

We follow Abbott et al. (2019) to search for short-duration signals (as potentially emitted by *f*-modes) and long-duration signals (such as might accompany an observed QPO). Each search combines the data from two (or more when available in the case of the short-duration search) detectors into a time–frequency map and then forms groups of pixels, called clusters, to search for gravitational-wave signals. The three electromagnetic bursts without a known source are only analyzed with the short-duration search. The searches are described in the following sections.

2.1. Short-duration Search

The search for short-duration transient gravitational waves (milliseconds to seconds) is motivated by a potential signal associated with *f*-mode oscillations in the magnetar's core. Because the frequencies of the expected gravitational-wave signals can be as high as several kilohertz (Wen et al. 2019; Ho et al. 2020), the search ranges in frequency from 50 to 4000 Hz, extending to higher frequencies than the other unmodeled searches (most notably LIGO–Virgo–KAGRA's burst searches

Figure 3. Spectrograms of the LHO (left) and LLO (right) data around the time of the most significant cluster found by the centered-window short-duration search of burst 2656. Even though the cluster is only barely visible in the LLO data, these spectrograms show that the ambient noise in each detector is in a normal state around the time of the flare.
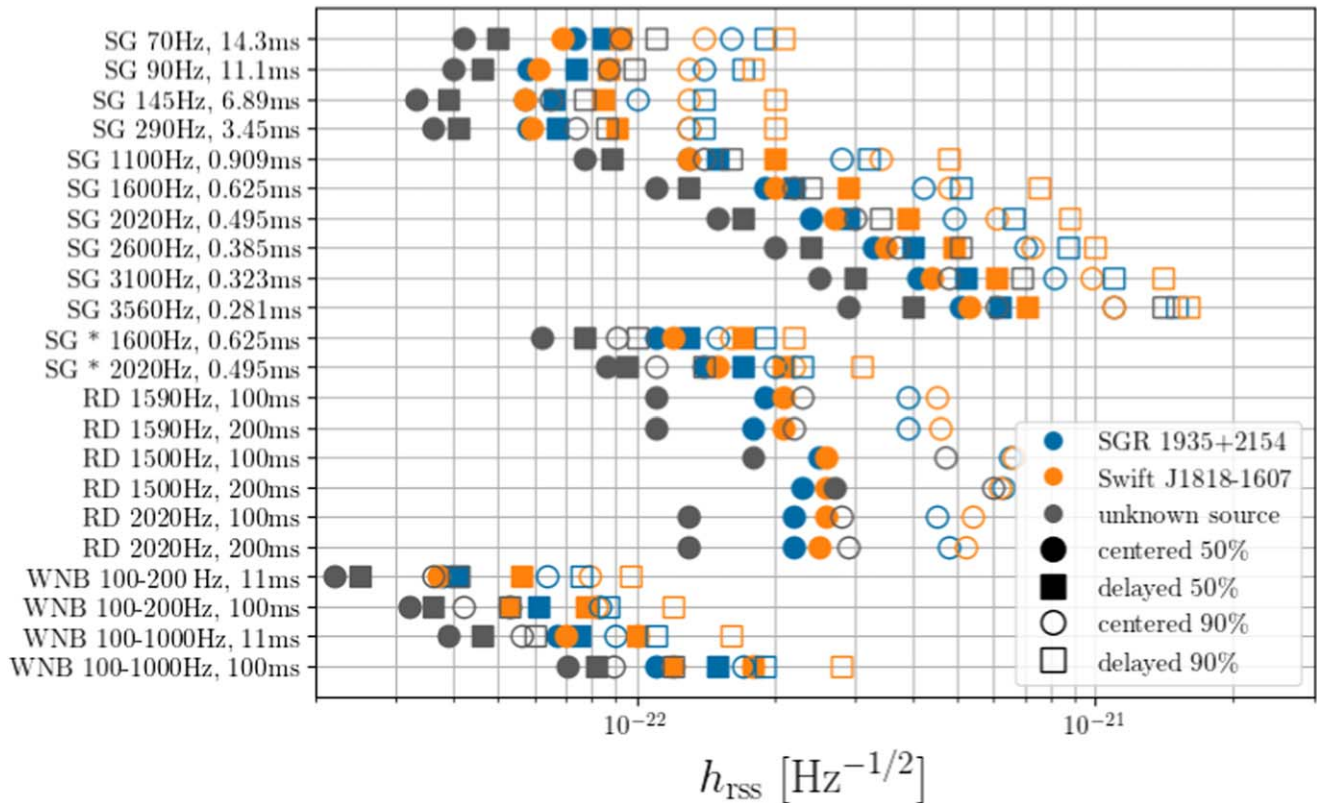
Figure 4. For each injection, we display the $h_{\rm rss}^{50\%}$ and $h_{\rm rss}^{90\%}$ values as measured by the most sensitive burst from each source in the short-duration search. The $h_{\rm rss}^{50\%}$ values are marked by filled-in shapes, and the $h_{\rm rss}^{90\%}$ values are not filled in. The vertical axis notes the waveform, where "SG" means sine-Gaussian and "RD" means ringdown. The frequency and duration of each injection are given as well. All of the sine-Gaussian and ringdown waveforms are eliptically polarized except for the ones denoted by "*," which are circularly polarized. The numerical values of $h_{\rm rss}^{50\%}$ can be found in Tables 6–8, while the numerical values of $h_{\rm rss}^{90\%}$ can be found in Tables 9–11.

associated with gamma-ray bursts, Abbott et al. 2021, 2022; and fast radio bursts, Abbott et al. 2023).

We analyze the data using X-pipeline: an unmodeled, coherent search pipeline (Sutton et al. 2010; Was et al. 2012). The X-pipeline algorithm coherently combines the data from each detector in the network to produce a multiresolution time–frequency map displaying the energy in each pixel. The brightest 1% of these pixels are then selected, and neighboring bright pixels are combined into clusters, which are then assigned a ranking statistic. A large fraction of background clusters are rejected by vetos built from the coherent and incoherent power across the detector network. Other details on the parameters of the short-duration search are summarized in Appendix A.

The search for short-duration gravitational waves is comprised of two components: an 8 s on-source window centered on the magnetar burst time (a "centered" on-source window) to optimize sensitivity when gravitational-wave emission is most probable, and a 500 s on-source window beginning just after the centered on-source window (a "delayed" on-source window). The longer delayed on-source window is intended to search for short-duration signals emitted during the time following the burst, analogous to the QPOs that have been observed in some giant flares. For each on-source window, we calculate the significance of clusters using 3 hr of data taken symmetrically about the burst time with a gap of 16 s before and after the on-source window.

Table 4
Values of $h_{rss}^{90\%}$ and $E_{GW}^{90\%}$ for the Centered On-source Short-duration Search for Each Burst and for Two Types of Waveforms that Best Model the Gravitational Wave One Would Expect in Conjuncture with an f-mode: the Elliptically Polarized 1600 Hz sine-Gaussian Waveform and 100 ms Ringdown Waveform at Central Frequency 1590 Hz

Burst	Source	Ringdown			Sine-Gaussian		
		$h_{rss}^{90\%}$ (Hz$^{-1/2}$)	$E_{GW}^{90\%}$ (erg)	$\dfrac{E_{GW}^{90\%}}{E_{EM}^{iso}}$	$h_{rss}^{90\%}$ (Hz$^{-1/2}$)	$E_{GW}^{90\%}$ (erg)	$\dfrac{E_{GW}^{90\%}}{E_{M}^{ISO}}$
2652	SGR 1935+2154	1.2×10^{-21}	4.2×10^{48}	3.0×10^{9}	1.3×10^{-21}	5.4×10^{48}	3.8×10^{9}
2653	SGR 1935+2154	5.2×10^{-22}	8.3×10^{47}	7.3×10^{8}	5.5×10^{-22}	9.4×10^{47}	8.3×10^{8}
2654	SGR 1935+2154	1.0×10^{-21}	3.1×10^{48}	...	9.9×10^{-22}	3.1×10^{48}	...
2655	SGR 1935+2154	3.9×10^{-22}	4.7×10^{47}	8.2×10^{7}	4.2×10^{-22}	5.5×10^{47}	9.6×10^{7}
2656	SGR 1935+2154	4.6×10^{-22}	6.7×10^{47}	3.0×10^{7}	4.5×10^{-22}	6.3×10^{47}	2.8×10^{7}
2657	SGR 1935+2154	4.9×10^{-22}	7.5×10^{47}	2.7×10^{8}	5.2×10^{-22}	8.4×10^{47}	3.1×10^{8}
2660	SGR 1935+2154	1.1×10^{-21}	3.6×10^{48}	3.0×10^{9}	8.8×10^{-22}	2.4×10^{48}	2.0×10^{9}
2661	SGR 1935+2154	7.4×10^{-22}	1.7×10^{48}	1.3×10^{9}	7.8×10^{-22}	1.9×10^{48}	1.4×10^{9}
2668	SGR 1935+2154	6.8×10^{-22}	1.4×10^{48}	1.9×10^{9}	6.5×10^{-22}	1.3×10^{48}	1.8×10^{9}
2669	unknown	2.5×10^{-22}	3.5×10^{46}	...	2.2×10^{-22}	2.6×10^{46}	...
2670	unknown	2.3×10^{-22}	3.0×10^{46}	...	2.2×10^{-22}	2.8×10^{46}	...
2671	unknown	4.1×10^{-22}	9.3×10^{46}	...	4.2×10^{-22}	9.7×10^{46}	...
2673	Swift J1818.0−1607	7.0×10^{-22}	1.2×10^{48}	...	7.3×10^{-22}	1.4×10^{48}	...
2674	Swift J1818.0−1607	4.5×10^{-22}	5.1×10^{47}	...	4.8×10^{-22}	5.9×10^{47}	...

Note. We calculate the energies using the source distances given in the caption of Table 1, and conservatively assuming a distance of 8.1 kpc for Swift J1818.0–1607. Because the gravitational-wave energy is proportional to the distance squared, the $E_{GW}^{90\%}$ upper limits pertaining to Swift J1818.0–1607 could scale by a factor as low as 0.35 if the source is at its nearest distance of 4.8 kpc. The burst numbers are consistent with those used in the catalog: http://www.ssl.berkeley.edu/ipn3/sgrlist.txt.

(This table is available in machine-readable form.)

Since the delayed on-source window starts just after the end of the centered on-source window and has a 500 s duration, it overlaps the off-source window for the centered on-source search. This introduces the possibility of a signal detected in the delayed on-source window being included in the background of the centered on-source window. We mitigate this possibility by examining the results of the delayed on-source window and verifying the absence of a signal before viewing the results of the centered on-source window. A summary of the pipeline, time window, and frequency range for the short-duration searches (and long-duration search) is reported in Table 2.

2.2. Long-duration Search

Following previous searches (Quitzow-James 2016; Quitzow-James et al. 2017; Abbott et al. 2019), we use the Stochastic Transient Analysis Multidetector Pipeline (STAMP; Thrane et al. 2011) to analyze data for the long-duration search. STAMP builds signal-to-noise ratio (S/N) time–frequency maps using the cross-power between two detectors. We then use STAMP's seedless clustering algorithm, which generates clusters with quadratic Bézier curves (Thrane & Coughlin 2013), to search for long-duration transient gravitational-wave signals. Restricting the variation of the clusters in frequency to a maximum of 10% allows us to target nearly monochromatic gravitational-wave signals potentially emitted from the mechanisms responsible for QPOs while reducing computational resources (Abbott et al. 2019). Clusters are ranked according to their S/N, defined as the sum of the S/N of the pixels that compose the cluster (Thrane & Coughlin 2013).

The on-source window starts 4 s before the burst time and ends 1600 s after, for 1604 s in total. Additional details are provided in Appendix B and in Thrane et al. (2011). The frequency range is 24–2500 Hz, limited by seismic noise at low frequencies, and going to just above the QPO's highest

frequency observed in the tail of the 2004 giant flare (Mereghetti et al. 2005). Data from LHO and LLO are used when available, with data from Virgo used for bursts that also have data from either LHO or LLO (see Table 1 for the available detectors for each burst).

The background for each burst is estimated using 59,040 s of off-source data as close as possible to the burst's on-source window while excluding the on-source windows of all of the other bursts. These data are broken up into 36 off-source analysis windows. We combine the data from one detector from each of these analysis windows with the data from the other detector from every other analysis window to create 1260 ($36^2 - 36$) S/N time–frequency maps (which we will refer to as background segments) in order to produce a background cluster distribution for each burst.

3. Results

The results of the short-duration and long-duration searches for each burst are presented in the following sections. Clusters found in the on-source windows of the short-duration search are ranked by their p-value, which is the probability of having a cluster of such significance in the on-source window under the null hypothesis. They are calculated considering the clusters in the background with a ranking statistic larger than the on-source cluster. Similarly we characterize the significance of the on-source clusters of the long-duration search with the fraction of background segments (FBS) as

$$\text{FBS} = N_{\geqslant}/N_{\text{Total}}, \qquad (1)$$

where $N_{\geqslant}$ is the number of segments in the respective burst's background whose loudest cluster has an S/N greater than or equal to the on-source cluster's S/N, and N_{Total} is the total number of segments in that background. The p-value in the short-duration search is found similarly to Equation (1), but where $N_{\geqslant}$ and N_{Total} include all clusters in the background with
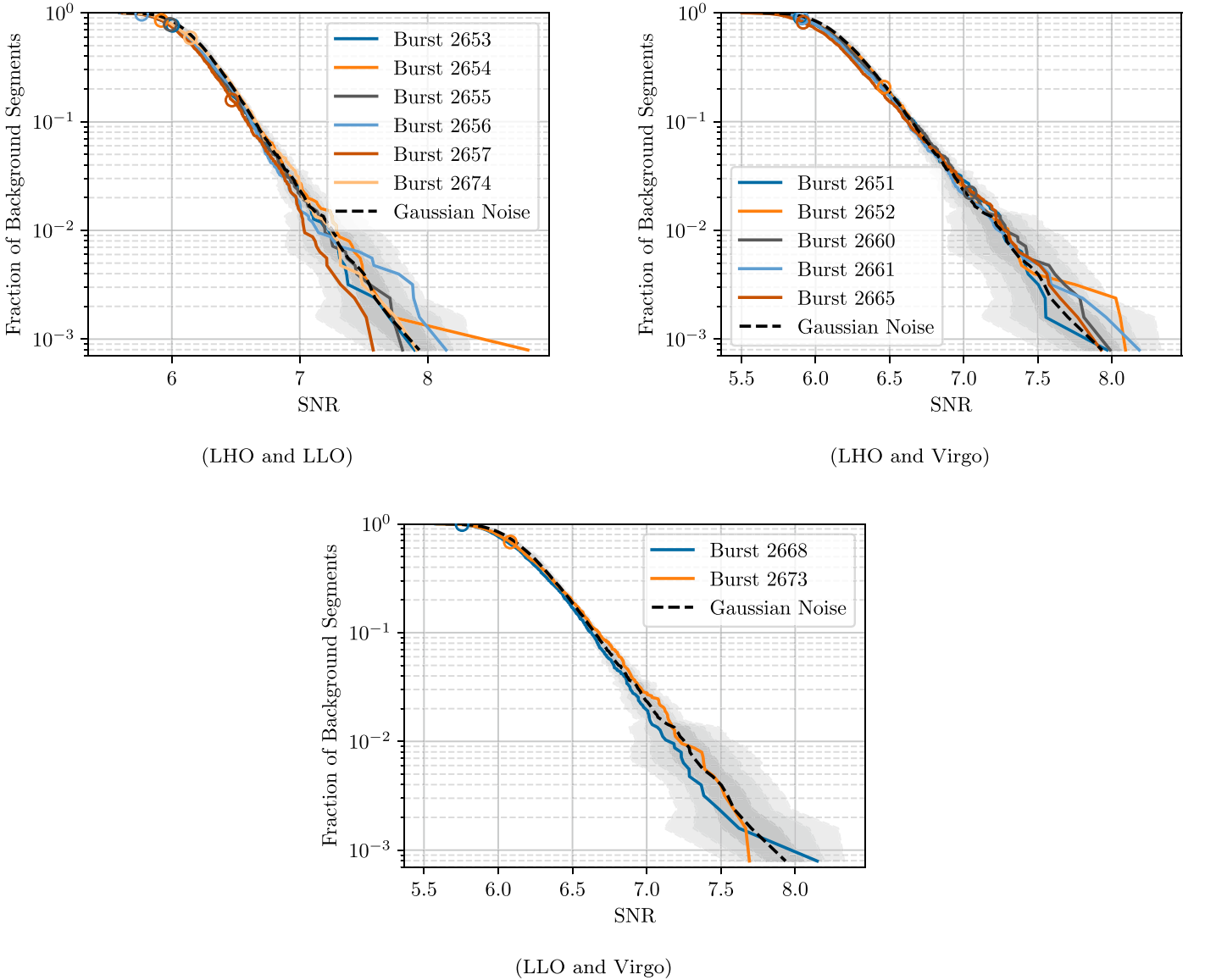
Figure 5. Distributions of background and on-source clusters found by the long-duration search for each burst analyzed with data from LHO, LLO, and Virgo. The background of each burst is displayed along with the S/N of its on-source cluster, denoted by a circle. The dashed black line is the mean, and the gray contours are the one, two, and three standard deviations of the distribution of FBS obtained simulating Gaussian noise colored with the Advanced LIGO design sensitivity curve (Barsotti et al. 2018).

a S/N higher than the on-source cluster rather than only the loudest cluster from each time segment.

The upper limit $h_{\text{rss}}^{90\%}$ ($E_{\text{GW}}^{90\%}$) is the value of the root-sum-square strain (gravitational-wave energy) of the magnetar signal such that 90% of a population of signals with that amplitude (energy) would have given rise to gravitational-wave candidates more significant than those found by our search. We also present the analogous upper limits pertaining to a 50% detection efficiency, $h_{\text{rss}}^{50\%}$ and $E_{\text{GW}}^{50\%}$. To estimate $h_{\text{rss}}^{50\%}$ and $h_{\text{rss}}^{90\%}$ for each burst, we inject waveforms into the data and calculate the amplitudes for which 50% and 90% of the signals have a detection statistic equal to or greater than the respective most significant on-source cluster. These waveforms are meant to encapsulate a broad range of different signals that could be produced in association with magnetar bursts, but are not associated with specific emission mechanisms.

We then derive the rms of the integrated incident gravitational-wave strain (h_{rss}) and gravitational-wave energy (E_{GW})

for these amplitudes. The definition of h_{rss} is

$$h_{\text{rss}} = \sqrt{\int_{-\infty}^{\infty} |h_{+}(t)|^2 + |h_{\times}(t)|^2 dt}, \qquad (2)$$

where $h_{+}(t)$ and $h_{\times}(t)$ are the two signal polarizations. In Appendix C we derive h_{rss} and E_{GW} for the different waveforms used in the analysis.

When calculating E_{GW}, we use 9 kpc for SGR 1935+2154 (Zhong et al. 2020). The distance to Swift J1818.0−1607 is estimated to be in the range of 4.8–8.1 kpc (Karuppusamy et al. 2020); we calculate E_{GW} with the larger distance of 8.1 kpc to be conservative. For the magnetar bursts with unknown source (s), we consider 1 RXS J170849 as the source and use 3.8 kpc for the distance (Olausen & Kaspi 2014). The gravitational-wave energy upper limits corresponding to the h_{rss} upper limits are calculated according to the discussion in Appendix C, and in all cases the energy is proportional to the source distance
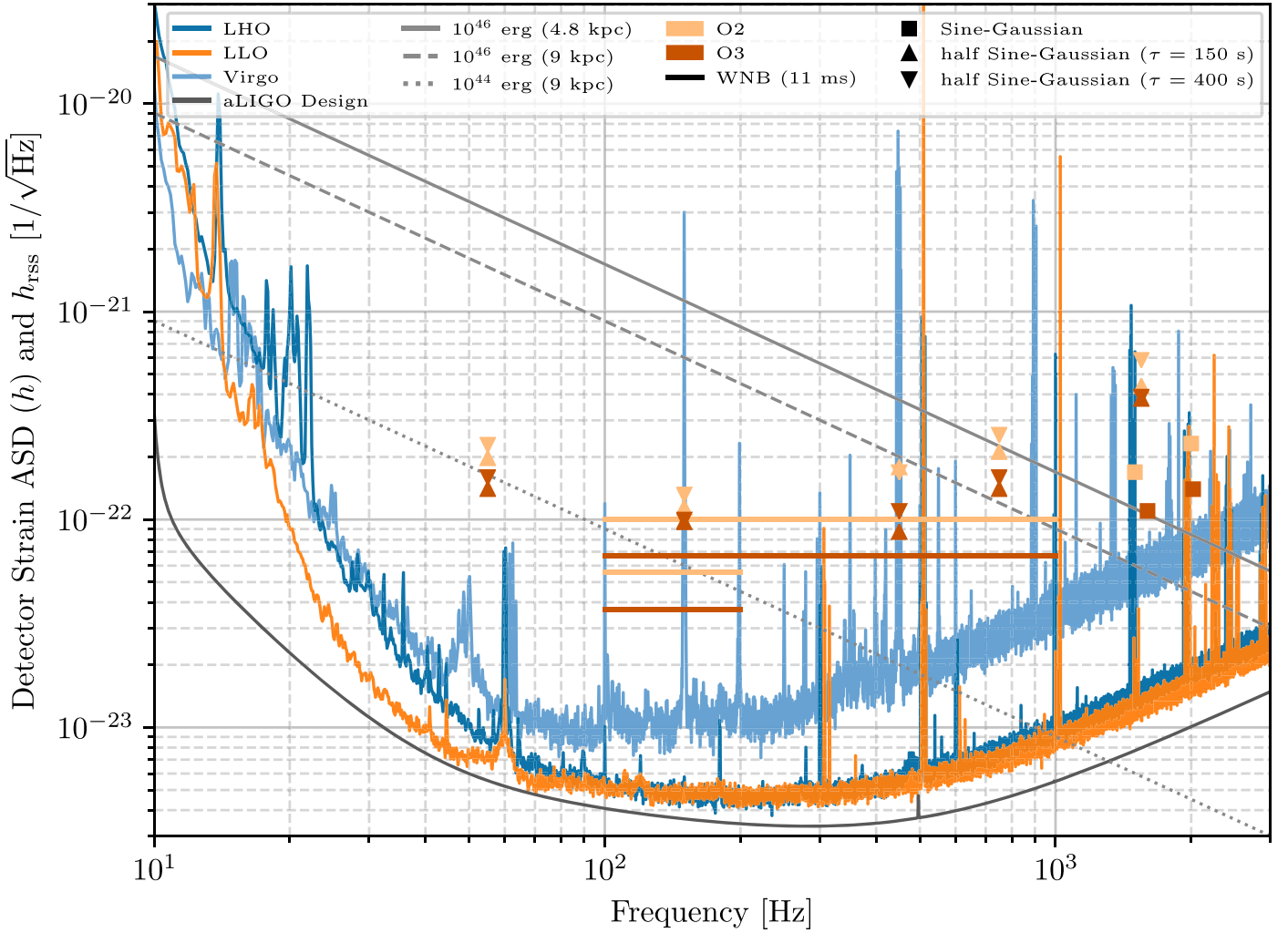
Figure 6. The lowest $h_{\mathrm{rss}}^{50\%}$ value across all bursts with known sources are displayed and compared to O2 results for the long-duration search. The detectors' amplitude strain density curves correspond to the representative sensitivity for each detector during O3 (Buikema et al. 2020; Kissel 2020; Verkindt 2021).

squared. Any uncertainty in these distances will also effect the energy upper limits.

3.1. Short-duration Search Results

All bursts listed in Table 1 have been considered by the short-duration search except bursts 2651 and 2665 because of missing data in the on-source windows. For the bursts considered, the short-duration centered and delayed on-source searches find clusters whose p-values are reported in Table 3. The cumulative distribution of these p-values is represented in Figure 1. The two most significant (p-value < 1%) clusters found for bursts 2653 and 2656 by the short-duration search are discussed.

Burst 2653. Two significant clusters are detected by the delayed on-source search. The most significant cluster has a p-value of 3.5×10^{-3}, a peak frequency of 97 Hz, and duration of 31 ms. This is the outlier displayed in Figure 2. X-pipeline identifies another loud cluster 50 s earlier with the same p-value, a peak frequency of 228 Hz, and a duration of 7.8 ms. Given their frequency and duration, each of these clusters is only a couple of cycles long. Both clusters display similar characteristics in the LHO data, appearing in spectrograms as a short-duration, low-frequency spike. In both cases, another

high-S/N spike is seen in the data ∼0.3 s from the time of the cluster as shown in Figure 2. Several other of these high-S/N features are detected on the same day as trigger 2653, and these are also in groups of two spaced out by ∼0.3 s. While X-pipeline does not reconstruct either of these neighboring spikes in a coherent cluster, their presence at such a consistent and short time separation from the cluster strongly suggests that each of these clusters has a terrestrial origin. While X-pipeline conducts a coherent search, there remains poor coherence across the two-detector network for these clusters. When the energy per time–frequency pixel is standardized to be 1 unit for Gaussian data, this signal is detected with 165.3 units in LHO, and only 6.2 units and 12.8 units of energy in LLO and Virgo, respectively. The ratio between the LHO and LLO energies is more than can be accounted for by the ratio of antenna factors squared, which gives a measure of the directional sensitivity (4.8 for LHO–LLO and 1.3 for LHO–Virgo) at the time of the burst. Finally, neither of these clusters is visibly identifiable in the LLO nor the Virgo time–frequency maps, meaning they are likely instrumental artifacts in LHO only.

Burst 2656. The most significant cluster found by the centered on-source search has a p-value of 8.6×10^{-3}. This cluster is 63 ms long, and its frequency extends from 1560 to
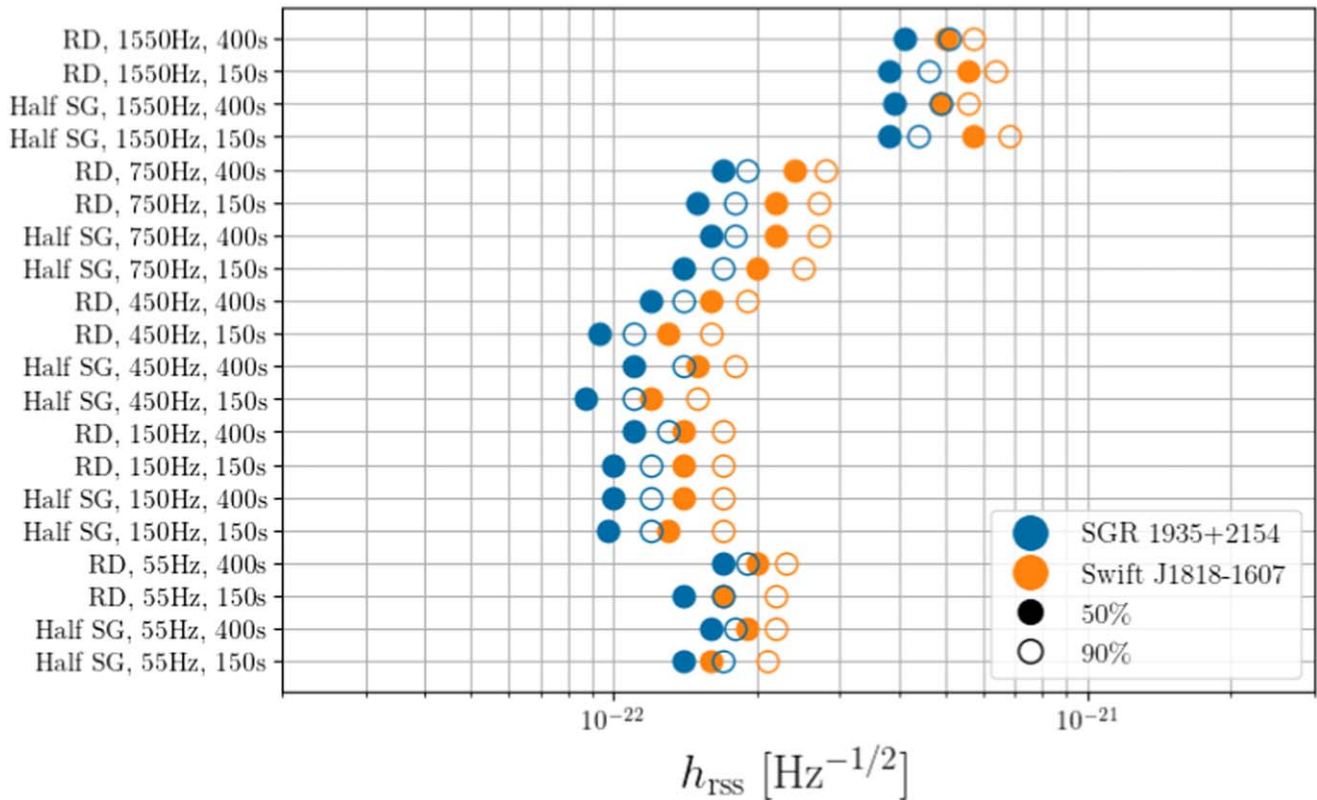
Figure 7. For each injection, we display the $h_{\rm rss}^{50\%}$ values of the burst with the lowest value at 50% detection efficiency from each source in the long-duration search, and the $h_{\rm rss}^{90\%}$ values for the same burst. The $h_{\rm rss}^{50\%}$ values are marked by filled-in shapes, and the $h_{\rm rss}^{90\%}$ values are not filled in. The vertical axis notes the waveform, where "Half SG" means half sine-Gaussian and "RD" means ringdown. The frequency and duration of each injection are given as well. In general the $h_{\rm rss}^{90\%}$ values are less than a factor of 1.5 greater than their corresponding $h_{\rm rss}^{50\%}$. The numerical values of the upper limits pertaining to SGR 1935+2154 can be found in Table 12, while the upper limits for Swift J1818.0–1607 can be found in Table 13.

1608 Hz, which matches the expected frequency range of neutron star f-mode oscillations. The cluster appears $\sim$3.1 s before the burst time. There are no known physical mechanisms to produce gravitational waves so long before the electromagnetic emission; while this does not rule out this cluster being astrophysical, it makes it less plausible.

Unlike the clusters found for burst 2653, this one is only visible in the LLO data spectrogram shown in Figure 3, which also illustrates that no high-S/N glitches are present in the ambient noise at the time of the burst. The imbalance in detector energies for this cluster also suggests that it is an instrumental artifact.

When considering the number of analyses in the long-duration and short-duration searches (40 in total across the three on-source windows of 16 bursts), the probability of having a p-value as low as that of burst 2656 is 29%. This, and the high probability that the cluster is due to an instrumental artifact, imply it is highly unlikely to be a signal of astrophysical origin. Nevertheless, we can calculate the strain and gravitational-wave energy required for such a signal assuming it is of astrophysical origin. Using the ringdown waveform with a 100 ms damping time and 1590 Hz frequency, $h_{\rm rss}^{50\%}$ and $E_{\rm GW}^{50\%}$ are 2.2×10^{-22} Hz$^{-1/2}$ and 1×10^{47} erg, respectively. This implies a ratio of gravitational-wave energy to electromagnetic energy of $E_{\rm GW}^{50\%}/E_{\rm EM}^{\rm iso} = 6 \times 10^{6}$. It is difficult to imagine a physical scenario whereby this much more energy is deposited into gravitational rather than electromagnetic waves, adding further weight to the conclusion that this cluster is not of astrophysical origin.

In the short-duration searches, simulated signals are added into the on-source data and the resulting time–frequency maps are processed similarly to the on-source time–frequency maps. The injected signals are chosen such that they adequately model a short-duration transient consistent with a magnetar f-mode signal, and also such that they cover a reasonable range of frequencies outside of the f-mode frequency range. We inject sine-Gaussian waveforms, described in Appendix C, at a range of frequencies between 70 and 3560 Hz and standardize the damping time of each injection to be the inverse of the frequency. We also inject a series of ringdown waveforms characterized by sinusoids with an exponentially decaying amplitude as described in Appendix C. These ringdown waveforms have damping times of 100 ms and 200 ms, and frequencies ranging from 1500 to 2020 Hz for consistency with previous searches. We also include a series of white noise burst (WNB) signals ranging in frequency from 100 to 1000 Hz to probe $h_{\rm rss}$ upper limits at lower frequencies. The ringdown and sine-Gaussian waveforms are eliptically polarized such that the analysis makes no assumptions on the source orientation. The exception to this are two circularly polarized sine-Gaussian waveforms injected at 1600 and 2020 Hz, which assume an optimally oriented source and are used for comparison with previous searches.

In Figure 4, we present the $h_{\rm rss}^{50\%}$ and $h_{\rm rss}^{90\%}$ values of the most sensitive burst from each source for the short-duration search. Overall, the $h_{\rm rss}$ upper limits follow the detectors' sensitivity frequency evolution and we also see that for most waveforms, $h_{\rm rss}^{90\%}$ is approximately a factor of 2 greater than the

Table 5
Parameters Used in the Centered On-source and Delayed On-source Short-duration Searches

Burst	Parameters of the Delayed On-source Search	Parameters of the Centered On-source Search
2652	Background asymmetry factor = 0.3726, background length = 8090 s, frequency range = 300 Hz to 4000 Hz	Background asymmetry factor = 0.3858, background length = 9056 s
2653	Background asymmetry factor = 0.4711, background length = 10,790 s, frequency range = 65 Hz to 4000 Hz, error region = 1°	
2655	Background asymmetry factor = 0.5677, background length = 10,790 s	Background asymmetry factor = 0.5225, background length = 10,790 s
2656	Background asymmetry factor = 0.4331, background length = 10,790 s	Background asymmetry factor = 0.4775, background length = 10,790 s
2660	Background asymmetry factor = 0.3421, background length = 10,790 s	Background asymmetry factor = 0.3403, background length = 10,790 s
2661	Error region = 1°	
2668	Error region = 1°	Frequency range = 85 Hz to 4000 Hz
2669	Background asymmetry factor = 0.8993, background length = 10,790 s	Background asymmetry factor = 0.854, background length = 10,790 s
2670	Background asymmetry factor = 0.1015, background length = 10,790 s	Background asymmetry factor = 0.1459, background length = 10,790 s
2671		Background length = 10,790 s
2673	Frequency range = 60–4000 Hz, error region = 1°	

Note. When no value is specified, the search was run with the default parameters, including frequency ranging from 50 to 4000 Hz, a symmetric background window 10,800 s in length, and a 0° error region. The background asymmetry factor is defined as the fraction of the background time before the burst time, with 0.5 corresponding to a symmetric background. The error region is defined as the 1σ uncertainty in the sky position of the source. Using a nonzero error region on a point source can sometimes optimize the $h_{\rm rss}$ and $E_{\rm GW}$ upper limits because it counters the effects of the Earth's rotation during the on-source window.

Table 6
$h_{\rm rss}^{50\%}$ and $E_{\rm GW}^{50\%}$ for the Most Sensitive Burst from SGR 1935+2154 for Each Injected Waveform in the Centered and Delayed On-source Windows of the Short-duration Search

Injection Type	Frequency	Duration/	Centered (8 s)			Delayed (500 s)		
	(Hz)	τ (ms)	Burst	$h_{\rm rss}^{50\%}$ (Hz$^{-1/2}$)	$E_{\rm GW}^{50\%}$ ($\frac{d^2}{(9\,{\rm kpc})^2}$ erg)	Burst	$h_{\rm rss}^{50\%}$ (Hz$^{-1/2}$)	$E_{\rm GW}^{50\%}$ ($\frac{d^2}{(9\,{\rm kpc})^2}$ erg)
Sine-Gaussian	70	14.3	2655	7.3×10^{-23}	3.2×10^{43}	2656	8.5×10^{-23}	4.4×10^{43}
Sine-Gaussian	90	11.1	2668	5.8×10^{-23}	3.3×10^{43}	2656	7.4×10^{-23}	5.5×10^{43}
Sine-Gaussian	145	6.89	2668	5.7×10^{-23}	8.4×10^{43}	2656	6.6×10^{-23}	1.1×10^{44}
Sine-Gaussian	290	3.45	2655	5.8×10^{-23}	3.5×10^{44}	2656	6.7×10^{-23}	4.7×10^{44}
Sine-Gaussian	1100	0.909	2655	1.3×10^{-22}	2.6×10^{46}	2656	1.5×10^{-22}	3.4×10^{46}
Sine-Gaussian	1600	0.625	2655	1.9×10^{-22}	1.1×10^{47}	2656	2.2×10^{-22}	1.6×10^{47}
Sine-Gaussian	2020	0.495	2655	2.4×10^{-22}	3.0×10^{47}	2656	2.9×10^{-22}	4.3×10^{47}
Sine-Gaussian	2600	0.385	2655	3.3×10^{-22}	9.2×10^{47}	2656	4.0×10^{-22}	1.3×10^{48}
Sine-Gaussian	3100	0.323	2655	4.1×10^{-22}	2.0×10^{48}	2652	5.2×10^{-22}	3.1×10^{48}
Sine-Gaussian	3560	0.281	2655	5.1×10^{-22}	4.0×10^{48}	2652	6.2×10^{-22}	6.0×10^{48}
Sine-Gaussian*	1600	0.625	2655	1.1×10^{-22}	3.8×10^{46}	2656	1.3×10^{-22}	5.2×10^{46}
Sine-Gaussian*	2020	0.495	2655	1.4×10^{-22}	9.6×10^{46}	2656	1.7×10^{-22}	1.4×10^{47}
Ringdown	1590	100	2655	1.9×10^{-22}	1.1×10^{47}	...	...	...
Ringdown	1590	200	2655	1.8×10^{-22}	9.6×10^{46}	...	...	...
Ringdown	1500	100	2668	2.5×10^{-22}	1.8×10^{47}	...	...	...
Ringdown	1500	200	2668	2.3×10^{-22}	1.5×10^{47}	...	...	...
Ringdown	2020	100	2655	2.2×10^{-22}	2.4×10^{47}	...	...	...
Ringdown	2020	200	2655	2.2×10^{-22}	2.3×10^{47}	...	...	...
WNB	100–200	11	2668	3.8×10^{-23}	1.0×10^{44}	2656	4.1×10^{-23}	1.2×10^{44}
WNB	100–200	100	2668	5.3×10^{-23}	2.0×10^{44}	2656	6.1×10^{-23}	2.7×10^{44}
WNB	100–1000	11	2655	6.7×10^{-23}	5.1×10^{45}	2656	7.5×10^{-23}	6.4×10^{45}
WNB	100–1000	100	2655	1.1×10^{-22}	1.5×10^{46}	2656	1.5×10^{-22}	2.4×10^{46}

Note. The energy is calculated assuming a distance of 9 kpc. Taking into account the uncertainty on the distance to SGR 1935+2154 given in the caption of Table 1, the energies could scale by a factor ranging from 0.52 to 1.6. All waveforms are elliptically polarized, except those denoted by an "*," which have circular polarization, and the WNBs, which are unpolarized.

(This table is available in machine-readable form.)

Table 7

$h_{\rm rss}^{50\%}$ and $E_{\rm GW}^{50\%}$ for the Most Sensitive Burst from Swift J1818.0−1607 for Each Injected Waveform in the Centered and Delayed On-source Windows of the Short-duration Search

Injection Type	Frequency	Duration/	Centered (8 s)			Delayed (500 s)		
	(Hz)	τ (ms)	Burst	$h_{\rm rss}^{50\%}$ (Hz$^{-1/2}$)	$E_{\rm GW}^{50\%}$ ($\frac{d^2}{(8.1\ {\rm kpc})^2}$ erg)	Burst	$h_{\rm rss}^{50\%}$ (Hz$^{-1/2}$)	$E_{\rm GW}^{50\%}$ ($\frac{d^2}{(8.1\ {\rm kpc})^2}$ erg)
Sine-Gaussian	70	14.3	2674	6.9×10^{-23}	2.3×10^{43}	2673	9.2×10^{-23}	4.1×10^{43}
Sine-Gaussian	90	11.1	2674	6.1×10^{-23}	3.0×10^{43}	2673	8.7×10^{-23}	6.1×10^{43}
Sine-Gaussian	145	6.89	2674	5.7×10^{-23}	6.9×10^{43}	2674	8.5×10^{-23}	1.5×10^{44}
Sine-Gaussian	290	3.45	2674	5.9×10^{-23}	3.0×10^{44}	2674	9.1×10^{-23}	6.9×10^{44}
Sine-Gaussian	1100	0.909	2674	1.3×10^{-22}	2.1×10^{46}	2674	2.0×10^{-22}	4.8×10^{46}
Sine-Gaussian	1600	0.625	2674	2.0×10^{-22}	1.0×10^{47}	2674	2.9×10^{-22}	2.1×10^{47}
Sine-Gaussian	2020	0.495	2674	2.7×10^{-22}	3.0×10^{47}	2674	3.9×10^{-22}	6.1×10^{47}
Sine-Gaussian	2600	0.385	2674	3.5×10^{-22}	8.2×10^{47}	2674	4.9×10^{-22}	1.6×10^{48}
Sine-Gaussian	3100	0.323	2674	4.4×10^{-22}	1.8×10^{48}	2674	6.1×10^{-22}	3.5×10^{48}
Sine-Gaussian	3560	0.281	2674	5.3×10^{-22}	3.5×10^{48}	2674	7.1×10^{-22}	6.3×10^{48}
Sine-Gaussian	1600	0.625	2674	1.2×10^{-22}	3.5×10^{46}	2674	1.7×10^{-22}	7.4×10^{46}
Sine-Gaussian	2020	0.495	2674	1.5×10^{-22}	9.0×10^{46}	2674	2.1×10^{-22}	1.8×10^{47}
Ringdown	1590	100	2674	2.1×10^{-22}	1.1×10^{47}	…	…	…
Ringdown	1590	200	2674	2.1×10^{-22}	1.1×10^{47}	…	…	…
Ringdown	1500	100	2673	2.6×10^{-22}	1.5×10^{47}	…	…	…
Ringdown	1500	200	2673	2.6×10^{-22}	1.5×10^{47}	…	…	…
Ringdown	2020	100	2674	2.6×10^{-22}	2.6×10^{47}	…	…	…
Ringdown	2020	200	2674	2.5×10^{-22}	2.5×10^{47}	…	…	…
WNB	100–200	11	2674	3.7×10^{-23}	8.1×10^{43}	2673	5.6×10^{-23}	1.8×10^{44}
WNB	100–200	100	2674	5.3×10^{-23}	1.6×10^{44}	2673	7.8×10^{-23}	3.5×10^{44}
WNB	100–1000	11	2674	7.0×10^{-23}	4.5×10^{45}	2674	1.0×10^{-22}	9.4×10^{45}
WNB	100–1000	100	2674	1.2×10^{-22}	1.3×10^{46}	2674	1.8×10^{-22}	3.1×10^{46}

Note. The energy is calculated assuming a distance of 8.1 kpc, the most conservative value in the range of accepted distances. Taking into account the distance range to Swift J1818.0−1607 given in the caption of Table 1, the energies could scale by a factor as low as 0.35. All waveforms are elliptically polarized, except those denoted by an "*," which have circular polarization, and the WNBs, which are unpolarized.

(This table is available in machine-readable form.)

Table 8

$h_{\rm rss}^{50\%}$ and $E_{\rm GW}^{50\%}$ for the Most Sensitive Burst from the Unknown Source for Each Injected Waveform in the Centered and Delayed On-source Windows of the Short-duration Search

Injection Type	Frequency	Duration/	Centered (8 s)			Delayed (500 s)		
	(Hz)	τ (ms)	Burst	$h_{\rm rss}^{50\%}$ (Hz$^{-1/2}$)	$E_{\rm GW}^{50\%}$ ($\frac{d^2}{(3.8\ {\rm kpc})^2}$ erg)	Burst	$h_{\rm rss}^{50\%}$ (Hz$^{-1/2}$)	$E_{\rm GW}^{50\%}$ ($\frac{d^2}{(3.8\ {\rm kpc})^2}$ erg)
Sine-Gaussian	70	14.3	2669	4.2×10^{-23}	1.9×10^{42}	2669	5.0×10^{-23}	2.7×10^{42}
Sine-Gaussian	90	11.1	2669	4.0×10^{-23}	2.8×10^{42}	2669	4.6×10^{-23}	3.8×10^{42}
Sine-Gaussian	145	6.89	2669	3.3×10^{-23}	5.1×10^{42}	2669	3.9×10^{-23}	7.0×10^{42}
Sine-Gaussian	290	3.45	2669	3.6×10^{-23}	2.4×10^{43}	2669	4.1×10^{-23}	3.1×10^{43}
Sine-Gaussian	1100	0.909	2669	7.7×10^{-23}	1.6×10^{45}	2669	8.8×10^{-23}	2.1×10^{45}
Sine-Gaussian	1600	0.625	2669	1.1×10^{-22}	7.1×10^{45}	2670	1.3×10^{-22}	9.5×10^{45}
Sine-Gaussian	2020	0.495	2669	1.5×10^{-22}	1.9×10^{46}	2669	1.7×10^{-22}	2.5×10^{46}
Sine-Gaussian	2600	0.385	2669	2.0×10^{-22}	5.9×10^{46}	2669	2.4×10^{-22}	8.8×10^{46}
Sine-Gaussian	3100	0.323	2669	2.5×10^{-22}	1.3×10^{47}	2670	3.0×10^{-22}	1.9×10^{47}
Sine-Gaussian	3560	0.281	2669	2.9×10^{-22}	2.3×10^{47}	2670	4.0×10^{-22}	4.5×10^{47}
Sine-Gaussian*	1600	0.625	2669	6.2×10^{-23}	2.2×10^{45}	2669	7.7×10^{-23}	3.3×10^{45}
Sine-Gaussian*	2020	0.495	2669	8.6×10^{-23}	6.6×10^{45}	2670	9.5×10^{-23}	8.1×10^{45}
Ringdown	1590	100	2670	1.1×10^{-22}	6.8×10^{45}	…	…	…
Ringdown	1590	200	2670	1.1×10^{-22}	7.0×10^{45}	…	…	…
Ringdown	1500	100	2669	1.8×10^{-22}	1.6×10^{46}	…	…	…
Ringdown	1500	200	2671	2.7×10^{-22}	3.6×10^{46}	…	…	…
Ringdown	2020	100	2670	1.3×10^{-22}	1.6×10^{46}	…	…	…
Ringdown	2020	200	2670	1.3×10^{-22}	1.6×10^{46}	…	…	…
WNB	100–200	11	2669	2.2×10^{-23}	6.2×10^{42}	2669	2.5×10^{-23}	8.2×10^{42}
WNB	100–200	100	2669	3.2×10^{-23}	1.3×10^{43}	2670	3.6×10^{-23}	1.7×10^{43}
WNB	100–1000	11	2669	3.9×10^{-23}	3.0×10^{44}	2669	4.6×10^{-23}	4.4×10^{44}
WNB	100–1000	100	2669	7.1×10^{-23}	1.0×10^{45}	2669	8.2×10^{-23}	1.4×10^{45}

Note. The energy is calculated assuming a distance of 3.8 kpc. Taking into account the uncertainty on the distance to 1 RXS J170849 given in the caption of Table 1, the energies could scale by a factor ranging from 0.75 to 1.3. All waveforms are elliptically polarized, except those denoted by an "*," which have circular polarization, and the WNBs, which are unpolarized.

(This table is available in machine-readable form.)

Table 9

$h_{\rm rss}^{90\%}$ and $E_{\rm GW}^{90\%}$ for the Most Sensitive Burst from SGR 1935+2154 for Each Injected Waveform in the Centered and Delayed On-source Windows of the Short-duration Search

Injection Type	Frequency	Duration/	Centered (8 s)			Delayed (500 s)		
	(Hz)	τ (ms)	Burst	$h_{\rm rss}^{90\%}$ (Hz$^{-1/2}$)	$E_{\rm GW}^{90\%}$ ($\frac{d^2}{(9\ {\rm kpc})^2}$ erg)	Burst	$h_{\rm rss}^{90\%}$ (Hz$^{-1/2}$)	$E_{\rm GW}^{90\%}$ ($\frac{d^2}{(9\ {\rm kpc})^2}$ erg)
Sine-Gaussian	70	14.3	2655	1.6×10^{-22}	1.5×10^{44}	2656	1.9×10^{-22}	2.1×10^{44}
Sine-Gaussian	90	11.1	2655	1.4×10^{-22}	1.9×10^{44}	2656	1.7×10^{-22}	2.9×10^{44}
Sine-Gaussian	145	6.89	2655	1.0×10^{-22}	2.8×10^{44}	2655	1.4×10^{-22}	5.1×10^{44}
Sine-Gaussian	290	3.45	2655	1.3×10^{-22}	1.7×10^{45}	2656	1.4×10^{-22}	2.0×10^{45}
Sine-Gaussian	1100	0.909	2655	2.8×10^{-22}	1.2×10^{47}	2656	3.2×10^{-22}	1.5×10^{47}
Sine-Gaussian	1600	0.625	2655	4.2×10^{-22}	5.5×10^{47}	2656	5.1×10^{-22}	8.1×10^{47}
Sine-Gaussian	2020	0.495	2655	4.9×10^{-22}	1.2×10^{48}	2652	6.6×10^{-22}	2.2×10^{48}
Sine-Gaussian	2600	0.385	2655	7.0×10^{-22}	4.0×10^{48}	2656	8.7×10^{-22}	6.3×10^{48}
Sine-Gaussian	3100	0.323	2655	8.1×10^{-22}	7.8×10^{48}	2652	1.1×10^{-21}	1.3×10^{49}
Sine-Gaussian	3560	0.281	2656	1.1×10^{-21}	2.0×10^{49}	2652	1.5×10^{-21}	3.3×10^{49}
Sine-Gaussian	1600*	0.625	2655	1.5×10^{-22}	7.0×10^{46}	2656	1.9×10^{-22}	1.1×10^{47}
Sine-Gaussian	2020*	0.495	2655	2.0×10^{-22}	2.1×10^{47}	2656	2.3×10^{-22}	2.6×10^{47}
Ringdown	1590	100	2655	3.9×10^{-22}	4.7×10^{47}	...	...	...
Ringdown	1590	200	2655	3.9×10^{-22}	4.8×10^{47}	...	...	...
Ringdown	1500	100	2655	6.5×10^{-22}	1.2×10^{48}	...	...	...
Ringdown	1500	200	2668	6.3×10^{-22}	1.1×10^{48}	...	...	...
Ringdown	2020	100	2655	4.5×10^{-22}	1.0×10^{48}	...	...	...
Ringdown	2020	200	2655	4.8×10^{-22}	1.2×10^{48}	...	...	...
WNB	100–200	11	2655	6.4×10^{-23}	2.9×10^{44}	2656	7.6×10^{-23}	4.1×10^{44}
WNB	100–200	100	2655	8.3×10^{-23}	4.9×10^{44}	2656	8.7×10^{-23}	5.4×10^{44}
WNB	100–1000	11	2655	9.0×10^{-23}	9.2×10^{45}	2656	1.1×10^{-22}	1.4×10^{46}
WNB	100–1000	100	2655	1.7×10^{-22}	3.3×10^{46}	2656	1.9×10^{-22}	4.0×10^{46}

Note. The energy is calculated assuming a distance of 9 kpc. Taking into account the uncertainty on the distance to SGR 1935+2154 given in Table 1, the energies could scale by a factor ranging from 0.52 to 1.6. All waveforms are elliptically polarized, except those denoted by an "*," which have circular polarization, and the WNBs, which are unpolarized.

(This table is available in machine-readable form.)

Table 10

$h_{\rm rss}^{90\%}$ and $E_{\rm GW}^{90\%}$ for the Most Sensitive Burst from Swift J1818.0−1607 for Each Injected Waveform in the Centered and Delayed On-source Windows of the Short-duration Search

Injection Type	Frequency	Duration/	Centered (8 s)			Delayed (500 s)		
	(Hz)	τ (ms)	Burst	$h_{\rm rss}^{90\%}$ (Hz$^{-1/2}$)	$E_{\rm GW}^{90\%}$ ($\frac{d^2}{(8.1\ {\rm kpc})^2}$ erg)	Burst	$h_{\rm rss}^{90\%}$ (Hz$^{-1/2}$)	$E_{\rm GW}^{90\%}$ ($\frac{d^2}{(8.1\ {\rm kpc})^2}$ erg)
Sine-Gaussian	70	14.3	2674	1.4×10^{-22}	9.4×10^{43}	2673	2.1×10^{-22}	2.1×10^{44}
Sine-Gaussian	90	11.1	2674	1.3×10^{-22}	1.4×10^{44}	2673	1.8×10^{-22}	2.7×10^{44}
Sine-Gaussian	145	6.89	2674	1.3×10^{-22}	3.6×10^{44}	2673	2.0×10^{-22}	8.2×10^{44}
Sine-Gaussian	290	3.45	2674	1.3×10^{-22}	1.4×10^{45}	2674	2.0×10^{-22}	3.4×10^{45}
Sine-Gaussian	1100	0.909	2674	3.4×10^{-22}	1.4×10^{47}	2674	4.8×10^{-22}	2.7×10^{47}
Sine-Gaussian	1600	0.625	2674	4.8×10^{-22}	5.9×10^{47}	2674	7.5×10^{-22}	1.4×10^{48}
Sine-Gaussian	2020	0.495	2674	6.1×10^{-22}	1.5×10^{48}	2674	8.8×10^{-22}	3.1×10^{48}
Sine-Gaussian	2600	0.385	2674	7.3×10^{-22}	3.6×10^{48}	2674	1.0×10^{-21}	7.1×10^{48}
Sine-Gaussian	3100	0.323	2674	9.8×10^{-22}	9.2×10^{48}	2674	1.4×10^{-21}	1.8×10^{49}
Sine-Gaussian	3560	0.281	2674	1.1×10^{-21}	1.5×10^{49}	2674	1.6×10^{-21}	3.1×10^{49}
Sine-Gaussian	1600*	0.625	2674	1.6×10^{-22}	6.9×10^{46}	2674	2.2×10^{-22}	1.3×10^{47}
Sine-Gaussian	2020*	0.495	2674	2.2×10^{-22}	2.0×10^{47}	2674	3.1×10^{-22}	3.9×10^{47}
Ringdown	1590	100	2674	4.5×10^{-22}	5.1×10^{47}	...	...	...
Ringdown	1590	200	2674	4.6×10^{-22}	5.2×10^{47}	...	...	...
Ringdown	1500	100	2673	6.6×10^{-22}	9.8×10^{47}	...	...	...
Ringdown	1500	200	2673	6.2×10^{-22}	8.5×10^{47}	...	...	...
Ringdown	2020	100	2674	5.4×10^{-22}	1.2×10^{48}	...	...	...
Ringdown	2020	200	2674	5.2×10^{-22}	1.1×10^{48}	...	...	...
WNB	100–200	11	2673	7.9×10^{-23}	3.6×10^{44}	2673	9.7×10^{-23}	5.4×10^{44}
WNB	100–200	100	2674	8.2×10^{-23}	3.9×10^{44}	2673	1.2×10^{-22}	9.0×10^{44}
WNB	100–1000	11	2674	1.0×10^{-22}	9.4×10^{45}	2674	1.6×10^{-22}	2.4×10^{46}
WNB	100–1000	100	2674	1.8×10^{-22}	2.9×10^{46}	2674	2.8×10^{-22}	7.4×10^{46}

Note. The energy is calculated assuming a distance of 8.1 kpc, the most conservative value in the range of accepted distances. Taking into account the distance range to Swift J1818.0−1607 given in the caption of Table 1, the energies could scale by a factor as low as 0.35. All waveforms are elliptically polarized, except those denoted by an "*," which have circular polarization, and the WNBs, which are unpolarized.

(This table is available in machine-readable form.)

Table 11
$h_{\mathrm{rss}}^{90\%}$ and $E_{\mathrm{GW}}^{90\%}$ for the Most Sensitive Burst from the Unknown Source for Each Injected Waveform in the Centered and Delayed On-source Windows of the Short-duration Search

Injection Type	Frequency	Duration/	Centered (8 s)			Delayed (500 s)		
	(Hz)	τ (ms)	Burst	$h_{\mathrm{rss}}^{90\%}$ (Hz$^{-1/2}$)	$E_{\mathrm{GW}}^{90\%}$ ($\frac{d^2}{(3.8\ \mathrm{kpc})^2}$ erg)	Burst	$h_{\mathrm{rss}}^{90\%}$ (Hz$^{-1/2}$)	$E_{\mathrm{GW}}^{90\%}$ ($\frac{d^2}{(3.8\ \mathrm{kpc})^2}$ erg)
Sine-Gaussian	70	14.3	2669	9.2×10^{-23}	9.1×10^{42}	2669	1.1×10^{-22}	1.2×10^{43}
Sine-Gaussian	90	11.1	2669	8.7×10^{-23}	1.3×10^{43}	2669	9.9×10^{-23}	1.7×10^{43}
Sine-Gaussian	145	6.89	2669	6.5×10^{-23}	2.0×10^{43}	2669	7.7×10^{-23}	2.7×10^{43}
Sine-Gaussian	290	3.45	2670	7.4×10^{-23}	1.0×10^{44}	2669	8.6×10^{-23}	1.4×10^{44}
Sine-Gaussian	1100	0.909	2669	1.4×10^{-22}	5.5×10^{45}	2669	1.6×10^{-22}	6.8×10^{45}
Sine-Gaussian	1600	0.625	2669	2.2×10^{-22}	2.6×10^{46}	2669	2.4×10^{-22}	3.1×10^{46}
Sine-Gaussian	2020	0.495	2669	3.0×10^{-22}	8.0×10^{46}	2669	3.4×10^{-22}	1.0×10^{47}
Sine-Gaussian	2600	0.385	2669	3.7×10^{-22}	2.1×10^{47}	2670	5.1×10^{-22}	3.8×10^{47}
Sine-Gaussian	3100	0.323	2669	4.8×10^{-22}	4.8×10^{47}	2669	6.9×10^{-22}	1.0×10^{48}
Sine-Gaussian	3560	0.281	2669	6.1×10^{-22}	1.0×10^{48}	2670	1.4×10^{-21}	5.8×10^{48}
Sine-Gaussian	1600*	0.625	2669	9.1×10^{-23}	4.6×10^{45}	2670	1.0×10^{-22}	6.0×10^{45}
Sine-Gaussian	2020*	0.495	2669	1.1×10^{-22}	1.1×10^{46}	2670	1.4×10^{-22}	1.8×10^{46}
Ringdown	1590	100	2670	2.3×10^{-22}	3.0×10^{46}	...	...	...
Ringdown	1590	200	2670	2.2×10^{-22}	2.6×10^{46}	...	...	...
Ringdown	1500	100	2671	4.7×10^{-22}	1.1×10^{47}	...	...	...
Ringdown	1500	200	2671	6.0×10^{-22}	1.8×10^{47}	...	...	...
Ringdown	2020	100	2670	2.8×10^{-22}	6.9×10^{46}	...	...	...
Ringdown	2020	200	2670	2.9×10^{-22}	7.6×10^{46}	...	...	...
WNB	100–200	11	2669	3.6×10^{-23}	1.7×10^{43}	2669	4.1×10^{-23}	2.1×10^{43}
WNB	100–200	100	2669	4.2×10^{-23}	2.2×10^{43}	2669	5.3×10^{-23}	3.6×10^{43}
WNB	100–1000	11	2669	5.6×10^{-23}	6.4×10^{44}	2669	6.0×10^{-23}	7.4×10^{44}
WNB	100–1000	100	2669	8.9×10^{-23}	1.6×10^{45}	2669	1.2×10^{-22}	2.9×10^{45}

Note. The energy is calculated assuming a distance of 3.8 kpc. Taking into account the uncertainty on the distance to 1 RXS J170849 given in Table 1, the energies could scale by a factor ranging from 0.75 to 1.3. All waveforms are elliptically polarized, except those denoted by an "$*$," which have circular polarization, and the WNBs, which are unpolarized.

(This table is available in machine-readable form.)

Table 12
Upper Limits for h_{rss} and E_{GW} for Half Sine-Gaussian and Ringdown Waveforms for Burst 2656 from SGR 1935+2154 for the Long-duration Search

Frequency (Hz)	τ (s)	Detection Efficiency	Half Sine-Gaussian		Ringdown	
			h_{rss} (Hz$^{-1/2}$)	E_{GW} (erg)	h_{rss} (Hz$^{-1/2}$)	E_{GW} (erg)
55	150	50%	1.4×10^{-22}	7.3×10^{43}	1.4×10^{-22}	7.8×10^{43}
...	...	90%	1.7×10^{-22}	1.0×10^{44}	1.7×10^{-22}	1.1×10^{44}
...	400	50%	1.6×10^{-22}	9.3×10^{43}	1.7×10^{-22}	1.0×10^{44}
...	...	90%	1.8×10^{-22}	1.3×10^{44}	1.9×10^{-22}	1.4×10^{44}
150	150	50%	9.7×10^{-23}	2.6×10^{44}	1.0×10^{-22}	2.9×10^{44}
...	...	90%	1.2×10^{-22}	3.8×10^{44}	1.2×10^{-22}	4.1×10^{44}
...	400	50%	1.0×10^{-22}	2.9×10^{44}	1.1×10^{-22}	3.3×10^{44}
...	...	90%	1.2×10^{-22}	3.8×10^{44}	1.3×10^{-22}	4.4×10^{44}
450	150	50%	8.7×10^{-23}	1.9×10^{45}	9.3×10^{-23}	2.1×10^{45}
...	...	90%	1.1×10^{-22}	2.8×10^{45}	1.1×10^{-22}	3.2×10^{45}
-	400	50%	1.1×10^{-22}	3.1×10^{45}	1.2×10^{-22}	3.5×10^{45}
...	...	90%	1.4×10^{-22}	4.7×10^{45}	1.4×10^{-22}	5.0×10^{45}
750	150	50%	1.4×10^{-22}	1.4×10^{46}	1.5×10^{-22}	1.7×10^{46}
...	...	90%	1.7×10^{-22}	1.9×10^{46}	1.8×10^{-22}	2.2×10^{46}
...	400	50%	1.6×10^{-22}	1.7×10^{46}	1.7×10^{-22}	1.9×10^{46}
...	...	90%	1.8×10^{-22}	2.2×10^{46}	1.9×10^{-22}	2.6×10^{46}
1550	150	50%	3.8×10^{-22}	4.2×10^{47}	3.8×10^{-22}	4.2×10^{47}
...	...	90%	4.4×10^{-22}	5.8×10^{47}	4.6×10^{-22}	6.2×10^{47}
...	400	50%	3.9×10^{-22}	4.4×10^{47}	4.1×10^{-22}	5.0×10^{47}
...	...	90%	4.9×10^{-22}	7.0×10^{47}	5.1×10^{-22}	7.7×10^{47}

Note. Burst 2656 had the lowest upper limits for 50% detection efficiency. The value of E_{GW} is proportional to d^2, where d is the distance to the source. The energies are calculated assuming a distance of 9 kpc (the distance to SGR 1935+2154 is 9.0 ± 2.5 kpc; Zhong et al. 2020); given the uncertainty on the distance to SGR 1935+2154, the energies could scale by a factor ranging from 0.52 to 1.6.

(This table is available in machine-readable form.)

Table 13
Upper Limits for h_{rss} and E_{GW} for Half Sine-Gaussian and Ringdown Waveforms for Swift J1818.0−1607 for the Long-duration Search

Frequency (Hz)	τ (s)	Detection Efficiency	Half Sine-Gaussian		Ringdown	
			h_{rss} (Hz$^{-1/2}$)	E_{GW} (erg)	h_{rss} (Hz$^{-1/2}$)	E_{GW} (erg)
55	150	50%	1.6×10^{-22}	7.9×10^{43}	1.7×10^{-22}	8.8×10^{43}
…	…	90%	2.1×10^{-22}	1.3×10^{44}	2.2×10^{-22}	1.5×10^{44}
…	400	50%	1.9×10^{-22}	1.1×10^{44}	2.0×10^{-22}	1.2×10^{44}
…	…	90%	2.2×10^{-22}	1.5×10^{44}	2.3×10^{-22}	1.6×10^{44}
150	150	50%	1.3×10^{-22}	3.8×10^{44}	1.4×10^{-22}	4.2×10^{44}
…	…	90%	1.7×10^{-22}	6.1×10^{44}	1.7×10^{-22}	6.7×10^{44}
…	400	50%	1.4×10^{-22}	4.2×10^{44}	1.4×10^{-22}	4.5×10^{44}
…	…	90%	1.7×10^{-22}	6.2×10^{44}	1.7×10^{-22}	6.7×10^{44}
450	150	50%	1.2×10^{-22}	3.0×10^{45}	1.3×10^{-22}	3.5×10^{45}
…	…	90%	1.5×10^{-22}	4.5×10^{45}	1.6×10^{-22}	5.1×10^{45}
…	400	50%	1.5×10^{-22}	4.5×10^{45}	1.6×10^{-22}	5.0×10^{45}
…	…	90%	1.8×10^{-22}	6.6×10^{45}	1.9×10^{-22}	7.5×10^{45}
750	150	50%	2.0×10^{-22}	2.3×10^{46}	2.2×10^{-22}	2.7×10^{46}
…	…	90%	2.5×10^{-22}	3.4×10^{46}	2.7×10^{-22}	4.0×10^{46}
…	400	50%	2.2×10^{-22}	2.8×10^{46}	2.4×10^{-22}	3.2×10^{46}
…	…	90%	2.7×10^{-22}	4.1×10^{46}	2.8×10^{-22}	4.4×10^{46}
1550	150	50%	5.7×10^{-22}	7.8×10^{47}	5.6×10^{-22}	7.5×10^{47}
…	…	90%	6.8×10^{-22}	1.1×10^{48}	6.4×10^{-22}	9.9×10^{47}
…	400	50%	4.9×10^{-22}	5.7×10^{47}	5.0×10^{-22}	6.0×10^{47}
…	…	90%	5.6×10^{-22}	7.5×10^{47}	5.7×10^{-22}	7.9×10^{47}

Note. The upper limits are given for burst 2673 for 55 Hz waveforms with $\tau = 400$ s and given for burst 2674 for all other waveforms; these bursts had the lowest upper limits for 50% detection efficiency for these respective waveforms. The energy upper limits are calculated conservatively assuming a distance of 8.1 kpc for Swift J1818.0–1607, although we note that these upper limits could scale by a factor as low as 0.35 if the source is at the close end of its distance range (4.8 kpc).

(This table is available in machine-readable form.)

corresponding $h_{rss}^{50\%}$. In Table 4 we provide $h_{rss}^{90\%}$ and $E_{GW}^{90\%}$ for two waveforms that best model the f-mode for each burst. Finally, in Appendix D we give for each waveform the lowest value of $h_{rss}^{50\%}$ and $E_{GW}^{50\%}$ considering all bursts from SGR 1935+2154, Swift J1818.0−1607, and the unknown source for each waveform in Tables 6–8, respectively. The lowest values of $h_{rss}^{90\%}$ and $E_{GW}^{90\%}$ are in Tables 9–11.

3.2. Long-duration Search Results

All bursts from Table 1 have been analyzed by the long-duration search except the three bursts from the unknown source(s). The search results for each burst are shown in Table 3, which lists the FBS of the most significant cluster for each burst. No interesting cluster has been found as the most significant cluster has an FBS of 0.02. Figure 5 compares the most significant on-source cluster to the corresponding background distribution for each burst.

As in the O2 search (Abbott et al. 2019), two families of waveforms, half sine-Gaussians and ringdowns, are injected at five frequencies (55, 150, 450, 750, and 1550 Hz) and two damping times (150 and 400 s). The lowest value of $h_{rss}^{50\%}$ comes from burst 2656, identified with SGR 1935+2154, which has the largest sum squared antenna factors. The results for burst 2656 indicate an improvement in $h_{rss}^{50\%}$ from O2 to O3, ranging from a factor of 1.25–2, which follow roughly the detectors' sensitivity improvement between the runs, although it also depends on additional considerations such as the detector antenna factors at the time of the burst. The half sine-Gaussian $h_{rss}^{50\%}$ values for burst 2656 are plotted against

representative sensitivity curves of LHO, LLO, and Virgo during O3 (Buikema et al. 2020; Kissel 2020; Verkindt 2021) in Figure 6, along with $h_{rss}^{50\%}$ from O2 as a comparison.

In Figure 7, we plot $h_{rss}^{50\%}$ and $h_{rss}^{90\%}$ for bursts 2656 and 2674 (2673 for waveforms at 55 Hz with a damping time of 400 s for Swift J1818.0−1607), which provide the lowest values at 50% detection efficiency among all bursts emitted by SGR 1935+2154 and Swift J1818.0−1607, respectively. Tables 12 and 13 provide the 50% and 90% detection efficiency upper limits on h_{rss} and E_{GW} for these same bursts for each waveform.

4. Conclusions

In this study, we search for and find no evidence of gravitational waves coincident with 16 bursts (13 magnetar short bursts and three electromagnetic bursts thought to be magnetar short bursts but with no identified source object) during O3. We search for both short-duration signals produced by excited f-modes in the neutron star's core, and for long-duration signals that may be generated from core buoyancy or Alfvén modes. The detection statistics for both the short-duration and long-duration searches are consistent with background noise: the most significant cluster found that was not clearly identified as an instrumental artifact has a p-value of 0.00857; a cluster with this p-value or lower has a 29% probability of appearing in one or more of the 40 searches performed over all of the bursts under the null hypothesis.

For bursts with known sources, the lowest $E_{GW}^{50\%}$ in the short-duration search for waveforms with frequencies from 1500 to 2020 Hz ranged from 4×10^{46} to 6×10^{47} erg. The $E_{GW}^{90\%}$

values of these waveforms ranged from 7×10^{46} erg to 3×10^{48} erg. In Tables 6–8, we report the lowest $h_{\rm rss}^{50\%}$ values over all bursts for each waveform; the lowest $h_{\rm rss}^{90\%}$ values are given in Tables 9–11. The only injected waveforms with exactly the same parameters as the O2 search are the WNBs; we see a factor of improvement in $h_{\rm rss}^{50\%}$ of 1.1 for the $100-200$ Hz, 11 ms WNB. To obtain an approximate metric of improvement, we compare injected circularly polarized sine-Gaussian waveforms at 1600 Hz and 2020 Hz from O3 to sine-Gaussian waveforms of 1500 Hz and 2000 Hz in O2 and see factors of improvement of 1.5 and 1.7 in $h_{\rm rss}^{50\%}$, respectively. This is roughly in agreement with the detector's sensitivity improvement between O2 and O3.

The long-duration search sets the lowest upper limits on long-duration gravitational-wave emission from magnetar bursts to date. We report the long-duration upper limits for each waveform for the burst which had the lowest $h_{\rm rss}$ values at 50% detection efficiency in Table 12 for SGR 1935+2154 and in Table 13 for Swift J1818.0−1607. Of these results, the half sine-Gaussian waveform injected into burst 2656 (from SGR 1935+2154) at 450 Hz produced the lowest $h_{\rm rss}^{90\%}$ upper limit of $1.1 \times 10^{-22}/\sqrt{\rm Hz}$. This corresponds to a gravitational-wave energy of 2.8×10^{45} erg. The lowest $E_{\rm GW}^{90\%}$ values from these results for SGR 1935+2154 and Swift J1818.0–1607 are measured by the sine-Gaussian waveform at 55 Hz, and are 1.0×10^{44} erg and 0.5–1.3×10^{44} erg, respectively. The energy upper limits scale with the distance squared to the source, and here we give the full range of $E_{\rm GW}^{90\%}$ for Swift J1818.0–1607 that corresponds to the distance range of 4.9–8.1 kpc.

We also place upper limits on the ratio of gravitational-wave energy to electromagnetic energy emitted by SGR 1935+2154 (the only source whose bursts have published electromagnetic fluences) using the calculated isotropic electromagnetic energies given in Table 1. For the short-duration search, the most constraining ratio when taking the gravitational-wave energy from the 1590 Hz, 100 ms ringdown waveform is $E_{\rm GW}^{90\%}/E_{\rm EM}^{\rm iso} = 3.0 \times 10^7$. For the long-duration search, the lowest ratio from burst 2656 is $E_{\rm GW}^{90\%}/E_{\rm EM}^{\rm iso} = 4.5 \times 10^3$, which comes from a half sine-Gaussian at 55 Hz with $\tau = 150$ s. These upper limits are less constraining than those of the 2004 giant flare from SGR 1806−20, which had $E_{\rm GW}^{90\%}/E_{\rm EM}^{\rm iso} = 9 \times 10^4$ for a 200 ms ringdown waveform at 1590 Hz (Abbott et al. 2008a) and $E_{\rm GW}^{90\%}/E_{\rm EM}^{\rm iso} \approx 5$ for a band surrounding the 92.5 Hz QPO in the giant flare's tail (Abbott et al. 2007, 2008a).

With the current sensitivities of the LIGO and Virgo detectors, we can now probe well below the potential energy budgets available to generate gravitational waves from catastrophic rearrangements of the star's internal magnetic field (Ioka 2001; Corsi & Owen 2011). However, even the lowest upper limits provided here are well above the expected gravitational-wave energy one would expect from f-mode emission from giant flares (e.g., Levin 2007; Ciolfi & Rezzolla 2012; Zink et al. 2012), let alone the lower-energy bursts being considered here. As gravitational-wave observatories continue to improve in sensitivity, and more observatories such as KAGRA (Akutsu et al. 2019) reach comparable sensitivity, searches for gravitational waves from magnetar bursts will eventually probe several orders of magnitude below the electromagnetic energy of giant flares, increasing the probability of a discovery of gravitational waves from magnetar flares.

Appendix A
Modifications to the Parameters of the Short-duration Search

It should be noted that the burst times are distributed such that the standard 3 hr symmetric background in the short-duration searches would in some cases include the time of the previous or subsequent burst. We mitigate this by either reducing the background length or adjusting the background asymmetry factor (the fraction of background time before the burst) to optimize the amount of background data that could be used for each burst. Full details of these modifications are provided in Table 5.

In addition to modifying the length and background asymmetry factor to exclude neighboring bursts, there are also modifications to the search that we do in order to optimize the upper limits of $h_{rss}^{50\%}$ and $h_{rss}^{90\%}$ for each burst. These include vetoing events in specific frequency bands that display high non-Gaussianity and introducing an error region around the source direction to adjust for the motion of the Earth during the on-source window. A full list of these changes is given in Table 5.

Appendix B
Data Removed from Long-duration Search Windows

Data are required both before and after each pixel in the long-duration time–frequency map to estimate the pixel background (see Thrane et al. 2011 for details). In this search, we use 18 s of data before and after each pixel, as was done in Quitzow-James (2016), Quitzow-James et al. (2017), and Abbott et al. (2019). Thus, any data removed from the long-duration on-source window include up to an additional 36 s, with 18 s both before and after the interval to be removed. We note that 1640 s of data are required for the full 1604 s long-duration on-source window.

Two on-source windows are missing data. One of these is the on-source window of burst 2651, which starts 87 s after the burst; since the on-source window starts 4 s before the burst and 18 s is needed to estimate the pixel background, the time–frequency map starts 109 s after the start of the on-source window (105 s after the burst). Data are available for the first 1121 s of the on-source window of burst 2665, leading to the time–frequency map ending after 1103 s. The on-source windows for bursts 2652, 2660, and 2665 each had 8 s of data removed due to data quality issues, leading to gaps of 44 s in the time–frequency maps. As was done in previous searches (including the O2 search; Abbott et al. 2019), noisy spectral lines, such as 60 Hz power-line harmonics, are identified and removed from the time–frequency maps for each detector pair. Of special note, 55 and 150 Hz are removed for the LHO/Virgo detector pair and 150 Hz for LLO/Virgo; thus, these detector pairs are not sensitive to injected waveforms in these respective frequencies. The Bezier curves for the clusters are generated identically to the other windows, with the missing times (and data removed due to noisy lines) not included in the calculation of the cluster S/N. The background segments are treated identically to their respective on-source windows.

Appendix C
Injected Waveforms and Upper Limit Calculations

For both short-duration and long-duration searches, we consider sine-Gaussian and ringdown waveforms whose plus (+) and cross (×) polarizations are given respectively by

$$\begin{bmatrix} h_+^{SG}(t) \\ h_\times^{SG}(t) \end{bmatrix} = \frac{h_0}{\sqrt{2}} \begin{bmatrix} \dfrac{1+\cos^2\iota}{2} \times \cos(2\pi f_0 t) \\ \cos\iota \times \sin(2\pi f_0 t) \end{bmatrix} e^{-\frac{t^2}{\tau^2}}, \qquad (C1)$$

and

$$\begin{bmatrix} h_+^{RD}(t) \\ h_\times^{RD}(t) \end{bmatrix} = \frac{h_0}{\sqrt{2}} \begin{bmatrix} \dfrac{1+\cos^2\iota}{2} \times \cos(2\pi f_0 t) \\ \cos\iota \times \sin(2\pi f_0 t) \end{bmatrix} e^{-\frac{t}{\tau}} \qquad \text{for t > 0,} \tag{C2}$$

where ι is the inclination angle and τ is the damping time. An injection is circularly polarized in the case where $\cos\iota$ is 1 or -1, linearly polarized when $\cos\iota = 0$, and elliptically polarized when $\cos\iota$ is between -1 and 1. All waveforms in the long-duration search (half sine-Gaussians and ringdowns) have circular polarization. For the short-duration search, the ringdown and most of the sine-Gaussian waveforms are elliptically polarized so as not to assume a source orientation. The polarization angle around the line of sight to the source is set to zero for the long-duration search (which results in an overall phase shift for circularly polarized waveforms), and is uniformly distributed from 0 to π for the waveforms in the short-duration search.

We calculate $E_{GW}^{50\%}$ ($E_{GW}^{90\%}$) for the short-duration search from the corresponding $h_{rss}^{50\%}$ ($h_{rss}^{90\%}$) using the rotating system emission formula in the narrow-band approximation given by Equation (17) of Sutton (2013)

$$E_{GW} \approx \frac{2}{5}\frac{c^3\pi^2}{G}d^2 f_0^2 h_{rss}^2, \qquad (C3)$$

where d is the distance to the source and f_0 is the central frequency. We note that Equation (17) of Sutton (2013) is valid regardless of waveform polarization.

We calculate the $E_{GW}^{50\%}$ and $E_{GW}^{90\%}$ of the WNB waveforms using Equation (11) of Sutton (2013) for isotropic emission,

with correction factors to account for our waveforms being broadband. Specifically, we use

$$E_{\rm GW} = 1.0370 \times \frac{c^3\pi^2}{G}d^2f_0^2\,h_{\rm rss}^2, \tag{C4}$$

for WNBs with a frequency range from 100 to 200 Hz, and

$$E_{\rm GW} = 1.2231 \times \frac{c^3\pi^2}{G}d^2f_0^2\,h_{\rm rss}^2, \tag{C5}$$

for WNBs with a frequency range of 100–1000 Hz.

The $h_{\rm rss}$ of a sine-Gaussian waveform derived from Equation (2) is (Quitzow-James 2016)

$$h_{\rm rss}^{\rm SG} = h_0\tau^{1/2}\frac{\pi^{1/4}}{2\left(2^{1/4}\right)}\sqrt{\left(\frac{(1+\cos^2\iota)^2}{4}+\cos^2\iota\right)+\left(\frac{(1+\cos^2\iota)^2}{4}-\cos^2\iota\right)e^{-2\pi^2f_0^2\tau^2}}. \tag{C6}$$

The $h_{\rm rss}$ of a sine-Gaussian when the inclination angle $\iota = 0$ is

$$h_{\rm rss,\iota=0}^{\rm SG} = h_0\sqrt{\tau}\frac{\pi^{1/4}}{2^{3/4}}. \tag{C7}$$

The $E_{\rm GW}$ of a sine-Gaussian waveform is (Quitzow-James 2016)

$$E_{\rm GW}^{\rm SG} = \frac{c^3\pi^{5/2}}{5\sqrt{2}\,G}h_0^2d^2f_0^2\tau$$
$$\times\left[1+\frac{1}{4\pi^2f_0^2\tau^2}\left(1+\frac{1}{6}e^{-2\pi^2f_0^2\tau^2}\right)\right]. \tag{C8}$$

For $Q = \sqrt{2}\,\pi f_0\tau \gg 1$, this can be approximated as

$$E_{\rm GW}^{\rm SG} \approx \frac{c^3\pi^{5/2}}{5\sqrt{2}\,G}h_0^2d^2f_0^2\tau. \tag{C9}$$

The $E_{\rm GW}$ of a half sine-Gaussian is half of the $E_{\rm GW}$ of a sine-Gaussian, and the $h_{\rm rss}$ of a half sine-Gaussian is the $h_{\rm rss}$ of a sine-Gaussian divided by $\sqrt{2}$. The $h_{\rm rss}$ of a half sine-Gaussian with $\iota = 0$ is (Quitzow-James 2016)

$$h_{\rm rss,\iota=0}^{\rm hSG} = \frac{h_{\rm rss,\iota=0}^{\rm SG}}{\sqrt{2}} = h_0\sqrt{\tau}\frac{\pi^{1/4}}{2^{5/4}}. \tag{C10}$$

The $E_{\rm GW}$ of a half sine-Gaussian waveform with $Q = \sqrt{2}\,\pi f_0\tau \gg 1$ can be approximated as (Quitzow-James 2016)

$$E_{\rm GW}^{\rm hSG} \approx \frac{c^3\pi^{5/2}}{10\sqrt{2}\,G}h_0^2d^2f_0^2\tau. \tag{C11}$$

The $h_{\rm rss}$ of a ringdown waveform can be derived from Equation (2) as

$$h_{\rm rss}^{\rm ringdown} = \frac{h_0}{2}\sqrt{\frac{\tau}{2}}\left[\left(\frac{(1+\cos^2\iota)^2}{4}+\cos^2\iota\right)\right.$$
$$\left.+\frac{1}{1+4\pi^2f_0^2\tau^2}\left(\frac{(1+\cos^2\iota)^2}{4}-\cos^2\iota\right)\right]^{1/2}. \tag{C12}$$

For $\iota = 0$ this becomes

$$h_{\rm rss,\iota=0}^{\rm ringdown} = \frac{h_0}{2}\sqrt{\tau}. \tag{C13}$$

$E_{\rm GW}$ can be calculated as

$$E_{\rm GW}^{\rm ringdown} = \frac{c^3}{40G}h_0^2d^2\left(\frac{1+4\pi^2f_0^2\tau^2}{\tau}\right)$$
$$\times\left(1+\left(\frac{1}{6}\right)\frac{1}{1+4\pi^2f_0^2\tau^2}\right). \tag{C14}$$

For $Q = \sqrt{2}\,\pi f_0\tau \gg 1$

$$E_{\rm GW}^{\rm ringdown} \approx \frac{\pi^2c^3}{10\,G}d^2f_0^2\,h_0^2\tau. \tag{C15}$$

It is important to note that the short-duration ringdown waveforms include a ringup right before the injection time for the purpose of avoiding a discontinuous jump in the signal. This ringup has a rise time that is one-tenth of the ringdown damping time. When including this ringup, the $h_{\rm rss}$ of the total waveform is the $h_{\rm rss}$ of the ringup and ringdown added in quadrature while the $E_{\rm GW}$ of the ringup and ringdown are add linearly. This gives

$$h_{\rm rss,\iota=0}^{\rm ringup+ringdown} = \frac{h_0}{2}\sqrt{\tau+\tau\frac{1}{10}} = \frac{h_0}{2}\sqrt{\tau\frac{11}{10}}, \tag{C16}$$

and (for $\sqrt{2}\,\pi f_0\tau \gg 1$)

$$E_{\rm GW}^{\rm ringup+ringdown} \approx \frac{\pi^2c^3}{10G}d^2f_0^2\,h_0^2\tau(11/10). \tag{C17}$$

Appendix D
Search Upper Limit Tables

This section of the appendix contains the tables whose values are displayed in Figures 4, 6 and 7. The upper limits pertaining to both a 50% and 90% detection efficiency are included in Tables 6–13 to provide a complete picture of the search sensitivity.

ORCID iDs

K. Ackley https://orcid.org/0000-0002-8648-0767
N. Adhikari https://orcid.org/0000-0002-4559-8427
R. X. Adhikari https://orcid.org/0000-0002-5731-5076
M. Agathos https://orcid.org/0000-0002-9072-1121
K. Agatsuma https://orcid.org/0000-0002-3952-5985
O. D. Aguiar https://orcid.org/0000-0002-2139-4390
L. Aiello https://orcid.org/0000-0003-2771-8816
P. Ajith https://orcid.org/0000-0001-7519-2439
T. Akutsu https://orcid.org/0000-0003-0733-7530
A. Allocca https://orcid.org/0000-0002-5288-1351

P. A. Altin https://orcid.org/0000-0001-8193-5825
A. Amato https://orcid.org/0000-0001-9557-651X
S. B. Anderson https://orcid.org/0000-0003-2219-9383
W. G. Anderson https://orcid.org/0000-0003-0482-5942
N. Andres https://orcid.org/0000-0002-5360-943X
M. Andrés-Carcasona https://orcid.org/0000-0002-8738-1672
T. Andrić https://orcid.org/0000-0002-9277-9773
J. M. Antelis https://orcid.org/0000-0003-3377-0813
S. Antier https://orcid.org/0000-0002-7686-3334
K. Arai https://orcid.org/0000-0001-8916-8915
A. Araya https://orcid.org/0000-0002-6884-2875
M. C. Araya https://orcid.org/0000-0002-6018-6447
J. S. Areeda https://orcid.org/0000-0003-0266-7936
N. Aritomi https://orcid.org/0000-0003-4424-7657
N. Arnaud https://orcid.org/0000-0001-6589-8673
H. Asada https://orcid.org/0000-0001-9442-6050
G. Ashton https://orcid.org/0000-0001-7288-2231
Y. Aso https://orcid.org/0000-0002-1902-6695
P. Astone https://orcid.org/0000-0003-4981-4120
F. Aubin https://orcid.org/0000-0003-1613-3142
K. AultONeal https://orcid.org/0000-0002-6645-4473
S. Babak https://orcid.org/0000-0001-7469-4250
F. Badaracco https://orcid.org/0000-0001-8553-7904
S. Bae https://orcid.org/0000-0003-2429-3357
S. Bagnasco https://orcid.org/0000-0001-6062-6505
R. Bajpai https://orcid.org/0000-0003-0495-5720
G. Baltus https://orcid.org/0000-0002-0304-8152
S. Banagiri https://orcid.org/0000-0001-7852-7484
B. Banerjee https://orcid.org/0000-0002-8008-2485
D. Bankar https://orcid.org/0000-0002-6068-2993
P. Barneo https://orcid.org/0000-0002-8883-7280
F. Barone https://orcid.org/0000-0002-8069-8490
B. Barr https://orcid.org/0000-0002-5232-2736
L. Barsotti https://orcid.org/0000-0001-9819-2562
M. Barsuglia https://orcid.org/0000-0002-1180-4050
D. Barta https://orcid.org/0000-0001-6841-550X
M. A. Barton https://orcid.org/0000-0002-9948-306X
R. Bassiri https://orcid.org/0000-0001-8171-6833
M. Bawaj https://orcid.org/0000-0003-3611-3042
J. C. Bayley https://orcid.org/0000-0003-2306-4106
B. Bécsy https://orcid.org/0000-0003-0909-5563
F. Beirnaert https://orcid.org/0000-0002-4003-7233
M. Bejger https://orcid.org/0000-0002-4991-8213
J. D. Bentley https://orcid.org/0000-0002-4736-7403
M. Berbel https://orcid.org/0000-0001-6345-1798
B. K. Berger https://orcid.org/0000-0002-4845-8737
S. Bernuzzi https://orcid.org/0000-0002-2334-0935
D. Bersanetti https://orcid.org/0000-0002-7377-415X
J. Betzwieser https://orcid.org/0000-0003-1533-9229
D. Beveridge https://orcid.org/0000-0002-1481-1993
U. Bhardwaj https://orcid.org/0000-0003-1233-4174
D. Bhattacharjee https://orcid.org/0000-0001-6623-9506
S. Bhaumik https://orcid.org/0000-0001-8492-2202
G. Billingsley https://orcid.org/0000-0002-4141-2744
O. Birnholtz https://orcid.org/0000-0002-7562-9263
S. Biscoveanu https://orcid.org/0000-0001-7616-7366
B. Biswas https://orcid.org/0000-0003-2131-1476
M.-A. Bizouard https://orcid.org/0000-0002-4618-1674
J. K. Blackburn https://orcid.org/0000-0002-3838-2986
G. N. Bolingbroke https://orcid.org/0000-0002-7350-5291
E. Bonilla https://orcid.org/0000-0002-6284-9769

R. Bonnand https://orcid.org/0000-0001-5013-5913
V. Boschi https://orcid.org/0000-0001-8665-2293
V. Boudart https://orcid.org/0000-0001-9923-4154
P. R. Brady https://orcid.org/0000-0002-4611-9387
M. Branchesi https://orcid.org/0000-0003-1643-0526
J. E. Brau https://orcid.org/0000-0003-1292-9725
M. Breschi https://orcid.org/0000-0002-3327-3676
T. Briant https://orcid.org/0000-0002-6013-1729
A. F. Brooks https://orcid.org/0000-0003-4295-792X
R. Bruntz https://orcid.org/0000-0002-0840-8567
A. Buonanno https://orcid.org/0000-0002-5433-1409
R. Buscicchio https://orcid.org/0000-0002-7387-6754
C. Buy https://orcid.org/0000-0003-2872-8186
G. S. Cabourn Davies https://orcid.org/0000-0002-4289-3439
G. Cabras https://orcid.org/0000-0002-6852-6856
R. Cabrita https://orcid.org/0000-0003-0133-1306
L. Cadonati https://orcid.org/0000-0002-9846-166X
G. Cagnoli https://orcid.org/0000-0002-7086-6550
K. C. Cannon https://orcid.org/0000-0003-4068-6572
Z. Cao https://orcid.org/0000-0002-1932-7295
E. Capocasa https://orcid.org/0000-0003-3762-6958
J. B. Carlin https://orcid.org/0000-0001-5694-0809
G. Carullo https://orcid.org/0000-0001-9090-1862
M. Cavaglià https://orcid.org/0000-0002-3835-6729
F. Cavalier https://orcid.org/0000-0002-3658-7240
R. Cavalieri https://orcid.org/0000-0001-6064-0569
G. Cella https://orcid.org/0000-0002-0752-0338
E. Cesarini https://orcid.org/0000-0001-9127-3167
S. Chalathadka Subrahmanya https://orcid.org/0000-0002-9207-4669
E. Champion https://orcid.org/0000-0002-7901-4100
C. L. Chan https://orcid.org/0000-0002-3377-4737
P. Chanial https://orcid.org/0000-0003-1753-524X
C. Chapman-Bird https://orcid.org/0000-0002-2728-9612
P. Charlton https://orcid.org/0000-0002-4263-2706
E. A. Chase https://orcid.org/0000-0003-1005-0792
E. Chassande-Mottin https://orcid.org/0000-0003-3768-9908
C. Chatterjee https://orcid.org/0000-0001-8700-3455
Debarati Chatterjee https://orcid.org/0000-0002-0995-2329
Deep Chatterjee https://orcid.org/0000-0003-0038-5468
S. Chaty https://orcid.org/0000-0002-5769-8601
C. Chen https://orcid.org/0000-0002-3354-0105
D. Chen https://orcid.org/0000-0003-1433-0716
H. Y. Chen https://orcid.org/0000-0001-5403-3762
F. Chiadini https://orcid.org/0000-0002-9339-8622
A. Chincarini https://orcid.org/0000-0003-4094-9942
A. Chiummo https://orcid.org/0000-0003-2165-2967
S. Choudhary https://orcid.org/0000-0003-0949-7298
N. Christensen https://orcid.org/0000-0002-6870-4202
S. S. Y. Chua https://orcid.org/0000-0001-8026-7597
G. Ciani https://orcid.org/0000-0003-4258-9338
M. Cieślar https://orcid.org/0000-0001-8912-5587
R. Ciolfi https://orcid.org/0000-0003-3140-8933
J. A. Clark https://orcid.org/0000-0003-3243-1393
E. Codazzo https://orcid.org/0000-0001-7170-8733
P.-F. Cohadon https://orcid.org/0000-0003-3452-9415
D. E. Cohen https://orcid.org/0000-0002-0583-9919
M. Colleoni https://orcid.org/0000-0002-7214-9088
A. Colombo https://orcid.org/0000-0002-7439-4773
L. Conti https://orcid.org/0000-0003-2731-2656

T. R. Corbitt ⓘ https://orcid.org/0000-0002-5520-8541
I. Cordero-Carrión ⓘ https://orcid.org/0000-0002-1985-1361
N. J. Cornish ⓘ https://orcid.org/0000-0002-7435-0869
S. Cortese ⓘ https://orcid.org/0000-0002-6504-0973
M. W. Coughlin ⓘ https://orcid.org/0000-0002-8262-2924
B. Cousins ⓘ https://orcid.org/0000-0002-7026-1340
P. Couvares ⓘ https://orcid.org/0000-0002-2823-3127
D. C. Coyne ⓘ https://orcid.org/0000-0002-6427-3222
R. Coyne ⓘ https://orcid.org/0000-0002-5243-5917
J. D. E. Creighton ⓘ https://orcid.org/0000-0003-3600-2406
A. W. Criswell ⓘ https://orcid.org/0000-0002-9225-7756
M. Croquette ⓘ https://orcid.org/0000-0002-8581-5393
J. R. Cudell ⓘ https://orcid.org/0000-0002-2003-4238
R. Cummings ⓘ https://orcid.org/0000-0002-8042-9047
T. Dal Canton ⓘ https://orcid.org/0000-0001-5078-9044
S. Dall'Osso ⓘ https://orcid.org/0000-0003-4366-8265
G. Dálya ⓘ https://orcid.org/0000-0003-3258-5763
B. D'Angelo ⓘ https://orcid.org/0000-0001-9143-8427
S. Danilishin ⓘ https://orcid.org/0000-0001-7758-7493
C. Darsow-Fromm ⓘ https://orcid.org/0000-0001-9602-0388
Sayantani Datta ⓘ https://orcid.org/0000-0001-9200-8867
D. Davis ⓘ https://orcid.org/0000-0001-5620-6751
M. C. Davis ⓘ https://orcid.org/0000-0001-7663-0808
E. J. Daw ⓘ https://orcid.org/0000-0002-3780-5430
J. Degallaix ⓘ https://orcid.org/0000-0002-1019-6911
S. Deléglise ⓘ https://orcid.org/0000-0002-8680-5170
F. De Lillo ⓘ https://orcid.org/0000-0003-4977-0789
D. Dell'Aquila ⓘ https://orcid.org/0000-0001-5895-0664
T. Dent ⓘ https://orcid.org/0000-0003-1354-7809
A. Depasse ⓘ https://orcid.org/0000-0003-1014-8394
R. De Pietri ⓘ https://orcid.org/0000-0003-1556-8304
R. De Rosa ⓘ https://orcid.org/0000-0002-4004-947X
R. DeSalvo ⓘ https://orcid.org/0000-0002-4818-0296
M. C. Díaz ⓘ https://orcid.org/0000-0002-7555-8856
T. Dietrich ⓘ https://orcid.org/0000-0003-2374-307X
C. Di Giorgio ⓘ https://orcid.org/0000-0003-2127-3991
F. Di Giovanni ⓘ https://orcid.org/0000-0001-8568-9334
T. Di Girolamo ⓘ https://orcid.org/0000-0003-2339-4471
A. Di Lieto ⓘ https://orcid.org/0000-0002-4787-0754
A. Di Michele ⓘ https://orcid.org/0000-0002-0357-2608
S. Di Pace ⓘ https://orcid.org/0000-0001-6759-5676
I. Di Palma ⓘ https://orcid.org/0000-0003-1544-8943
F. Di Renzo ⓘ https://orcid.org/0000-0002-5447-3810
A. Dmitriev ⓘ https://orcid.org/0000-0002-0314-956X
L. D'Onofrio ⓘ https://orcid.org/0000-0001-9546-5959
S. Doravari ⓘ https://orcid.org/0000-0001-8750-8330
M. Drago ⓘ https://orcid.org/0000-0002-3738-2431
J. C. Driggers ⓘ https://orcid.org/0000-0002-6134-7628
D. D'Urso ⓘ https://orcid.org/0000-0002-8215-4542
T. Eckhardt ⓘ https://orcid.org/0000-0002-1224-4681
G. Eddolls ⓘ https://orcid.org/0000-0002-5895-4523
B. Edelman ⓘ https://orcid.org/0000-0001-7648-1689
O. Edy ⓘ https://orcid.org/0000-0001-9617-8724
A. Effler ⓘ https://orcid.org/0000-0001-8242-3944
S. Eguchi ⓘ https://orcid.org/0000-0003-2814-9336
J. Eichholz ⓘ https://orcid.org/0000-0002-2643-163X
A. Ejlli ⓘ https://orcid.org/0000-0002-4149-4532
Y. Enomoto ⓘ https://orcid.org/0000-0001-6426-7079
R. C. Essick ⓘ https://orcid.org/0000-0001-8196-9267
D. Estevez ⓘ https://orcid.org/0000-0002-3021-5964
M. Evans ⓘ https://orcid.org/0000-0001-8459-4499
F. Fabrizi ⓘ https://orcid.org/0000-0002-3809-065X

V. Fafone ⓘ https://orcid.org/0000-0003-1314-1622
P. C. Fan ⓘ https://orcid.org/0000-0003-3988-9022
A. M. Farah ⓘ https://orcid.org/0000-0002-6121-0285
B. Farr ⓘ https://orcid.org/0000-0002-2916-9200
W. M. Farr ⓘ https://orcid.org/0000-0003-1540-8562
G. Favaro ⓘ https://orcid.org/0000-0002-0351-6833
M. Favata ⓘ https://orcid.org/0000-0001-8270-9512
M. Fays ⓘ https://orcid.org/0000-0002-4390-9746
E. Fenyvesi ⓘ https://orcid.org/0000-0003-2777-3719
D. L. Ferguson ⓘ https://orcid.org/0000-0002-4406-591X
A. Fernandez-Galiana ⓘ https://orcid.org/0000-0002-8940-9261
I. Ferrante ⓘ https://orcid.org/0000-0002-0083-7228
F. Fidecaro ⓘ https://orcid.org/0000-0002-6189-3311
P. Figura ⓘ https://orcid.org/0000-0002-8925-0393
A. Fiori ⓘ https://orcid.org/0000-0003-3174-0688
I. Fiori ⓘ https://orcid.org/0000-0002-0210-516X
M. Fishbach ⓘ https://orcid.org/0000-0002-1980-5293
J. A. Font ⓘ https://orcid.org/0000-0001-6650-2634
B. Fornal ⓘ https://orcid.org/0000-0003-3271-2080
F. Frasconi ⓘ https://orcid.org/0000-0003-4204-6587
Z. Frei ⓘ https://orcid.org/0000-0002-0181-8491
A. Freise ⓘ https://orcid.org/0000-0001-6586-9901
R. Frey ⓘ https://orcid.org/0000-0003-0341-2636
G. G. Fronzé ⓘ https://orcid.org/0000-0003-0966-4279
B. U. Gadre ⓘ https://orcid.org/0000-0002-1534-9761
J. R. Gair ⓘ https://orcid.org/0000-0002-1671-3668
D. Ganapathy ⓘ https://orcid.org/0000-0003-3028-4174
A. Ganguly ⓘ https://orcid.org/0000-0001-7394-0755
D. Gao ⓘ https://orcid.org/0000-0002-1697-7153
B. Garaventa ⓘ https://orcid.org/0000-0003-2490-404X
F. Garufi ⓘ https://orcid.org/0000-0003-1391-6168
G.-G. Ge ⓘ https://orcid.org/0000-0003-2601-6484
G. Gemme ⓘ https://orcid.org/0000-0002-1127-7406
A. Gennai ⓘ https://orcid.org/0000-0003-0149-2089
O. Gerberding ⓘ https://orcid.org/0000-0001-7740-2698
L. Gergely ⓘ https://orcid.org/0000-0003-3146-6201
S. Ghonge ⓘ https://orcid.org/0000-0002-5476-938X
Abhirup Ghosh ⓘ https://orcid.org/0000-0002-2112-8578
Archisman Ghosh ⓘ https://orcid.org/0000-0003-0423-3533
Shaon Ghosh ⓘ https://orcid.org/0000-0001-9901-6253
Tathagata Ghosh ⓘ https://orcid.org/0000-0001-9848-9905
B. Giacomazzo ⓘ https://orcid.org/0000-0002-6947-4023
J. A. Giaime ⓘ https://orcid.org/0000-0002-3531-817X
M. Giesler ⓘ https://orcid.org/0000-0003-2300-893X
P. Giri ⓘ https://orcid.org/0000-0002-4628-2432
S. Gkaitatzis ⓘ https://orcid.org/0000-0001-9420-7499
E. Goetz ⓘ https://orcid.org/0000-0003-2666-721X
R. Goetz ⓘ https://orcid.org/0000-0002-9617-5520
B. Goncharov ⓘ https://orcid.org/0000-0003-3189-5807
G. González ⓘ https://orcid.org/0000-0003-0199-3158
A. Grado ⓘ https://orcid.org/0000-0002-0501-8256
M. Granata ⓘ https://orcid.org/0000-0003-3275-1186
R. Gray ⓘ https://orcid.org/0000-0002-5556-9873
A. C. Green ⓘ https://orcid.org/0000-0002-6287-8746
W. L. Griffiths ⓘ https://orcid.org/0000-0001-8366-0108
H. L. Griggs ⓘ https://orcid.org/0000-0001-5018-7908
A. Grimaldi ⓘ https://orcid.org/0000-0002-6956-4301
H. Grote ⓘ https://orcid.org/0000-0002-0797-3943
D. Guerra ⓘ https://orcid.org/0000-0003-0029-5390
G. M. Guidi ⓘ https://orcid.org/0000-0002-3061-9870
H.-K. Guo ⓘ https://orcid.org/0000-0002-3777-3117

Anuradha Gupta https://orcid.org/0000-0002-5441-9013
F. Guzman https://orcid.org/0000-0001-9136-929X
L. Haegel https://orcid.org/0000-0002-3680-5519
O. Halim https://orcid.org/0000-0003-1326-5481
E. D. Hall https://orcid.org/0000-0001-9018-666X
W.-B. Han https://orcid.org/0000-0002-2039-0726
M. Haney https://orcid.org/0000-0001-7554-3665
J. Harms https://orcid.org/0000-0002-7332-9806
G. M. Harry https://orcid.org/0000-0002-8905-7622
I. W. Harry https://orcid.org/0000-0002-5304-9372
D. Hartwig https://orcid.org/0000-0002-9742-0794
C.-J. Haster https://orcid.org/0000-0001-8040-9807
J. Healy https://orcid.org/0000-0002-5233-3320
A. Heidmann https://orcid.org/0000-0002-0784-5175
J. Heinze https://orcid.org/0000-0001-8692-2724
H. Heitmann https://orcid.org/0000-0003-0625-5461
F. Hellman https://orcid.org/0000-0002-9135-6330
A. F. Helmling-Cornell https://orcid.org/0000-0002-7709-8638
G. Hemming https://orcid.org/0000-0001-5268-4465
M. Hendry https://orcid.org/0000-0001-8322-5405
E. Hennes https://orcid.org/0000-0002-2246-5496
M. H. Hennig https://orcid.org/0000-0003-1531-8460
M. Heurs https://orcid.org/0000-0002-5577-2273
A. L. Hewitt https://orcid.org/0000-0002-1255-3492
D. G. Holcomb https://orcid.org/0000-0001-5987-769X
I. J. Hollows https://orcid.org/0000-0002-3404-6459
Z. J. Holmes https://orcid.org/0000-0003-1311-4691
D. E. Holz https://orcid.org/0000-0002-0175-5064
E. J. Howell https://orcid.org/0000-0001-7891-2817
C. G. Hoy https://orcid.org/0000-0002-8843-6719
H-F. Hsieh https://orcid.org/0000-0002-8947-723X
H-Y. Huang https://orcid.org/0000-0002-1665-2383
P. Huang https://orcid.org/0000-0002-3812-2180
Y-C. Huang https://orcid.org/0000-0001-8786-7026
Y.-J. Huang https://orcid.org/0000-0002-2952-8429
M. T. Hübner https://orcid.org/0000-0002-9642-3029
D. C. Y. Hui https://orcid.org/0000-0003-1753-1660
V. Hui https://orcid.org/0000-0002-0233-2346
B. Idzkowski https://orcid.org/0000-0001-5869-2714
K. Inayoshi https://orcid.org/0000-0001-9840-4959
P. Iosif https://orcid.org/0000-0003-1621-7709
M. Isi https://orcid.org/0000-0001-8830-8672
Y. Itoh https://orcid.org/0000-0003-2694-8935
B. R. Iyer https://orcid.org/0000-0002-4141-5179
V. JaberianHamedan https://orcid.org/0000-0003-3605-4169
T. Jacqmin https://orcid.org/0000-0002-0693-4838
P.-E. Jacquet https://orcid.org/0000-0001-9552-0057
S. P. Jadhav https://orcid.org/0000-0003-0554-0084
A. L. James https://orcid.org/0000-0001-9165-0807
A. Z. Jan https://orcid.org/0000-0003-2050-7231
K. Janssens https://orcid.org/0000-0001-8760-4429
P. Jaranowski https://orcid.org/0000-0001-8085-3414
R. Jaume https://orcid.org/0000-0001-8691-3166
A. C. Jenkins https://orcid.org/0000-0003-1785-5841
J. Jiang https://orcid.org/0000-0002-0154-3854
H.-B. Jin https://orcid.org/0000-0002-6217-2428
A. W. Jones https://orcid.org/0000-0002-0395-0680
L. Ju https://orcid.org/0000-0002-7951-4295
P. Jung https://orcid.org/0000-0003-2974-4604
J. Junker https://orcid.org/0000-0002-3051-4374
T. Kajita https://orcid.org/0000-0003-1207-6638
M. Kakizaki https://orcid.org/0000-0003-1430-3339
V. Kalogera https://orcid.org/0000-0001-9236-5469
M. Kamiizumi https://orcid.org/0000-0001-7216-1784
N. Kanda https://orcid.org/0000-0001-6291-0227
S. Kandhasamy https://orcid.org/0000-0002-4825-6764
G. Kang https://orcid.org/0000-0002-6072-8189
D. P. Kapasi https://orcid.org/0000-0001-8189-4920
C. Karathanasis https://orcid.org/0000-0002-0642-5507
M. Kasprzack https://orcid.org/0000-0003-4618-5939
S. Katsanevas https://orcid.org/0000-0003-0324-0758
K. Kawaguchi https://orcid.org/0000-0003-4443-6984
D. Keitel https://orcid.org/0000-0002-2824-626X
J. S. Key https://orcid.org/0000-0003-0123-7600
F. Y. Khalili https://orcid.org/0000-0001-7068-2332
S. Khan https://orcid.org/0000-0003-4953-5754
N. Kijbunchoo https://orcid.org/0000-0002-2874-1228
C. Kim https://orcid.org/0000-0003-3040-8456
J. Kim https://orcid.org/0000-0001-9145-0530
K. Kim https://orcid.org/0000-0003-1653-3795
Y.-M. Kim https://orcid.org/0000-0001-8720-6113
M. Kinley-Hanlon https://orcid.org/0000-0002-7367-8002
R. Kirchhoff https://orcid.org/0000-0003-0224-8600
J. S. Kissel https://orcid.org/0000-0002-1702-9577
A. M. Knee https://orcid.org/0000-0003-0703-947X
K. Kokeyama https://orcid.org/0000-0002-2896-1992
S. Koley https://orcid.org/0000-0002-5793-6665
P. Kolitsidou https://orcid.org/0000-0002-6719-8686
M. Kolstein https://orcid.org/0000-0002-5482-6743
A. K. H. Kong https://orcid.org/0000-0002-5105-344X
A. Kontos https://orcid.org/0000-0002-1347-0680
M. Korobko https://orcid.org/0000-0002-3839-3909
C. Kozakai https://orcid.org/0000-0003-2853-869X
N. V. Krishnendu https://orcid.org/0000-0002-3483-7517
A. Królak https://orcid.org/0000-0003-4514-7690
P. Kuijer https://orcid.org/0000-0002-6987-2048
Prayush Kumar https://orcid.org/0000-0001-5523-4603
K. Kuns https://orcid.org/0000-0003-0630-3902
S. Kuroyanagi https://orcid.org/0000-0001-6538-1447
K. Kwak https://orcid.org/0000-0002-2304-7798
D. Laghi https://orcid.org/0000-0001-7462-3794
R. N. Lang https://orcid.org/0000-0002-4804-5537
B. Lantz https://orcid.org/0000-0002-7404-4845
P. D. Lasky https://orcid.org/0000-0003-3763-1386
M. Laxen https://orcid.org/0000-0001-7515-9639
A. Lazzarini https://orcid.org/0000-0002-5993-8808
P. Leaci https://orcid.org/0000-0002-3997-5046
S. Leavey https://orcid.org/0000-0001-8253-0272
Y. K. Lecoeuche https://orcid.org/0000-0002-9186-7034
H. M. Lee https://orcid.org/0000-0003-4412-7161
H. W. Lee https://orcid.org/0000-0002-1998-3209
K. Lee https://orcid.org/0000-0003-0470-3718
R. Lee https://orcid.org/0000-0002-7171-7274
M. Lenti https://orcid.org/0000-0002-2765-3955
M. Leonardi https://orcid.org/0000-0002-7641-0060
N. Leroy https://orcid.org/0000-0002-2321-1017
K. L. Li https://orcid.org/0000-0001-8229-2024
X. Li https://orcid.org/0000-0002-3780-7735
C-Y. Lin https://orcid.org/0000-0002-7489-7418
E. T. Lin https://orcid.org/0000-0002-0030-8051
F-L. Lin https://orcid.org/0000-0002-4277-7219
H. L. Lin https://orcid.org/0000-0002-3528-5726

L. C.-C. Lin https://orcid.org/0000-0003-4083-9567
G. C. Liu https://orcid.org/0000-0001-5663-3016
J. Liu https://orcid.org/0000-0001-6726-3268
R. K. L. Lo https://orcid.org/0000-0003-1561-6716
A. Longo https://orcid.org/0000-0003-4254-8579
M. Lorenzini https://orcid.org/0000-0002-2765-7905
G. Losurdo https://orcid.org/0000-0003-0452-746X
J. D. Lough https://orcid.org/0000-0002-5160-0239
C. O. Lousto https://orcid.org/0000-0002-6400-9640
D. Lumaca https://orcid.org/0000-0002-3628-1591
L.-W. Luo https://orcid.org/0000-0002-2761-8877
R. Macas https://orcid.org/0000-0002-6096-8297
D. M. Macleod https://orcid.org/0000-0002-1395-8694
I. A. O. MacMillan https://orcid.org/0000-0002-6927-1031
C. Magazzù https://orcid.org/0000-0002-9913-381X
R. M. Magee https://orcid.org/0000-0001-9769-531X
R. Maggiore https://orcid.org/0000-0001-5140-779X
M. Magnozzi https://orcid.org/0000-0003-4512-8430
E. Majorana https://orcid.org/0000-0002-2383-3692
V. Mandic https://orcid.org/0000-0001-6333-8621
V. Mangano https://orcid.org/0000-0001-7902-8505
M. Manske https://orcid.org/0000-0002-7778-1189
M. Mantovani https://orcid.org/0000-0002-4424-5726
M. Mapelli https://orcid.org/0000-0001-8799-2548
D. Marín Pina https://orcid.org/0000-0001-6482-1842
S. Márka https://orcid.org/0000-0002-3957-1324
Z. Márka https://orcid.org/0000-0003-1306-5260
S. Marsat https://orcid.org/0000-0001-9449-1071
I. W. Martin https://orcid.org/0000-0001-7300-9151
H. Masalehdan https://orcid.org/0000-0002-4589-0815
M. Masso-Reid https://orcid.org/0000-0001-6177-8105
S. Mastrogiovanni https://orcid.org/0000-0003-1606-4183
M. Mateu-Lucena https://orcid.org/0000-0003-4817-6913
M. Matiushechkina https://orcid.org/0000-0002-9957-8720
N. Mavalvala https://orcid.org/0000-0003-0219-9706
D. E. McClelland https://orcid.org/0000-0001-6210-5842
J. McIver https://orcid.org/0000-0003-0316-1355
D. Meacher https://orcid.org/0000-0001-5882-0368
M. Mehmet https://orcid.org/0000-0001-9432-7108
C. S. Menoni https://orcid.org/0000-0001-9185-2572
K. Merfeld https://orcid.org/0000-0003-1773-5372
C. Messenger https://orcid.org/0000-0001-7488-5022
P. M. Meyers https://orcid.org/0000-0002-2689-0190
F. Meylahn https://orcid.org/0000-0002-9556-142X
A. Miani https://orcid.org/0000-0001-7737-3129
I. Michaloliakos https://orcid.org/0000-0003-2980-358X
C. Michel https://orcid.org/0000-0003-0606-725X
Y. Michimura https://orcid.org/0000-0002-2218-4002
H. Middleton https://orcid.org/0000-0001-5532-3622
D. P. Mihaylov https://orcid.org/0000-0002-8820-407X
M. Miravet-Tenés https://orcid.org/0000-0002-8766-1156
T. Mishra https://orcid.org/0000-0002-7881-1677
S. Mitra https://orcid.org/0000-0002-0800-4626
V. P. Mitrofanov https://orcid.org/0000-0002-6983-4981
G. Mitselmakher https://orcid.org/0000-0001-5745-3658
O. Miyakawa https://orcid.org/0000-0002-9085-7600
K. Miyo https://orcid.org/0000-0001-6976-1252
S. Miyoki https://orcid.org/0000-0002-1213-8416
Geoffrey Mo https://orcid.org/0000-0001-6331-112X
L. M. Modafferi https://orcid.org/0000-0002-3422-6986
S. R. Mohite https://orcid.org/0000-0003-1356-7156
M. Molina-Ruiz https://orcid.org/0000-0003-4892-3042

A. More https://orcid.org/0000-0001-7714-7076
C. Moreno https://orcid.org/0000-0002-0496-032X
S. Morisaki https://orcid.org/0000-0002-8445-6747
B. Mours https://orcid.org/0000-0002-6444-6402
C. M. Mow-Lowry https://orcid.org/0000-0002-0351-4555
S. Mozzon https://orcid.org/0000-0002-8855-2509
D. Mukherjee https://orcid.org/0000-0001-7335-9418
Suvodip Mukherjee https://orcid.org/0000-0002-3373-5236
N. Mukund https://orcid.org/0000-0002-8666-9156
E. A. Muñiz https://orcid.org/0000-0001-8844-421X
P. G. Murray https://orcid.org/0000-0002-8218-2404
R. Musenich https://orcid.org/0000-0002-2168-5462
K. Nagano https://orcid.org/0000-0001-6686-1637
K. Nakamura https://orcid.org/0000-0001-6148-4289
H. Nakano https://orcid.org/0000-0001-7665-0796
I. Nardecchia https://orcid.org/0000-0001-5558-2595
L. Naticchioni https://orcid.org/0000-0003-2918-0730
R. K. Nayak https://orcid.org/0000-0002-6814-7792
S. W. S. Ng https://orcid.org/0000-0001-5843-1434
C. Nguyen https://orcid.org/0000-0001-8623-0306
L. Nguyen Quynh https://orcid.org/0000-0002-1828-3702
W.-T. Ni https://orcid.org/0000-0001-6792-4708
A. Nishizawa https://orcid.org/0000-0003-3562-0990
E. Nitoglia https://orcid.org/0000-0001-8906-9159
L. K. Nuttall https://orcid.org/0000-0002-8599-8791
Y. Obayashi https://orcid.org/0000-0001-8791-2608
E. Oelker https://orcid.org/0000-0002-3916-1595
J. J. Oh https://orcid.org/0000-0001-5417-862X
K. Oh https://orcid.org/0000-0002-9672-3742
S. H. Oh https://orcid.org/0000-0003-1184-7453
M. Ohashi https://orcid.org/0000-0001-8072-0304
M. Ohkawa https://orcid.org/0000-0002-1380-1419
F. Ohme https://orcid.org/0000-0003-0493-5607
K. Oohara https://orcid.org/0000-0002-7518-6677
B. O'Reilly https://orcid.org/0000-0002-3874-8335
R. O'Shaughnessy https://orcid.org/0000-0001-5832-8517
E. O'Shea https://orcid.org/0000-0002-0230-9533
S. Oshino https://orcid.org/0000-0002-2794-6029
S. Ossokine https://orcid.org/0000-0002-2579-1246
D. J. Ottaway https://orcid.org/0000-0001-6794-1591
C. Palomba https://orcid.org/0000-0002-4450-9883
K.-C. Pan https://orcid.org/0000-0002-1473-9880
F. Pannarale https://orcid.org/0000-0002-7537-3210
F. Paoletti https://orcid.org/0000-0001-8898-1963
A. Parisi https://orcid.org/0000-0003-0251-8914
J. Park https://orcid.org/0000-0002-7510-0079
W. Parker https://orcid.org/0000-0002-7711-4423
D. Pascucci https://orcid.org/0000-0003-1907-0175
R. Passaquieti https://orcid.org/0000-0003-4753-9428
B. Patricelli https://orcid.org/0000-0001-6709-0969
S. Paul https://orcid.org/0000-0002-4449-1732
F. E. Peña Arellano https://orcid.org/0000-0002-8516-5159
S. Penn https://orcid.org/0000-0003-4956-0853
T. Pereira https://orcid.org/0000-0003-1856-6881
A. Perreca https://orcid.org/0000-0002-6269-2490
J. Petermann https://orcid.org/0000-0002-8949-3803
H. P. Pfeiffer https://orcid.org/0000-0001-9288-519X
K. A. Pham https://orcid.org/0000-0002-7650-1034
K. S. Phukon https://orcid.org/0000-0003-1561-0760
O. J. Piccinni https://orcid.org/0000-0001-5478-3950
M. Pichot https://orcid.org/0000-0002-4439-8968
L. Pierini https://orcid.org/0000-0003-0945-2196

V. Pierro https://orcid.org/0000-0002-6020-5521
M. D. Pitkin https://orcid.org/0000-0003-4548-526X
A. Placidi https://orcid.org/0000-0001-8032-4416
M. L. Planas https://orcid.org/0000-0001-8278-7406
W. Plastino https://orcid.org/0000-0002-5737-6346
R. Poggiani https://orcid.org/0000-0002-9968-2464
E. Polini https://orcid.org/0000-0003-4059-0765
R. Poulton https://orcid.org/0000-0003-2049-520X
G. Pratten https://orcid.org/0000-0003-4984-0775
G. A. Prodi https://orcid.org/0000-0001-5256-915X
M. Punturo https://orcid.org/0000-0001-8722-4485
M. Pürrer https://orcid.org/0000-0002-3329-9788
H. Qi https://orcid.org/0000-0001-6339-1537
R. Quitzow-James https://orcid.org/0000-0003-1233-633X
P. Raffai https://orcid.org/0000-0001-7576-0141
K. E. Ramirez https://orcid.org/0000-0003-2194-7669
A. Ramos-Buades https://orcid.org/0000-0002-6874-7421
V. Raymond https://orcid.org/0000-0003-0066-0095
N. Raza https://orcid.org/0000-0002-8549-9124
M. Razzano https://orcid.org/0000-0003-4825-1629
L. Rei https://orcid.org/0000-0002-8690-9180
P. Relton https://orcid.org/0000-0003-2756-3391
P. Rettegno https://orcid.org/0000-0001-8088-3517
B. Revenu https://orcid.org/0000-0002-7629-4805
J. W. Richardson https://orcid.org/0000-0002-1472-4806
K. Riles https://orcid.org/0000-0002-6418-5812
S. Rinaldi https://orcid.org/0000-0001-5799-4155
K. Rink https://orcid.org/0000-0002-1494-3494
A. Rocchi https://orcid.org/0000-0002-1382-9016
L. Rolland https://orcid.org/0000-0003-0589-9687
J. G. Rollins https://orcid.org/0000-0002-9388-2799
A. Romero https://orcid.org/0000-0003-2275-4164
S. Ronchini https://orcid.org/0000-0003-0020-687X
M. P. Ross https://orcid.org/0000-0002-8955-5269
D. Rozza https://orcid.org/0000-0002-7378-6353
J. Sadiq https://orcid.org/0000-0001-5931-3624
S. Saha https://orcid.org/0000-0002-3333-8070
M. Sakellariadou https://orcid.org/0000-0002-2715-1517
O. S. Salafia https://orcid.org/0000-0003-4924-7322
F. Salces-Carcoba https://orcid.org/0000-0001-7049-4438
M. Saleem https://orcid.org/0000-0002-3836-7751
F. Salemi https://orcid.org/0000-0002-9511-3846
A. Samajdar https://orcid.org/0000-0002-0857-6018
N. Sanchis-Gual https://orcid.org/0000-0001-5375-7494
A. Sanuy https://orcid.org/0000-0002-5767-3623
B. S. Sathyaprakash https://orcid.org/0000-0003-3845-7586
O. Sauter https://orcid.org/0000-0003-2293-1554
R. L. Savage https://orcid.org/0000-0003-3317-1036
T. Sawada https://orcid.org/0000-0001-5726-7150
M. G. Schiworski https://orcid.org/0000-0001-9298-004X
P. Schmidt https://orcid.org/0000-0003-1542-1791
R. Schnabel https://orcid.org/0000-0003-2896-4218
E. Schwartz https://orcid.org/0000-0001-8922-7794
J. Scott https://orcid.org/0000-0001-6701-6515
S. M. Scott https://orcid.org/0000-0002-9875-7700
M. Seglar-Arroyo https://orcid.org/0000-0001-8654-409X
Y. Sekiguchi https://orcid.org/0000-0002-2648-3835
Y. Setyawati https://orcid.org/0000-0003-3718-4491
M. S. Shahriar https://orcid.org/0000-0002-7981-954X
M. A. Shaikh https://orcid.org/0000-0003-0826-6164
L. Shao https://orcid.org/0000-0002-1334-8853

P. Shawhan https://orcid.org/0000-0002-8249-8070
N. S. Shcheblanov https://orcid.org/0000-0001-8696-2435
Y. Shikano https://orcid.org/0000-0003-2107-7536
H. Shimizu https://orcid.org/0000-0002-4221-0300
K. Shimode https://orcid.org/0000-0002-5682-8750
H. Shinkai https://orcid.org/0000-0003-1082-2844
A. Shoda https://orcid.org/0000-0002-0236-4735
D. H. Shoemaker https://orcid.org/0000-0002-4147-2560
D. M. Shoemaker https://orcid.org/0000-0002-9899-6357
D. Sigg https://orcid.org/0000-0003-4606-6526
L. Silenzi https://orcid.org/0000-0001-7316-3239
L. P. Singer https://orcid.org/0000-0001-9898-5597
D. Singh https://orcid.org/0000-0001-9675-4584
M. K. Singh https://orcid.org/0000-0001-8081-4888
N. Singh https://orcid.org/0000-0002-1135-3456
A. Singha https://orcid.org/0000-0002-9944-5573
A. M. Sintes https://orcid.org/0000-0001-9050-7515
B. J. J. Slagmolen https://orcid.org/0000-0002-2471-3828
J. R. Smith https://orcid.org/0000-0003-0638-9670
R. J. E. Smith https://orcid.org/0000-0001-8516-3324
J. Soldateschi https://orcid.org/0000-0002-5458-5206
S. N. Somala https://orcid.org/0000-0003-2663-3351
K. Somiya https://orcid.org/0000-0003-2601-2264
I. Song https://orcid.org/0000-0002-4301-8281
K. Soni https://orcid.org/0000-0001-8051-7883
N. Sorrentino https://orcid.org/0000-0002-1855-5966
A. P. Spencer https://orcid.org/0000-0003-4418-3366
M. Spera https://orcid.org/0000-0003-0930-6930
D. A. Steer https://orcid.org/0000-0002-8781-1273
S. Steinlechner https://orcid.org/0000-0003-4710-8548
K. A. Strain https://orcid.org/0000-0002-2066-5355
G. Stratta https://orcid.org/0000-0003-1055-7980
A. L. Stuver https://orcid.org/0000-0003-0324-5735
S. Sudhagar https://orcid.org/0000-0001-8578-4665
V. Sudhir https://orcid.org/0000-0002-5397-6950
R. Sugimoto https://orcid.org/0000-0001-6705-3658
H. G. Suh https://orcid.org/0000-0003-2662-3903
A. G. Sullivan https://orcid.org/0000-0002-9545-7286
T. Z. Summerscales https://orcid.org/0000-0002-4522-5591
L. Sun https://orcid.org/0000-0001-7959-892X
A. Sur https://orcid.org/0000-0001-6635-5080
J. Suresh https://orcid.org/0000-0003-2389-6666
P. J. Sutton https://orcid.org/0000-0003-1614-3922
Takamasa Suzuki https://orcid.org/0000-0003-3030-6599
B. L. Swinkels https://orcid.org/0000-0002-3066-3601
M. J. Szczepańczyk https://orcid.org/0000-0002-6167-6149
S. C. Tait https://orcid.org/0000-0003-0327-953X
H. Takahashi https://orcid.org/0000-0003-0596-4397
R. Takahashi https://orcid.org/0000-0003-1367-5149
H. Takeda https://orcid.org/0000-0001-9937-2557
Takahiro Tanaka https://orcid.org/0000-0001-8406-5183
S. Tanioka https://orcid.org/0000-0003-3321-1018
L. Tao https://orcid.org/0000-0003-4382-5507
E. N. Tapia San Martín https://orcid.org/0000-0002-4817-5606
A. Taruya https://orcid.org/0000-0002-4016-1955
J. D. Tasson https://orcid.org/0000-0002-4777-5087
R. Tenorio https://orcid.org/0000-0002-3582-2587
J. E. S. Terhune https://orcid.org/0000-0001-9078-4993
L. Terkowski https://orcid.org/0000-0003-4622-1215
J. E. Thompson https://orcid.org/0000-0002-0419-5517
Shubhanshu Tiwari https://orcid.org/0000-0003-1611-6625

V. Tiwari ⬤ https://orcid.org/0000-0002-1602-4176
A. E. Tolley ⬤ https://orcid.org/0000-0001-9841-943X
T. Tomaru ⬤ https://orcid.org/0000-0002-8927-9014
T. Tomura ⬤ https://orcid.org/0000-0002-7504-8258
A. Torres-Forné ⬤ https://orcid.org/0000-0001-8709-5118
I. Tosta e Melo ⬤ https://orcid.org/0000-0001-5833-4052
A. Trapananti ⬤ https://orcid.org/0000-0001-7763-5758
F. Travasso ⬤ https://orcid.org/0000-0002-4653-6156
M. C. Tringali ⬤ https://orcid.org/0000-0001-5087-189X
A. Tripathee ⬤ https://orcid.org/0000-0002-6976-5576
A. Trovato ⬤ https://orcid.org/0000-0002-9714-1904
L. Trozzo ⬤ https://orcid.org/0000-0002-8803-6715
T. Tsang ⬤ https://orcid.org/0000-0003-3666-686X
T. Tsutsui ⬤ https://orcid.org/0000-0002-2909-0471
K. Turbang ⬤ https://orcid.org/0000-0002-9296-8603
D. Tuyenbayev ⬤ https://orcid.org/0000-0002-4378-5835
A. S. Ubhi ⬤ https://orcid.org/0000-0002-3240-6000
N. Uchikata ⬤ https://orcid.org/0000-0003-0030-3653
T. Uchiyama ⬤ https://orcid.org/0000-0003-2148-1694
T. Uehara ⬤ https://orcid.org/0000-0003-4375-098X
K. Ueno ⬤ https://orcid.org/0000-0003-3227-6055
T. Ushiba ⬤ https://orcid.org/0000-0002-5059-4033
A. Utina ⬤ https://orcid.org/0000-0003-2975-9208
G. Vajente ⬤ https://orcid.org/0000-0002-7656-6882
G. Valdes ⬤ https://orcid.org/0000-0001-5411-380X
M. Valentini ⬤ https://orcid.org/0000-0003-1215-4552
M. van Beuzekom ⬤ https://orcid.org/0000-0002-0500-1286
J. F. J. van den Brand ⬤ https://orcid.org/0000-0003-4434-5353
H. van Haevermaet ⬤ https://orcid.org/0000-0003-2386-957X
J. V. van Heijningen ⬤ https://orcid.org/0000-0002-8391-7513
N. van Remortel ⬤ https://orcid.org/0000-0003-4180-8199
V. Varma ⬤ https://orcid.org/0000-0002-9994-1761
M. Vasúth ⬤ https://orcid.org/0000-0003-4573-8781
A. Vecchio ⬤ https://orcid.org/0000-0002-6254-1617
J. Veitch ⬤ https://orcid.org/0000-0002-6508-0713
P. J. Veitch ⬤ https://orcid.org/0000-0002-2597-435X
J. Venneberg ⬤ https://orcid.org/0000-0002-2508-2044
G. Venugopalan ⬤ https://orcid.org/0000-0003-4414-9918
D. Verkindt ⬤ https://orcid.org/0000-0003-4344-7227
Y. Verma ⬤ https://orcid.org/0000-0003-4147-3173
S. M. Vermeulen ⬤ https://orcid.org/0000-0003-4227-8214
D. Veske ⬤ https://orcid.org/0000-0003-4225-0895
A. Viceré ⬤ https://orcid.org/0000-0003-0624-6231
A. D. Viets ⬤ https://orcid.org/0000-0002-4241-1428
A. Vijaykumar ⬤ https://orcid.org/0000-0002-4103-0666
V. Villa-Ortega ⬤ https://orcid.org/0000-0001-7983-1963
S. Vitale ⬤ https://orcid.org/0000-0003-2700-0767
C. Vorvick ⬤ https://orcid.org/0000-0003-1591-3358
S. P. Vyatchanin ⬤ https://orcid.org/0000-0002-6823-911X
M. Wade ⬤ https://orcid.org/0000-0002-5703-4469
K. J. Wagner ⬤ https://orcid.org/0000-0002-7255-4251
J. Wang ⬤ https://orcid.org/0000-0002-1830-8527
M. Was ⬤ https://orcid.org/0000-0002-1890-1128
T. Washimi ⬤ https://orcid.org/0000-0001-5792-4907
J. Watchi ⬤ https://orcid.org/0000-0002-9154-6433
A. J. Weinstein ⬤ https://orcid.org/0000-0002-0928-6784
R. A. Weller ⬤ https://orcid.org/0000-0002-2280-219X
K. Wette ⬤ https://orcid.org/0000-0002-4394-7179
J. T. Whelan ⬤ https://orcid.org/0000-0001-5710-6576
B. F. Whiting ⬤ https://orcid.org/0000-0002-8501-8669

C. Whittle ⬤ https://orcid.org/0000-0002-8833-7438
D. Williams ⬤ https://orcid.org/0000-0003-3772-198X
M. J. Williams ⬤ https://orcid.org/0000-0003-2198-2974
A. R. Williamson ⬤ https://orcid.org/0000-0002-7627-8688
J. L. Willis ⬤ https://orcid.org/0000-0002-9929-0225
B. Willke ⬤ https://orcid.org/0000-0003-0524-2925
G. Woan ⬤ https://orcid.org/0000-0003-0381-0394
J. K. Wofford ⬤ https://orcid.org/0000-0002-4301-2859
I. C. F. Wong ⬤ https://orcid.org/0000-0003-2166-0027
C. Wu ⬤ https://orcid.org/0000-0003-3191-8845
D. S. Wu ⬤ https://orcid.org/0000-0003-2849-3751
L. Xiao ⬤ https://orcid.org/0000-0003-2703-449X
H. Yamamoto ⬤ https://orcid.org/0000-0002-3033-2845
K. Yamamoto ⬤ https://orcid.org/0000-0001-6919-9570
T. Yamamoto ⬤ https://orcid.org/0000-0002-0808-4822
F. W. Yang ⬤ https://orcid.org/0000-0001-9873-6259
K. Z. Yang ⬤ https://orcid.org/0000-0001-8083-4037
L. Yang ⬤ https://orcid.org/0000-0002-8868-5977
Y. Yang ⬤ https://orcid.org/0000-0002-3780-1413
A. B. Yelikar ⬤ https://orcid.org/0000-0002-8065-1174
J. Yokoyama ⬤ https://orcid.org/0000-0001-7127-4808
Hang Yu ⬤ https://orcid.org/0000-0002-6011-6190
Haocun Yu ⬤ https://orcid.org/0000-0002-7597-098X
S. Zeidler ⬤ https://orcid.org/0000-0001-7949-1292
M. Zevin ⬤ https://orcid.org/0000-0002-0147-0835
J. Zhang ⬤ https://orcid.org/0000-0002-3931-3851
R. Zhang ⬤ https://orcid.org/0000-0001-8095-483X
C. Zhao ⬤ https://orcid.org/0000-0001-5825-2401
Y. Zhao ⬤ https://orcid.org/0000-0003-2542-4734
X. J. Zhu ⬤ https://orcid.org/0000-0001-7049-6468
Z.-H. Zhu ⬤ https://orcid.org/0000-0002-3567-6743
J. Zweizig ⬤ https://orcid.org/0000-0002-1521-3397

References

Aasi, J., Abbott, B. P., Abbott, R., et al. 2015, CQGra, 32, 074001
Aasi, J., Abbott, B. P., Abbott, R., et al. 2014, PhRvL, 113, 011102
Abadie, J., Abbott, B. P., Abbott, R., et al. 2011, ApJL, 734, L35
Abadie, J., Abbott, B. P., Abbott, R., et al. 2012, ApJ, 755, 2
Abbott, B. P., Abbott, R., Adhikari, R., et al. 2007, PhRvD, 76, 062003
Abbott, B. P., Abbott, R., Abbott, T. D., et al. 2008a, PhRvL, 101, 211102
Abbott, B. P., Abbott, R., Adhikari, R., et al. 2008b, ApJ, 681, 1419
Abbott, B. P., Abbot, R., Adhikari, R., et al. 2009, ApJL, 701, L68
Abbott, B. P., Abbott, R., Abbott, T. D., et al. 2018, LRR, 21, 3
Abbott, B. P., Abbott, R., Abbott, T. D., et al. 2019, ApJ, 874, 163
Abbott, R., Abbott, T. D., Abraham, S., et al. 2021, ApJ, 915, 86
Abbott, R., Abbott, T. D., Acernese, F., et al. 2022, ApJ, 928, 186
Abbott, R., Abbott, T. D., Acerness, F., et al. 2023, ApJ, 955, 155
Acernese, F., Agathos, M., Agatsuma, K., et al. 2015, CQGra, 32, 024001
Ackley, K., Adya, V. B., Agrawal, P., et al. 2020, PASA, 37, e047
Akutsu, T., Ando, M., Arai, K., et al. 2019, NatAs, 3, 35
Akutsu, T., Ando, M., Arai, K., et al. 2021, PTEP, 2021, 05A102
Barat, C., Hayles, R. I., Hurley, K., et al. 1983, A&A, 126, 400
Barsotti, L., Gras, S., Evans, M., & Fritschel, P. 2018, Updated Advanced LIGO Sensitivity Design Curve, https://dcc.ligo.org/LIGO-T1800044/public
Boggs, S. E., Zoglauer, A., Bellm, E., et al. 2007, ApJ, 661, 458
Buikema, A., Cahillane, C., Mansell, G. L., et al. 2020, PhRvD, 102, 062003
Burns, E., Svinkin, D., Hurley, K., et al. 2021, ApJL, 907, L28
Ciolfi, R., Lander, S. K., Manca, G. M., & Rezzolla, L. 2011, ApJL, 736, L6
Ciolfi, R., & Rezzolla, L. 2012, ApJ, 760, 1
Colaiuda, A., & Kokkotas, K. D. 2011, MNRAS, 414, 3014
Corsi, A., & Owen, B. J. 2011, PhRvD, 83, 104014
Cummings, J., Barthelmy, S., Chester, M., & Page, K. 2014, ATel, 6294, 1
Davis, D., Areeda, J. S., Berger, B. K., et al. 2021, CQGra, 38, 135014
Duncan, R. C. 1998, ApJL, 498, L45
Durant, M., & van Kerkwijk, M. H. 2006, ApJ, 650, 1070
Evans, M., Adhikari, R.X., Afle, C., et al. 2021, arXiv:2109.09882

Evans, P., Gropp, J., Kennea, J., et al. 2020, GCN, 27373, 1, https://gcn.gsfc.nasa.gov/gcn/gcn3/27373.gcn3

Evans, W. D., Klebesadel, R. W., Laros, J. G., et al. 1980, ApJL, 237, L7

Glampedakis, K., & Jones, D. I. 2014, MNRAS, 439, 1522

Glampedakis, K., Samuelsson, L., & Andersson, N. 2006, MNRAS, 371, L74

Ho, W. C. G., Jones, D. I., Andersson, N., & Espinoza, C. M. 2020, PhRvD, 101, 103009

Huppenkothen, D., D'Angelo, C., Watts, A. L., et al. 2014a, ApJ, 787, 128

Huppenkothen, D., Heil, L. M., Watts, A. L., & Göğüş, E. 2014b, ApJ, 795, 114

Hurley, K., Boggs, S. E., Smith, D. M., et al. 2005, Natur, 434, 1098

Hurley, K., Cline, T., Mazets, E., et al. 1999, Natur, 397, 41

Hurley, K. 2021, SGR Burst List, http://www.ssl.berkeley.edu/ipn3/sgrlist.txt

Ioka, K. 2001, MNRAS, 327, 639

Israel, G. L., Belloni, T., Stella, L., et al. 2005, ApJL, 628, L53

Kalmus, P. 2009, PhD thesis, Columbia Univ.

Kalmus, P., Cannon, K. C., Márka, S., & Owen, B. J. 2009, PhRvD, 80, 042001

Kalmus, P., Khan, R., Matone, L., & Márka, S. 2007, CQGra, 24, S659

Karuppusamy, R., Desvignes, G., Kramer, M., et al. 2020, ATel, 13553

Kashiyama, K., & Ioka, K. 2011, PhRvD, 83, 081302

Kaspi, V. M., & Beloborodov, A. M. 2017, ARA&A, 55, 261

Kirsten, F., Snelders, M. P., Jenkins, M., et al. 2020, NatAs, 5, 414

Kissel, J. 2020, aLIGO, CAL, Official Advanced LIGO Sensitivity Plots, https://dcc.ligo.org/LIGO-G1500623/public

Lesage, S. 2020, GCN Circular 26980, https://gcn.gsfc.nasa.gov/gcn/gcn3/26980.gcn3

Levin, Y. 2007, MNRAS, 377, 159

Levin, Y., & van Hoven, M. 2011, MNRAS, 418, 659

Lin, L., Göğüş, E., Roberts, O. J., et al. 2020, ApJL, 902, L43

Lindblom, L., & Detweiler, S. L. 1983, ApJS, 53, 73

Macquet, A., Bizouard, M. A., Burns, E., et al. 2021, ApJ, 918, 80

Matone, L., & Márka, S. 2007, CQGra, 24, S649

Mazets, E. P., Aptekar, R. L., Cline, T. L., et al. 2008, ApJ, 680, 545

McDermott, P. N., van Horn, H. M., & Hansen, C. J. 1988, ApJ, 325, 725

Meegan, C., Lichti, G., Bhat, P. N., et al. 2009, ApJ, 702, 791

Mereghetti, S., Götz, D., von Kienlin, A., et al. 2005, ApJL, 624, L105

Messios, N., Papadopoulos, D. B., & Stergioulas, N. 2001, MNRAS, 328, 1161

Murphy, D., Tse, M., Raffai, P., et al. 2013, PhRvD, 87, 103008

Olausen, S. A., & Kaspi, V. M. 2014, ApJS, 212, 6

Piro, A. L. 2005, ApJL, 634, L153

Punturo, M., Abernathy, M., Acernese, F., et al. 2010, CQGra, 27, 194002

Quitzow-James, R. 2016, PhD thesis, Univ. of Oregon

Quitzow-James, R., Brau, J., Clarke, J., et al. 2017, CQGra, 34, 164002

Reitze, D., Adhikari, R. X., Ballmer, S., et al. 2019, BAAS, 51, 035

Robinet, F., Arnaud, N., Leroy, N., et al. 2020, SoftX, 12, 100620

Schale, P. 2019, PhD thesis, Univ. of Oregon, https://scholarsbank.uoregon.edu/xmlui/handle/1794/24835

Strohmayer, T. E., & Watts, A. L. 2005, ApJL, 632, L111

Strohmayer, T. E., & Watts, A. L. 2006, ApJ, 653, 593

Sutton, P. J. 2013, arXiv:1304.0210

Sutton, P. J., Jones, G., Chatterji, S., et al. 2010, NJPh, 12, 053034

Svinkin, D., Frederiks, D., Hurley, K., et al. 2021, Natur, 589, 211

Thrane, E., & Coughlin, M. 2013, PhRvD, 88, 083010

Thrane, E., Kandhasamy, S., Ott, C. D., et al. 2011, PhRvD, 83, 083004

Tsokaros, A., Ruiz, M., Shapiro, S. L., & Uryū, K. 2022, PhRvL, 128, 061101

Verkindt, D., 2021 Sensitivity Curves and BNS Range for Virgo in O2 and O3, Virgo TDS, https://tds.virgo-gw.eu/?content=3&r=19594

Was, M., Sutton, P. J., Jones, G., & Leonor, I. 2012, PhRvD, 86, 022003

Watts, A. L., & Strohmayer, T. E. 2006, ApJL, 637, L117

Wen, D.-H., Li, B.-A., Chen, H.-Y., & Zhang, N.-B. 2019, PhRvC, 99, 045806

Zhong, S.-Q., Dai, Z.-G., Zhang, H.-M., & Deng, C.-M. 2020, ApJL, 898, L5

Zink, B., Lasky, P. D., & Kokkotas, K. D. 2012, PhRvD, 85, 024030